uc3m | Universidad Carlos III de Madrid

University Degree in Aerospace engineering
Academic Year (e.g. 2016-2017)

Bachelor Thesis

"Parametric study of the orthogonal cut machining in composite materials"

Gonzalo Raba Serrahima

Víctor Criado del Álamo

Leganés, 26/09/2017

Abstract

Nowadays machining fiber reinforced plastic (FRP) composite materials is a compulsory process to satisfy functional requirements of the component. However, the fracture mechanics involved in the material removing process are quite complex. Since up to date the knowledge about this field is considerably poor, industrial machining process of FRP is not optimized yet. This results in low quality machined components where fiber pullouts or matrix delaminations are present. A experimental parametric study of orthogonal machining in multidirectional FRP laminates has been performed looking for the optimum cutting conditions where the machined quality is maximized. Cutting parameters such as cutting speed, depth of the cut or tool geometry have been studied. The influence of these parameters have been evaluated through force measurements, temperature monitoring and a complete damage inspection (external and internal). A meticulous analysis in each cutting condition has been performed and finally it was concluded that the optimum cutting condition was the maximum cutting speed, 200m/min, at the minimum depth of the cut, 0.05mm.

Table of contents

List of figures

List of tables

Chapter 1: Introduction

1.1. Introduccion

Nowadays the great advantages offered by fiber reinforced polymers (FRP) materials are being widely leveraged in a great vary of applications. Their characteristic high strength-to-weight ratio makes them the most suitable solution for many engineering problems. Evidently, tendencies show a sound increase in applications for the following decades and an imminent replacement of metals. Not only they will be used in high performance products like aircrafts but also the normal human user will be able to take advantage from them in daily products. However, as all materials, they need to be machined to satisfy product requirements: trimming surfaces, holes...etc. And now is when cost of their exceptional properties arises; FRP have a very poor machinability. Their multiphase constituents causes fibers pullout, matrix bursting on delaminations during the machining process resulting in low quality results. For this reason, machining FRP has been a great challenge for contemporary researchers since their discovery. Lots of cutting factors influence the machined workpiece and the relation cause-effect is not as intuitive as one would expect for metal cutting. The complex interactions between the different oriented laminas and the tool complicate understanding fracture mechanisms and consequently the optimization of the FRP machining process from an industrial point of view too. Great efforts are needed to minimized induced damage on the workpiece. The FRP machining problem not only includes minimizing damage, but also how to detect that the workpiece has been damaged. Unlike metals, FRP materials, can suffer internal damages that cannot be detected by visual inspection. Developing non-destructive methods to detect the internal methods is acquiring great importance in the industrial sector.

This project will try to deal with the overall problem, optimizing FRP machining and work on non-destructive damage detection.

1.2. Objectives

The main objective of this project is to study experimentally the orthogonal cutting on multidirectional Carbon Fiber Reinforce Polymers laminates as a simplification of other machining methods. It has been looked for a more practical/industrial standpoint which is basically seeking the optimum cutting conditions. Typical cutting parameters and tool geometries will be used to validate the results with the literature, but

A parametric analysis is going to be performed as function of the cutting parameters such as the velocity, depth and tool geometry to study the performance of the machining process.

The effect of these cutting parameters will be analyzed on the cutting forces measurements and induced damage on the workpiece and tool, during and after the machining process. Evaluating the induced damage includes studying the surface quality, internal defects, and thermal damage during the process. CFRP chip formation will be under consideration too.

It is expected that the obtained results will be used to validate numerical prediction models on multidirectional composite machining as well as in the industrial sector.

1.3. Structure

The project is divided in the following way:

- Chapter 1. Introduction: a brief introduction concerning FRP polymers and the general problem of composite machining is presented. The objectives of the project and its structure are also defined.
- Chapter 2. State of the art: In this chapter composite material and their current position concerning applications and future tendencies are included. The up-to-date FRP machining problem will be tackled and especial effort has been put on the simplified orthogonal machining process with the help of the literature. From a mechanical perspective fracture mechanics concepts as well as induced damaged will be presented. Moreover, current thermal monitoring methods and induced thermal effects in FRP machining will be introduced. A review of current non-destructive inspection methods in FRP laminates is also included. Finally the nowadays role of numerical simulations in FRP machining has been briefly commented.
- Chapter 3. Methodology: This chapter contains the entire experimental set-up (instruments, materials, tools...). But more important, it contains the description of the activities performed during the experiments. Basically in this section it is presented the why and how of the procedures and activities performed during the experiments and data acquisition/processing.
- Chapter 4. Results and discussion: The results obtained from the orthogonal machining forces, temperature profile, induced damage and chip formation are presented, analyzed and discussed.
- Chapter 5. Economic and legal framework: This brief chapter is dedicated to estimate the budget of the project and comment the guidelines followed to minimize the associated risk during the experimental procedure.
- Chapter 6. Conclusions: The conclusions drawn from the overall experimental study are presented in this chapter as well as possible future works related with this topic.

Chapter 2: State of the art

2.1. About Composite materials

The definition of composite material is very wide and flexible, but basically, a composite material is the combination of two or more constituents with significantly different properties and mechanical performance at a macroscopic level, and are not soluble between them (they must have different interface). The result is a composition where the interaction of the two constituents provides overall outstanding properties to the composite material. The properties of one constituent compliment the other, and vice versa; there is a synergy in the properties of the composite. Typically, it is composed of a matrix (for example a polymer) containing other elements, reinforcements, which strengthen it (generally fibers or particles).

Usually when we speak about composite materials we think about Carbon/epoxy or Glass/epoxy and their common applications in situations requiring high performance materials such as the *F1* or the aircraft industry. For this reason, the composite material concept might seem the last material solution of the contemporaneous engineers. However, the pioneer of this idea (as usually occurs with all kind of ideas) was the nature. The wood is composed of cellulose fibers, providing the stiffness, and polysaccharide lignin which plays the role of the matrix [1]. Moreover, composite materials have a huge historical background in construction. The Ancient Egyptians used straws in the mud to strengthen the bricks, and the Romans were famous for their *opus caementicium* (the Roman concrete) which was composed of pozzolana, quicklime and pumice and was used in the Pantheon in Rome. [2]

In spite of the general use of the composite on construction during the whole history, it was not until the last half century when the applications of the composite materials started to widespread to other engineering fields. Probably the catalyst of this evolution was the military researches during that century. From this point, material science was sufficiently developed and the manufacturing technology is advanced enough that nowadays composite materials are trending topic.

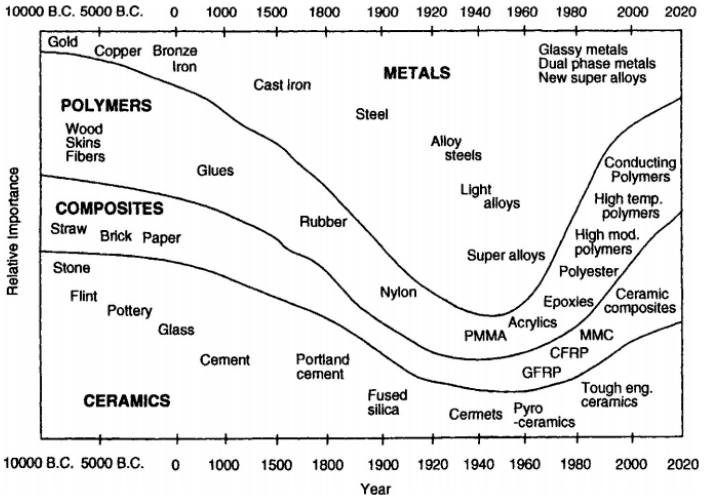

Figure 1: Relative importance of material development through history [3]

As the reader knows, composites are generally composed of reinforcement and a matrix. Since the reinforcement is the strongest component, it enhances the overall mechanical performance of the composite material. Typically are presented as fibers, which are the ones in charge of carrying the loads applied on the composite. However, the performance of the fibers by themselves would be inefficient. Due to their morphology, they are hard to control when loads are applied. For this reason a continuous binder component, a matrix, is needed. The function of the matrix is to hold the fibers together and aligned in a specific stress direction. It complements the fibers so the composite has an optimum performance. In the end, the matrix is the one that defines the shape of the final product. Consequently, the final result is non-homogeneous material that behaves anisotropically. This is the main reason why they are so attractive and at the same time generates so many difficulties in the machining processes.

We are not going to enter in detail in the classification of composite materials and all their characteristics. The type of composite material which is being studied in this project will be briefly commented in the following pages. It is considered as a laminate of unidirectional continuous fibers embedded in a polymer matrix.

Unidirectional continuous fibers composite materials are characterized for the geometry and disposition of these stiff fibers. The fibers are used to have a large length-diameter ratio and are uniquely oriented in the desired stress direction. The apparent elastic modulus and strength of some of the typical fibers used nowadays are presented in Table1:

Fiber	**Tensile modulus Msi (GPa)**	**Tensile strength ksi (MPa)**
Beryllium	35 (240)	189 (1300)
Boron	56 (385)	405 (2800)
Carbon: high tenacity, high modulus	10.2–87.5 (70–600)	254–509 (1750–3500)
PAN (polyacrylonitrite)	29.2–56.9 (200–390)	305–494 (2100–3400)
Pitch (mesophase)	24.8–100.6 (170–690)	189–349 (1300–2400)
Glass:		
E-glass	10.5 (72.4)	508 (3500)
S-glass	12.4 (85.5)	68 (4600)
M-glass	15.9 (110)	508 (3500)
Kevlar-29	8.6 (59)	384 (2640)
Kevlar-49	18.9 (128)	406 (2800)
Silica	16.5 (72.4)	482 (5800)
Tungsten	60 (414)	610 (4200)

Table 1: Typical strengths values of fibers [3]

These fibers are usually introduced in polymeric matrix such as resin, amber or pitch. Polymeric matrices are the most common ones for several reasons like: low cost, good mechanical properties are easily processed (low processing temperatures), good adhesion and provide good mechanical properties. Additionally, their low density constitutions make them even more attractive for structural materials. But, it can be significantly affected by external factors such as temperature and moisture. It can be distinguished thermoplastic and thermoset matrices. They differ in how their polymeric chains are linked, but the important

feature is that the first one can be remolded to a new shape when reheated to the same processing temperature (which is not very high) while for the second one not. Note that this is an important factor to be taken into account when machining this type of composite materials. When machining at high-speeds, high temperatures are reached in the zone near the tool. We must be careful with these temperatures since they can melt the matrix affecting the structural integrity of the composite material. Nevertheless, their overall performance makes them the most suitable matrices for structural composite materials.

When the continuous fibers are embedded uniderectionally in the matrix, they form what is called a lamina. It is assumed to have an orthotropic behavior, very stiff along the longitudinal direction of the fibers although is very weak in the transverse plane. To solve this problem, several unidirectional laminas are stacked combining different fibers orientations and forming what we all know as a laminate. This way, the material engineers can achieve the mechanical properties that they desire.

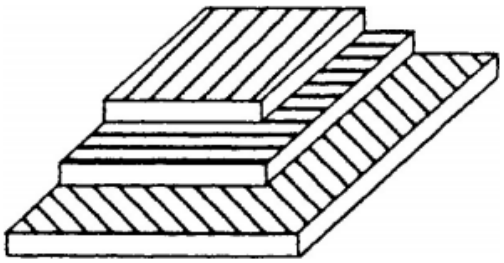

Figure 2: Composite material scheme [3]

The resultant composite material is highly dependent on the properties of its constituents and how they are arranged. At it is important to mention the volume fraction, the parameter that measures the percentage of fibers and matrix in the composite.

If the composite is properly designed and elaborated, it can afford significant advantages with respect other materials, and especially if it is for structural purposes. The most important advantages are:

- High strength and stiffness
- Low density
- Long fatigue life
- High adaptability of the properties to the requirements
- High corrosion resistance
- High dielectric resistance

What makes composite materials highly attractive for structural purposes is their large strength to weight ratio and the ease to control the material properties to fit specific requirements by adding, removing or changing the orientation of the laminas in the composite. Figure 3 shows the specific modulus (E/ρ) of common metals and the typical composite used for structural applications.

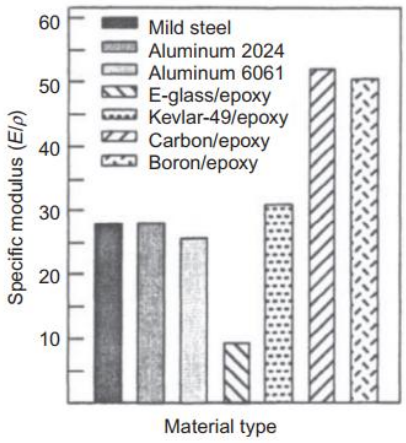

Figure 3: Comparison of specific modulus between metals and composite materials [3]

The emerging structural solutions with these composite materials are mainly characterized for their high-performance character and high strength-to-weight ratio. For these reasons now they are widely used, especially the aforementioned multidirectional continuous fibers laminates like Carbon/epoxy or Glass/epoxy.

Although the aeronautic and aerospace sector are the most demanding sector of this type of composite material (obviously for their exceptional properties), there also exists a constant increase of composite material applications in the whole engineering world. When engineers want to improve the performance of their work of art, for example by saving weight, they always look for composite materials. For example, in competitions it is highly demanded (bicycles, skis, raquets, *F1,* motoGP...) as well as in industrial sector directed to the consumer (cars, motorbikes, boats...). Figure 4 shows the trend of the worldwide usage of Carbon fibers from 2012 towards 2020, and definitely, composite materials are more present in our daily lives. For this reason we must continue researching in composite materials, but not only in improving more their qualities but also in their industrial process. The manufacturing process as well as the machining process needs to be optimized to give an opportunity to the normal consumer to have access to these materials. There is a composite material market that can be even more exploited.

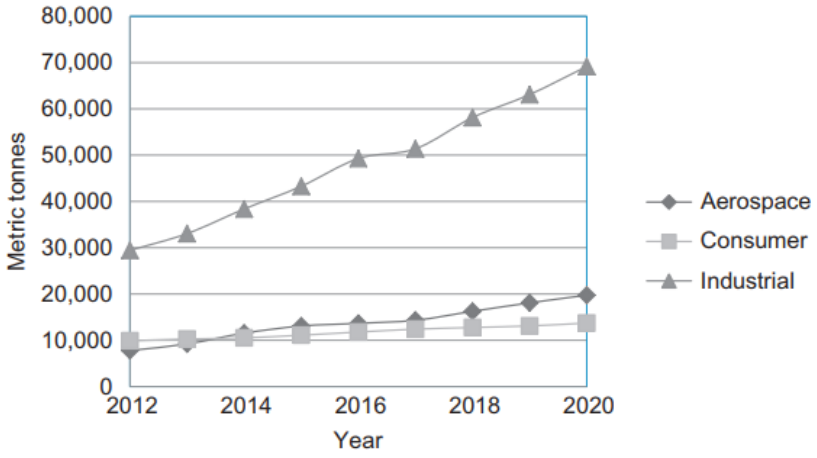

Figure 4: Historical tendency of the use of composite materials [3]

2.2. About orthogonal machining and mechanical behavior on composite materials

As previously mentioned, the fiber reinforced polymers (FRP) are being widely applied in lot of engineering solutions and are substituting the metals. This fact has motivated industrial companies and researchers to push further their knowledge limits of these materials in all related fields. Actually, the current manufacturing and net shape processing techniques for continuous fiber reinforced polymers have been deeply studied. Using the appropriate processing method, the composite material is almost ready to be used. Nevertheless, it is still needed post-manufacturing processes such as milling or drilling to satisfy certain functional and dimensional requirement; this are, holes, dimensional tolerances, a good surface quality...etc. However, due to the nature of the FRP they have a very poor machinability, obtaining good results is becoming a real challenge for nowadays engineers. The huge differences between the mechanical properties of fibers and polymeric matrices and how these ones are arranged are causing significant problems during the process and in the final workpiece. Several types of surface mechanical damage take place when machining FRP like fiber-matrix delamination, or fiber fragmentation and pullout leading to low surface quality results. Since the final results were not satisfying, lots of authors and companies have demanded to put more effort in researches related with FRP machining.

It can be considered that the main objectives of these studies are:

- Minimize the mechanical damage on the workpiece. Including internal and external damage.
- Maximize the service life of the FRP.
- Look for the optimum solution to machine FRP. It involves several variables like reducing forces, reducing machining time, maximizing tools life...

But to achieve these goals, the majority of the researches have suggested to deeply studying the mechanics of the most common machining techniques on FRP. They want to completely understand the mechanical behavior of the composite when machined. However, as it has been mentioned, the complexity of the material compared with an isotropic material, like the metal creates difficulties to understand its behavior. Additionally, the degree of difficulty of the study increases with multidirectional lay-ups FRP and complex machining methods like drilling.

Consequently, to understand the response of the FRP when machined, the majority of the researches have simplified the problem to specific conditions where uniquely the mechanical behavior is analyzed. How? [4]

- Instead of taking measurements from machining methods like a lathe, milling or drilling, the experiments were usually performed using orthogonal cutting.
- Instead of using multididirectional laminates they used unidirectional laminates, where the influences of the fiber orientation can be easily identified.
- In some studies, the velocity of the cut is relatively low compared with the industrial machining speeds for metals. This has been primarily done to avoid the induced

thermal effects. But for the interest of the reader, when these studies were performed, probably the researches of that time did not have enough resources to achieve high-speed orthogonal machining.

Performing the studies in this manner is attacking the root of the problem of FRP machining. This way researches can focus on the fracture mechanics involved in the process and analyze how the cutting parameter affect them. Basically they concentrate all their efforts in understanding the interaction between tool, fiber and matrix. In the end, the main idea is to fully understand the response of the FRP in simplified conditions to later extrapolate the conclusions to more complex case studies focused on more ambitious objectives like time reduction or optimum surface quality.

However, simplifying too much the experiments and working on the "most pure" response of the FRP to a cut may lead to reality flaws. This does not mean that the results and conclusions are incorrect, but in the more complex machining processes used in the industrial sector, there are some induced effects that are difficult to be taken into account in these simplified experiments. Therefore, from the industrial point of view, in first instance they could be considered incomplete or not too much practical. Some of these non-considered effects are:

- High-speed induced effects. When aiming time optimization in a machining processes, the industrial sector demands working at high cutting speeds. A number of authors have shown that using high cutting speeds on FRP reduces the cutting forces and a better quality is obtained [5]. Nevertheless, when high-speed machining induces thermal effects. The temperature reached in the area near the tool can be sufficiently high to melt the resin of the FRP. It can have non-desirable consequences like matrix degradation that will affect the overall mechanical performance of the machined composite [6].
- Additional effects in drilling. This is the most common machining method for FRP. Almost all the pieces need holes to be connected to other ones and form the structure. However, the large thrust forces of this machining process leads to internal delaminations, especially when the tool is drilling the last laminas. Figure 5 shows schematically what happens to the exit laminas. [7, 8]

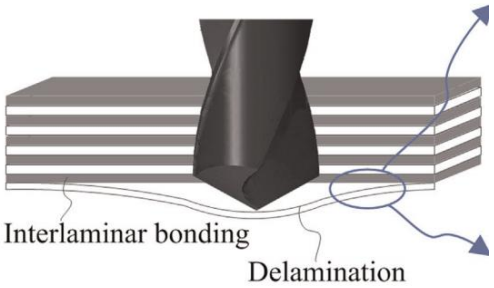

Figure 5: Scheme of induced damage by drilling [7]

- Multidirectional laminates effects. Analyzing fiber-tool interaction on unidirectional fibers leads to sound conclusions about fracture mechanics and cutting performance in

just one fiber orientation. However, usually the composites that are demanded to be machined are multidirectional laminates. The interactions between the different oriented fibers in a single laminate and the tool will lead to different cutting performance results. Therefore, to evaluate from a more practical point of view the performance of the cutting processes, multidirectional laminates are needed.

2.3. Laminate nomenclature

Generally laminas are defined according to the orientation of the fibers inside their matrix, although some researchers have adopted different defining systems. In this project, it is going to be used the traditional nomenclature which has been widely followed in most of the researches of the literature. The orientation of the fibers is measured from the horizontal axis depending on the cutting direction, as it can be seen in the following figures. It goes from 0° to 180°. From 0° to 90°, the orientation is considered positive (+) whiles the other half is defined negative (-). For example, a lamina with fibers oriented at 120° is considered as (-) 30° lamina. Figure 6 schematics the convection.

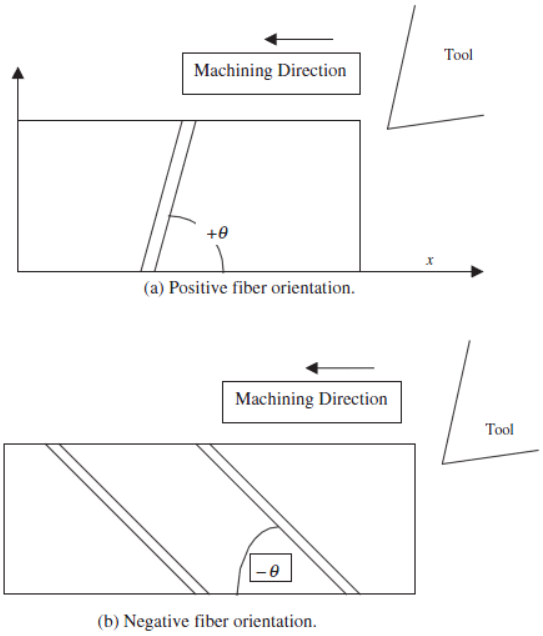

Figure 6: Fiber orientation scheme [9]

[9]

Figure 7is a schematization of the orthogonal cutting process where the cutting angles (clearance α and rake angle γ), fibers orientation angle θ, principal cutting force F_Z and thrust force F_Y are representated.

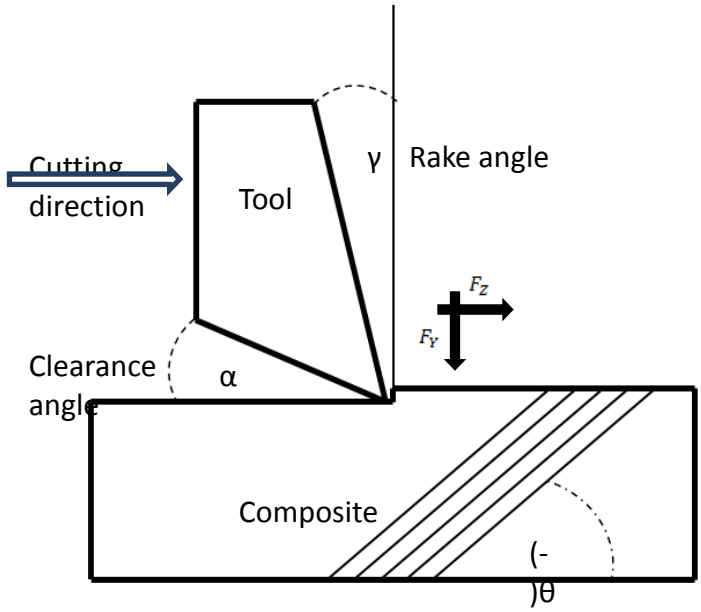

Figure 7: Cutting scheme

2.4. Parametric studies

Up-to-date, the majority of the experiments performed on orthogonal machining of FRP were aimed to understand the mechanical behavior of the laminate when being machined. In order to do so, several sensitivity analyses of different machining parameters (velocity, fiber orientation, tool geometry, depth of the cut...) have been made. The effects of these cutting parameters were collected as measurements in cutting forces or surface roughness. Therefore, each different cut had a different effect on the composite. In this way, researchers can apply their fracture mechanics theories and verify if they match with the reality. Figure 8 illustrates a typical scheme/flowchart of a parametric study in machining processes.

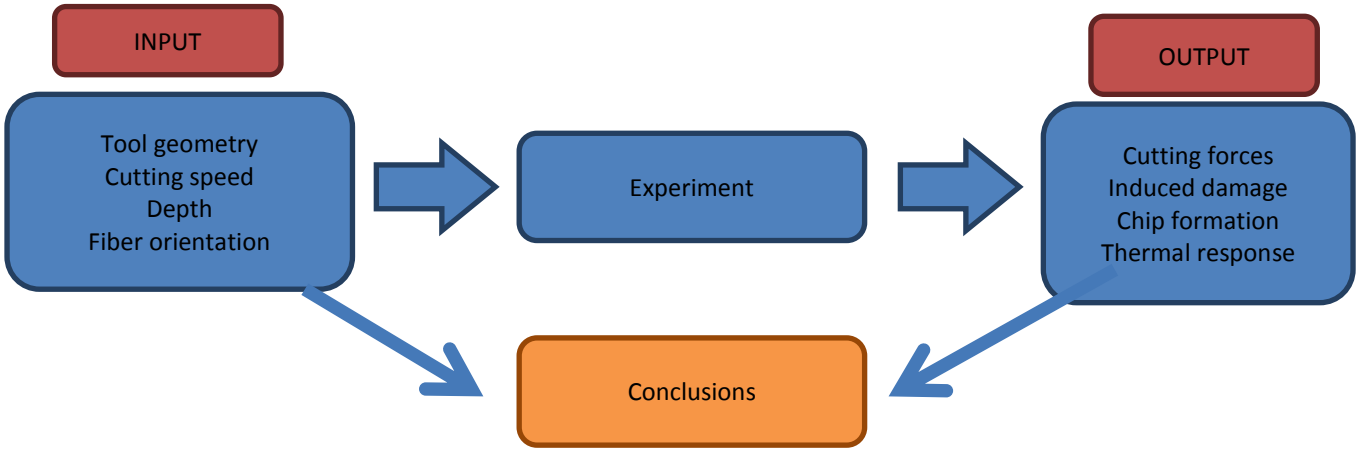

Figure 8: Conceptual parametric study scheme

2.5. Fracture mechanics in unidirectional laminates

Thanks to these parametric studies [4,5,9,10,11], we are able to understand the fracture mechanics of unidirectional FRP when orthogonally machined. The first experimental results about machining FRP were reported by Koplev *et al.* [10]. They showed that the chip formation was highly dependent on the orientation of the fibers with respect the cutting motion. Similar results and conclusions have been obtained in other researches about edge trimming in FRP. In addition to the high dependence on fiber orientations, the majority of the parametric studies indicate that most of the cutting parameters such as tool material and geometry or cutting speed have a significant influence on the chip formation, cutting forces and surface quality. The quality of the final machined result depends on lot of variables. Consequently, most of the researchers have aimed their experimental studies to collect quantitative data about orthogonal trimming. In this way, a database can be created with the purpose of assisting in the development, understanding and optimization of FRP orthogonal cutting.

Most of the authors that have studied experimentally the fracture mechanics of unidirectional FRP in orthogonal trimming have reached to the same conclusions that presented below [4,5,9,10,11].

Concerning chip formation, it has been analyzed in spite of the present difficulties in FRP trimming. For the ease, researchers have worked with unidirectional laminates at low velocities (4, 9, 14 m/min) [4]. In-situ analysis was taken to evaluate the mechanics of the process. The typical methods used were:

- Macrochip morphology study. The chip is collected and inspected at the moment with a Scanning Electron Microscope (SEM).
- Quick-stop method. The orthogonal trimming is stopped during the process and the contact zone between the composite and tool and the machined surface of the laminate are examined with a SEM to analyze how the material was fractured.

From this exhaustive analysis, it was concluded that chip formation is highly dependent on the fibers orientation. For 0° orientation (fibers aligned with the cutting direction), microbuckling was observed. The compressive tool loads along the longitudinal axis of the fibers generates a structural instability on the composite. The fracture could be considered as a mix mode of sliding and in-plane shearing loading modes. For negative fiber orientations, the chip is very discontinuous, like dust. For this reason, researchers were not able to find good records/measurements of the chip to be analyzed. For 90° and positive orientations, the chip was also very tiny but it has been observed delaminations and macro-cracks on the machined surface ahead of the tool.

To complement this in-situ analysis, researchers also recorded the cutting forces: principal and thrust. Figure 9 plots the characteristic force profile as a function of the fiber orientations.

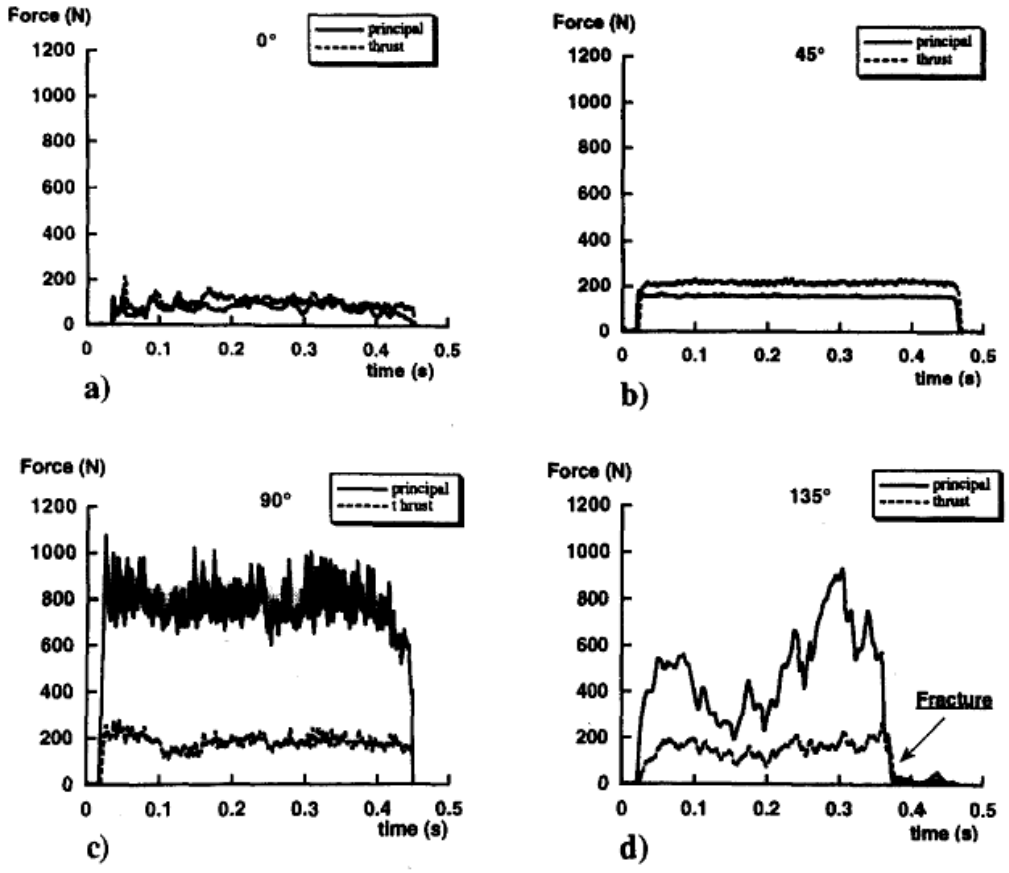

Figure 9: Force profile in unidirectional laminates trimming [4]

First of all, mention that the fiber orientation nomenclature followed by the authors of these results is the other way around. So the force records for Figure 9a and 9b corresponds to -45° and 45° respectively. From these results, it can be noted that for 0° orientations both force measurements have a high fluctuation degree. This is due to, as observed from chip formation analysis, microbuckiling. When fiber orientations are negative Figure 9b, the fluctuations have decreased significantly. The force records from 90° and positive orientations, clearly demonstrates that the fracture mechanics have different behavior.

From both analysis, in-situ chip formation and force measurements, several sound conclusion were found on the literature [4,11] concerning fracture mechanics in unidirectional FRP laminates. The schematic pictures in figure 10 will help to understand this behavior. For 0° degree oriented fibers, when microbuckling takes place, is characterized for being involved two loading modes (I and II). Loading mode I and fracture is along the fiber and matrix interface (Figure 10b). Loading mode II is due to tool's advancement bending the fibers and causing the crack perpendicular to these ones (Figure 10a). For negative fiber orientations (-30° to -75°), the chip formation mechanism is also due to the combination of two effects: compression induced shear across the longitudinal fiber axis, which breaks them, (Figure 10d) and the interfacial shearing along the fiber direction caused by the chip advancement (Figure 10d). Therefore, it can be considered that the fracture mechanism is determined by the in-

plane shear properties of the fibers. But on the other hand, mechanisms for positive fiber orientation until 90° are more complex. As it can be observed in Figure10e and Figure10f, the fracture mechanism is characterized for a perpendicular fracture to the fibers orientation, which is due to the compressive loads, and interlaminar shear fracture along the fiber-matrix interface. Generally, it is associated with fractures and out of plane displacements ahead of the tool; it is an induced macro deformation. The high fluctuation degree shown in the force measurements for this fracture mechanism (Figure 10f), is due to this discontinuous process. The tool does not break the fibers one by one; it needs to break a bunch of them at the same time.

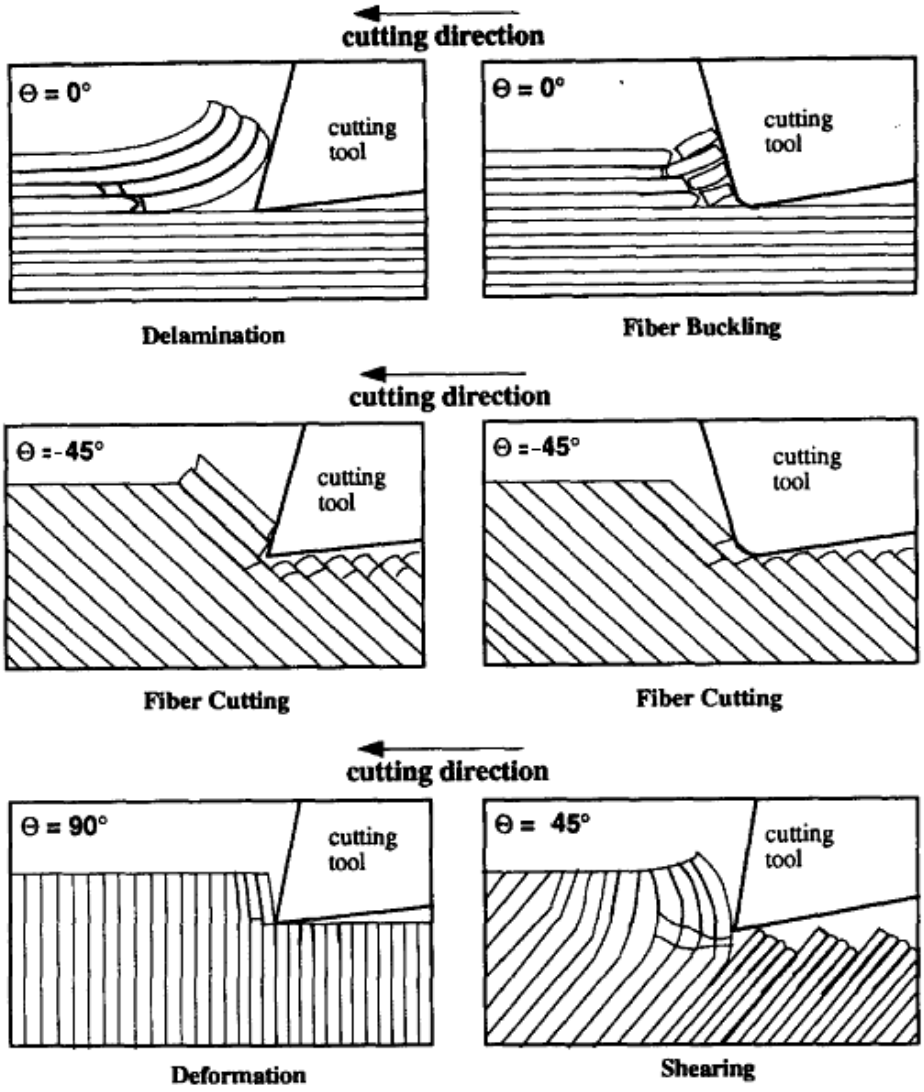

Figure 10: Cutting mechanics in othogonal unidirectional FRP laminates [4]

Influence of high speed machining on FRP

In the last decades, mechanism of material removal with conventional machining parameters in Carbon FRP using high-speed (∽200 m/min) rates have been performed [5]. All of them reported that increasing the cutting speed leads to a better surface quality and cutting force reduction.

2.6. Mechanical induced damage on orthogonal machining

Several authors [5, 9] noticed in their orthogonal trimming experiments on unidirectional FRP that there was induced internal damage that could affect the overall structural integrity of the composite; they analyzed it. For this reason, internal damage evaluation has also been under study in this project.

The typical internal damage that these authors evidenced was fiber-matrix delaminations and out of plane displacements. In order to evaluate the internal damage, Bhatnagar et al [9] used a fluorescent dye penetrant that was illuminated due to UV-ray excitation. In this way, the internal broken fibers were shown without causing any damage to the workpiece.

The results obtained, demonstrated that the maximum internal damage was for (+) positive fibers orientations, between 30° and 90°. For (-) negative orientations, the results were found to be insignificant on damage characteristics [5].

The results from Bhatnagar et al [5] on FRP were performed with a very low velocity[1] (0.5 m/min), depths of 0.1 and 0.2 mm and similar tool geometry to the one of the experiments of this project. It can be seen in Figure 11 the illuminated dye penetrant showing the internal delaminations. Note that low speed trimming requires higher cutting forces, and therefore more damage on the composite will be expected.

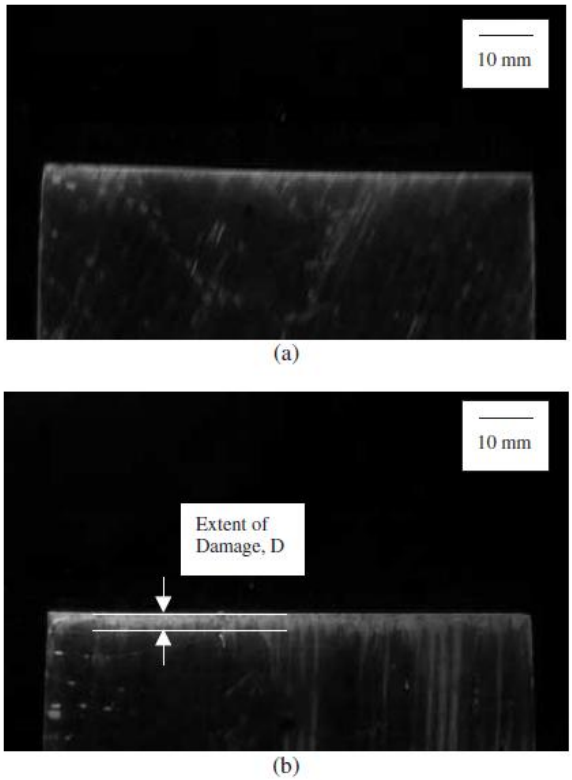

Figure 11: Induced damage in orthogonal cutting of unidirectional FRP

[1] Previously, some authors empirically showed that in FRP low speed trimming requires higher forces, and therefore will induce more damage on the composite.

Their experimental results are presented in Figure12.

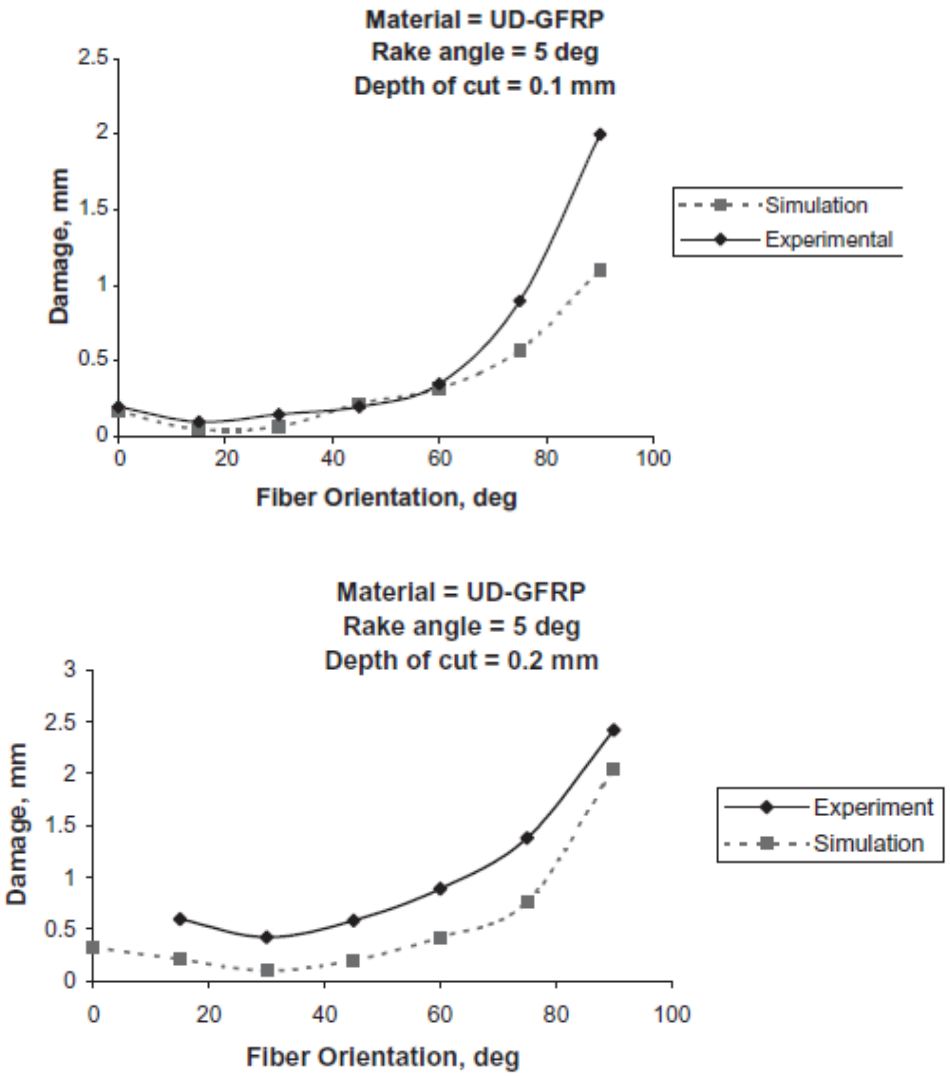

Figure 12: Induced damage extension in unidirectional laminates

Where Damage (mm) is the vertical extension of the induced damage showed by the fluorescent dye penetrant in Figure 10. These experimental results have been greatly helpful to this project because of the similar trimming conditions. They helped to take some procedure-decisions that later will be explained.

2.7. About thermal damage and monitoring on composite materials

Researchers have dedicated a great part of their time to measure temperatures in the interaction area between tool and workpiece. The following review [12] is devoted to explain

the most common techniques in machining experimental temperature measurements. These are: using thermocouples, infrared radiation techniques, and constant melting temperature point powders.

- Thermocouples. These instruments measure the temperature in a single point based on thermoelectric effect (Seedbeck-Peltier and Thomas effects) which is basically a conversion from temperature to voltage and the other way around. Generally they are used to measure temperature in the proximity of the machined surface or the in the tool. In order to do so, they are inserted and mounted in drilled holes on the target zone to take measurements. To have the best accuracy, the depth of these holes must be as close as possible to the temperature zone of interest. In the literature of metal and composite machining, they have been widely used for different for different purposes such as cutting effect temperature on the workpiece or heat flow in the tool. However, they have their limitations. Regarding their placement, they alter the heat flow and can limit the strength of the material where they are embedded. Moreover, their ability to measure the temperature transient response is not sufficiently developed [12].
- Infrared radiation techniques. These non-contact methods are based on the low and mid infrared radiation that thermographic cameras receive to estimate the temperature on zone of interest. The science that studies these methods is called infrared imaging thermography. It can be distinguished the instruments to measure a field temperature (Infrared radiation cameras) and instruments to measure temperature on a single point (Infrared pyrometers). They have several advantages over the other methods. The fact that they are non-contact methods allows taking measurement in difficult are without damaging the specimen. They are very suitable for high-speed machining processes where significantly high temperatures are reached in very small areas. Nevertheless, these advantages have a price. Taking accurate measurements with this method is quite complex, there are lot of factors affecting the radiation received by the instrument. For instance, the simply positioning of the camera can significantly affect the temperature measurements of the machining process or the wavelength or the emissivity… [12]. Therefore, all of these factors have to be carefully evaluated. Later we will go in detail of infrared thermography since it has been the method used in this project.
- Constant melting temperature point powder. These methods are generally used to evaluate temperature gradients in the tool's rake face. The temperature is estimating by watching the isothermal line that separates the melted powder from the unmelted. Using powder with different melting points, the gradient can be elaborated. However, this method takes too much time to be completed [12].

The complexity of the machining process makes very difficult to measure temperatures experimentally, and present even more difficulties when the workpiece to be machined is a composite material. For this reason, the literature about monitoring temperature in composite machining is not very extent. Nevertheless, more knowledge about thermal effect when machining composites is needed to ensure that the structural integrity of the composite is preserved. Currently, in the industrial sector, the most common machining process performed

on composite material is drilling. And more specifically, in the aeronautical field drilling achieves cutting speeds above 200m/min (High-speed drilling). As previously mentioned, this process can induce severe mechanical damage, but also the high-speed cutting induces very high temperature in the contact zone.

Guillaume Mullier and Jean François Chatelain worked on the induced thermal damage on trimming Carbon FRP [6]. In their study, they explain that temperatures above the glass-transition temperature[2] (T_g) of the resin can affect detrimentally the mechanical performance of the workpiece. The responsible for this undesirable effect is, unlike metals, the poor thermal conductivity of FRP. When they are trimmed, the heat produced by the cut is not dissipated over the entire workpiece. But it remains concentrated in the small machined zone causing a significant elevation of the temperatures. Achieving such temperature above T_g causes a degradation of the matrix in the cutting area. Additionally, this effect is aggravated with several cutting parameters such as increasing cutting speed or feed rate. But on the other hand, other researches [6] show that cutting temperatures above T_g do not significantly induced thermal damage on the specimen.

In metal cutting, a refrigerant fluid would be used to relieve these induced thermal effects. But, in the aeronautical field, the use of refrigerant fluid is considered damaging for composite materials, in particular for the resin properties. For this reason, drilling operations are dry, and consequently controlling the machining temperatures is of crucial importance regarding the entire composite integrity [13]. Even though up-to-date, we still do not know to what extent the mechanical performance reduction in a localized area affects the overall mechanical strength of the workpiece. This demonstrates how complex is the heat transfer in the cutting zone of FRP.

2.8. About infrared thermography [14]

Physics tells us that all objects above the absolute zero temperature emit electromagnetic radiation. But, the intensity of this radiation depends on the nature of the object. By definition, a blackbody is an object that absorbs 100% of the electromagnetic radiation received from every wavelength. By the same means, it emits energy at the maximum potential rate per unit area and unit wavelength at a given temperature. The interesting feature of these ideal radiators is that there exists a physical law called *Planck's law* which essentially relates the temperature of the blackbody with the energy that is radiating at a given wavelength. The following expression will explain it better:

$$I(\lambda, T) = \frac{2hc^2}{\lambda^5} \frac{1}{e^{\frac{hc}{\lambda kT}} - 1}$$

Where λ is the wavelength, c the speed of light, h and k are the Planck's and Boltzmann constants respectively and T the absolute temperature. The last variable is the spectral

[2] Characterize the range of temperatures over which a material passes from a "hard and brittle" state to a viscous state.

radiance, I, which is the energy per unit time per unit area per unit wavelength radiated by a surface at given angle and absolute temperature [K]. Figure13 shows the relationship of these 3 variables and the typical wavelength regions (low and mid infrared) where the thermographic cameras operate. Basically, they measure the intensity of the electromagnetic radiation in a range of wavelengths during a period of time called *integration time.*

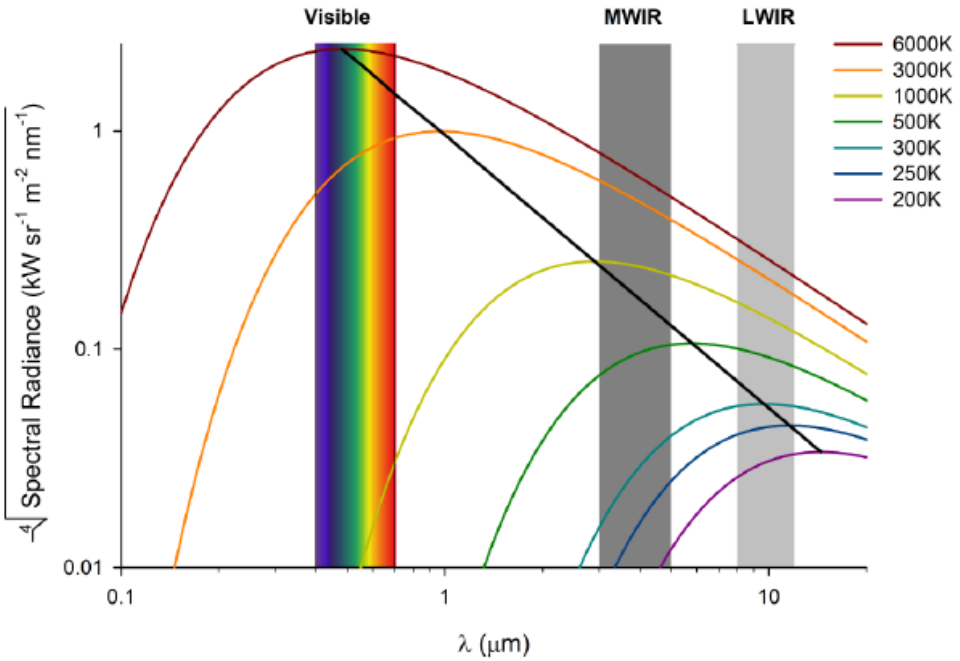

Figure 13: Planck's Law for different wave lengths and temperatures[14]

In the thermography science, there is also another equation of great importance, *Kirschoff's radiation law*. Basically summarizes the complex mechanisms radiative heat transfer in a body. It states in terms of heat flux that at a given wavelength, incident radiation is either absorbed, transmitted or reflected: $\phi_{incident} = \phi_{absoberd} + \phi_{transmitted} + \phi_{reflected}$. Normalized with the incident radiative heat flux, we obtain:

$$\alpha + \tau + \rho = 1$$

Where α, τ and ρ are the absorptivity, transmittivity and reflective of a body; they are physical properties that characterize an object. Since no radiant flux occurs through the bodies that we are going to study in this project τ can be set to 0. Consequently all the incident radiation is either absorbed or reflected.

If we take a body in thermodynamic equilibrium, all the radiation it has absorbed, must be emitted, otherwise the positive net balance of energy inside the body would increase its temperature, something that cannot occur because it violates the second law of thermodynamics. Therefore we arrive to the following Kirschoff's expression:

$$\varepsilon + \rho = 1$$

Where ε is the emissivity, a fundamental parameter when trying to figure out the true temperature of a body by means of infrared thermography. An ideal blackbody has an

emissivity $\varepsilon = 1$, it means that all the incident energy will be absorbed and emitted. Since no physical body can radiate more energy than a black body, the emissivity can also be understood as the ratio between the radiance flux of a body and the one of a blackbody at the same temperature; is like an efficiency parameter. Moreover, the emissivity is a property of the material that depends on lot of factors like the wavelength, the temperature or simply the morphology of the surface of the body. All of them must be taken into account when processing the experimental measurements.

Thermographic cameras have sensor that are capable of measuring the electromagnetic radiation of a given wavelength spectrum. However, all this infrared energy is not uniquely coming from the object of interest. There are multiple radiation sources in the environment affecting the sensors measurements. Therefore the signal arriving to the camera can be decomposed in the following way:

$$s = s_{body} + s_{reflections} + s_{atmoshphere}$$

Where $s_{reflections}$ is the reflected radiation from other bodies around our object of interest, and $s_{atmoshphere}$ is the radiation corresponding to atmospheric gasses. The most common way to deal with these two terms is through an in-situ empirical calibration of the camera that will be explained in section 3.7. Once s_{body} is known, we can apply *Planck's law* but taking into account the emissivity in the spectral radiance to estimate the true temperature of the object.

This process might seem easy, but when trying to estimate true temperatures in a machining process, several features must be taken into account [15]:

- Workpiece movement. Some difficulties regarding reflections and emissivity's uniformity can appear when measuring the temperature of the workpiece. But, it is also of great importance to adjust the camera for our experiment conditions; we must put special attention to the characteristic speed of the workpice's movement. As previously mentioned, the camera measures electromagnetic radiation's intensity over the integration time. If we are focused on a stationary object, each pixel would collect the spectral radiance of a given location of that object over a period of time. But when dealing with moving objects, *motion blur* can occur. This happens when the object moves a distance larger than the corresponding to 1 pixel during the integration time. Consequently, the radiation corresponding to a given location would be distributed along several pixels, giving rise to incorrect temperature measurements.
- Emissivity. Materials have different emissivity across the wavelength and temperature. Therefore, we have to carefully select the emissivity value for our body of interest. Moreover, this value is also influenced by the surface texture and oxide layers, resulting in a non-uniform emissivity value over the surface of the body. This effect is significantly enhanced in the material trimming processes because the machined surface and edges are drastically modified (and even more in FRP trimming). Since the emissivity is unknown in the machined zone, the zones where the temperature can be measured are limited.
- Chip. The chip temperature measurements are the most difficult ones to obtain, and even more in FRP trimming where the chip is almost dust. The combination of high-

speed movements with small chip size and a extremely non-uniform temperature map, makes the worst conditions to take measurements. Moreover, the significant deformations in the chip and its discontinuous morphology cause uncertain emissivity values. Additionally, the effect of temperatures discontinuities leads to incorrect measurements. Basically because the camera do not have enough resolution and the pixel takes the mean value of a given location where the high temperature of the chip can coexist with the ambient temperature. For these reasons, measuring chip's temperature in FRP machining with an infrared thermograhic camera is not recommended.

These features significantly limit the zones where the temperature can be measured in a machining process. The areas of interest where reliable measurements can be taken would be the zones in the workpiece where the emissivity is known and uniform, and the cutting tool.

2.9. Non-destructive damage inspections

Due to the different damage that composite materials can suffer, such as internal delaminations, determining if the laminate is still valid or not without damaging it is becoming a great challenge for the nowadays researchers. The simplest and most typical method is the visual/external inspection. It is generally used to evaluate surface quality and external damages, like for example, external delaminations when drilling (typically the thrust force tends to separate the last lamina of the composite). The usual instruments are profilometers to evaluate surface quality and microscopes to see if there is external fiber pull-out or kind of anomaly. But also, researchers have come up with interesting non-destructive inspections to measure and evaluate internal defects in FRP. A review of some of these techniques is presented in the following paragraphs:

- UV Dye penetrant. [9,16]. Firstly, UV dye is sprayed all over the workpiece. Later the excess is removed and only remains the dye inside the specimen that when exposed to UV light, it shows the internal defects.

- Pulse-echo UT [16]. Is based on the propagation of ultrasonic waves through the workpiece. The probe emits and receives the wave, but if there is any defect inside the specimen, this will show up as an anomaly in the received signal.
- Infrared thermography [17, 18]. This method is based on how the workpiece dissipates the thermal energy. Firstly, it is warmed up till a known temperature and later the dissipation of energy is monitored with an infrared thermographic camera. Internal defects will show as discontinuities in the thermal dissipation.

2.10. Numerical simulations

Nowadays we are lucky to count on high computation power. For this reason, researchers are directing their efforts to numerical simulations of FRP machining. Making use of this powerful tool, they are trying to predict the behavior of the laminates when trimmed as well as the

induced mechanical and thermal damage. In this way, an estimation of the final result in terms of quality and overall mechanical performance can be made as a function of the machining parameters. Obviously, these virtual studies are quite useful to optimize the machining process of FRP in the industrial sector. This new way of working bodes well for the machining of FRP researches. Nevertheless, all these models must be previously verified with experimental results. So, any kind of empirical data about FRP machining is welcomed by the science.

Chapter 3: Methodology

3.1. Description of the experimental methodology

In a first instance, the experimental methodology was aimed to study the overall orthogonal machining process of FRP, but as in every experimental research, resources are limited, hypothesis fail and non-expected problems arises. In this study, several orthogonal cuts on FRP have been performed varying the most important cutting parameters (cutting speed, depth of the cut and tool). During the process, forces corresponding to the considered cutting condition were measured because they provide relevant information concerning machining quality. Moreover, the test were monitored with a high-speed camera and an infrared thermographic camera with the purpose of obtaining results about chip formation and heat transfer mechanism during the orthogonal trimming. Later, the overall induced damage, external and internal, was evaluated on the tool and workpiece, two critical factors concerning industrial productivity. For the external damage a microscope was used while for the internal damage a non-destructive technique was utilized. Since not all the results were conclusive, during the project, some objectives were updated.

3.2. Experimental set-up

In order to satisfy the project objectives, the experiments must be properly settled. The following instruments were used:

- Orthgonal cutting machine. This machine was built by another student. It has exceptional capabilities to perform experimental machining studies because it achieves a wide range of constant cutting speeds. It is connected to a computer where the displacement of the workpiece along the rail is controlled. But, the drawback of this orthogonal cutting machine is that the feed of the cut is controlled manually. This is, every time a cut was performed, the tool was lifted manually to allow the workpiece moves back without being damaged. Obviously, these height movements of the tool needed to be regulated. In order to do so, the machine has a micrometer (error = ± 0.005mm) installed. It is also equipped with a *Nilfisk* industrial vacuum of 2 KW of power to remove the hazardous dust produced by the cut of FRP. Concerning security, this element is very important because when machining FRP, the tiny broken fibers hidden in the dust can be easily inhaled. And evidently, these particles are harmful for human's health.
- Dynamometer.(Figure14) To measure the cutting forces, the orthogonal cutting machine was equipped with a dynamometer Kistler Model 9257B which was able to measure forces (F_x, F_y, F_z) and moments (M_x, M_y, M_z), although for the purpose of this project only forces measurements were needed. The technical characteristics of the dynamometer are summarized in the Table 2 [19]:

Threshold	< 0,01 [N]
Linearity, all ranges	≤ ±1%
Hysteresis, al ranges	≤±0.5%
Cross talk	≤±2%

Table 2: Dynamomiter parameters

Figure 14: Dynamometer Kistler Model 9257B

Note that the force measurements will depend on how the dynamometer is oriented. The output of the dynamometer is then processed by a charge amplifier Type 5070 from Kistler. Later the signal is sampled, displayed and collected in a computer with a DAQ. The DAQ used was Adquisition DIgital I/O, model-3100 from Keithley. In the computer, the software used to sample the signal (at a 100 Hz sampling frequency) and record the data was *quickDATA.*

- High-speed camera. The orthogonal cut was monitored with the high-speed camera model MINI UX50 (Photron make). With this instrument, chip formation and the overall performance of the process could be analyzed. It was set to record at a frequency of 250 Hz (250 frames per second).
- Infrared thermographic camera. The camera used to estimate the temperature field was a FLIR SC4000 IR camera that has a noise equivalent temperature difference (NETD) of about 18 mK.
- Microscope. It allows to take digital pictures focusing in several planes at the same time. This tool was needed because the pulled-out fibers deteriorate the images.

For a better understanding of how all these instruments were arranged ,the overall set-up is shown in the Figure 15.

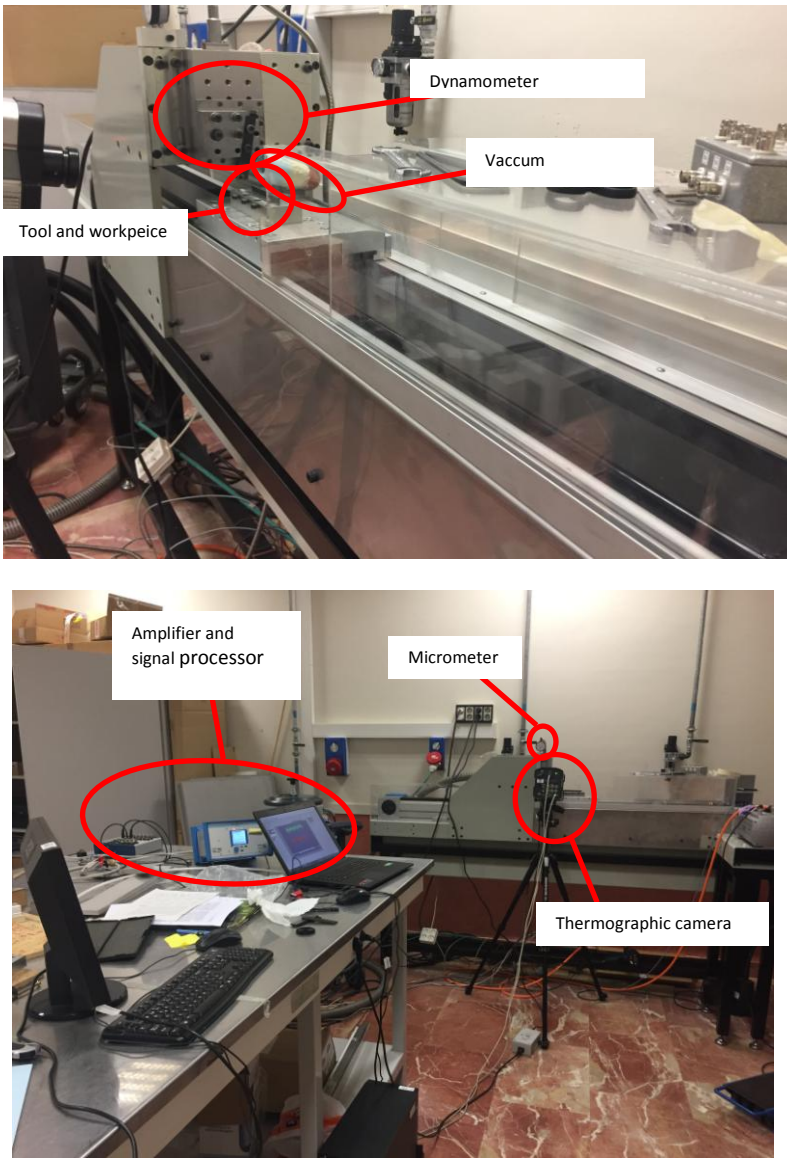

Figure 15: Experimental set up

3.3. Material tested

The FRP tested was Carbon Epoxy IM7 MTM-45-1 which was made by a company called *Advanced Composite Group.* The material is a laminate made up of carbon fiber IM7 embedded in epoxy matrix MTM45. The laminated is composed of 16 laminas oriented in 0°/90°/±45°. The workpiece has an approximate thickness of 2.2 mm. The mechanical properties of the laminate were provided by the same company and are summarized in Table3.

Carbon Epoxy IM7 MTM-45-1	
Longitudinal modulus, E_1 (GPa)	173
Transverse modulus, E_2 (GPa)	7.36
In-plane shear modulus, G_{12} (GPa)	3.89
Major Poisson's ratio, nu_{21}	0.33
Longitudinal tensile strength, X_T (MPa)	2998
Longitudinal compressive strength, X_c (MPa)	1414
Transverse tensile strength, Y_T (MPa)	37
Transverse compressive strength, Y_c (MPa)	169
In-plane shear strength, S_{12} (MPa)	120

Table 3: Mechanical properties of the workpiece material

To perform the experiments, 6 laminates were available. As it can be appreciated, it is a multidirectional laminate. Therefore, this is a perfect workpiece material to perform FRP machining experiments under industrial conditions.

In order to perform the temperature measurements, the emissivity of this laminate must be known. Since no surface emissivity measurements were made, a value of $\varepsilon = 0.8$ has been assumed for the FRP laminate. This surface emissivity value has been obtained from the total hemispherical emissivity measured in a similar carbon/epoxy material, typically used in the aeronautical industry, from research in FRP thermal behavior [20].

3.4. Tools

To perform the parametric study, two different tools were used with their corresponding toolholder:

- CCMT09T304-F2 TS2000. Is a carbide/cermet with a 7° clearance angle (α) and 0° rake angle (γ). It was held by SCACL1616H09 tool holder. As it can be appreciated in Figure16 the tool has two aggressive cutting edges, but only *side B* will be used during the tests. From now on, this tool will be referred as "***tool1"***.

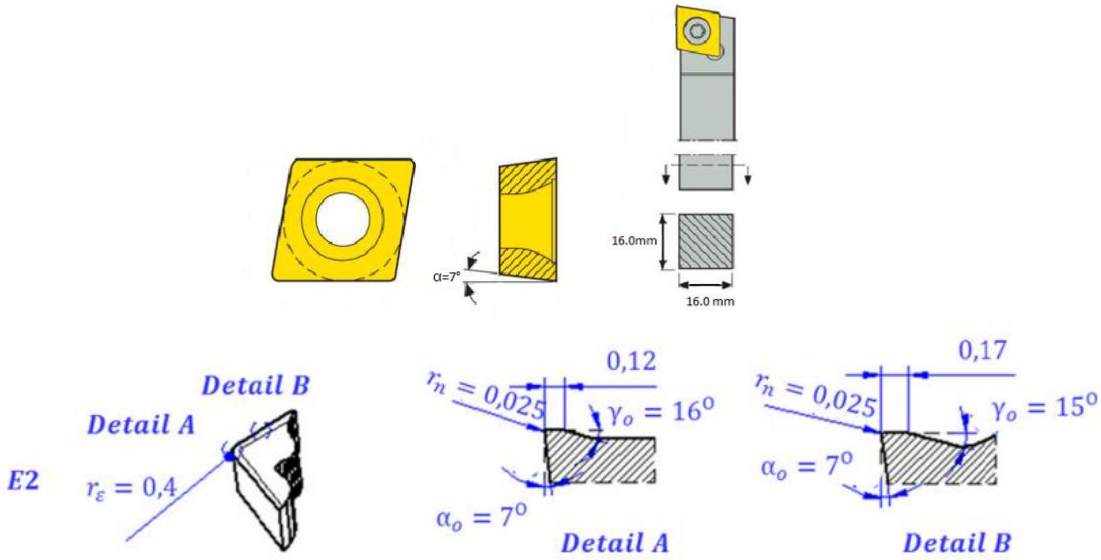

Figure 16: *Tool 1* (CCMT09T304-F2 TS2000) scheme [21]

- TCMW 16 T3 08 H13A (Figure17). Is also a carbide/cermet with a 7° clearance angle (α) and 0° rake angle (γ). It was held by STGCR 1616H 16 tool holder. The cutting edge of this tool is not aggressive; it can be observed that forms a 90° angle. From now on, this tool will be referred as "***tool2***".

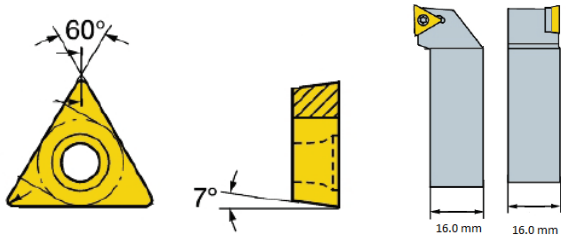

Figure 17: *Tool 2* (TCMW 16 T3 08 H13A) scheme

3.5. Selection of the cutting conditions

The cutting condition selected to perform the parametric study are presented in Table4. There are some reasons behind these choices and all of them are based on the same idea, to study FRP machining from an industrial point of view. For this reason, typical tool geometries and material have been selected. Moreover, since the common industrial machining processes, like drilling [5], are high-speed process, a cutting speed of 200 m/min has been included. In this way, it can be analyzed if the fracture mechanics and heat transfer mechanisms involved are different from low speed cutting conditions. A low speed cutting condition has also been included with purpose of having a reference to compare and verify the results of this project with the literature. Additionally, to avoid severe damage on the workpiece (excessive external delaminations that deteriorates the surface quality and the overall mechanical performance of

the laminate) no more than 0.2mm feed has been selected. It has also been decided that all the orthogonal cutting operations will be perform under dry conditions to satisfy the industrial requirements [13].

Tool	Tool1 and Tool2
Cutting speed	1, 50 and 200 m/min
Depth of the cut	0.05, 0.1 and 0.2 mm

Table 4: Experimental cutting parameters

3.6. Force measurements and processing

The force measurements depend on the orientation of the dynamometer. For all the tests, the principal force coincide with F_z and the thrust force with F_y. In reality, what the computer is receiving is an output voltage signal that will be transformed into force signal by multiplying it by the corresponding summation. The summation depends on how the amplifier is configured to avoid saturation. The following summations were applied for the two different rounds:

	Round 1 (*tool1*)	**Round 2 (*tool2*)**
$\boldsymbol{F_{principal}}$	200.0 [N/V]	400.0[N/V]
$\boldsymbol{F_{thrust}}$	40.0[N/V]	100.0[N/V]

Table 5: Force signal summation

The most reliable signals were taken to compute the mean force. If there was more than one reliable signal for a given test, the mean of the forces computed from the signals has been considered as the estimated value for that test. Note that sometimes the signals are a little bit displaced from the 0 reference value. This error was corrected by computing the mean value of the signal before the cut was performed.

3.7. Infrared thermographic calibration

Before talking about the calibration of the camera, it is important to remember that the camera measures all the electromagnetic radiation present in the laboratory. These measurements depend a lot on factor that can be controlled and others that cannot be so easily controlled. Within these factors we can include the ambient temperature of the laboratory or simply the position/orientation of the camera to take the measurements. For this reason, all the test measurements have been taken in the same conditions, such a way that all these factors affect equally the collected data. This means that the measurements during the shortest period of time and without moving the camera from its position.

The thermographic camera needs to be adjusted prior the tests according to the nature of the experiments. It can be considered that the experiments are characterized for its high-speed movement and a discontinuous temperature map with high peak values. For this reason there must be a balance between the integration time of the camera and the frequency at which the

camera is collecting the data. What does this mean? The integration time is equivalent to the exposition time in an optical camera. It is the time that the sensor is exposed to the electromagnetic radiation. However, if this time is too large the image will be saturated. So, this parameter is selected according to an estimation of the temperature scale present in the test. But at the same time, it will limit the frequency at which the camera can record the video. This might create problems with related with the previously mentioned *blur* effect. If the frequency is to low, the workpiece will move more than a pixel, leading to incorrect measurements. In the end, the limiting pre-test calibration factor was the speed of the workpiece. A 1500 Hz was selected, but it was only possible at the lowest resolution (128x128). The price to pay was saturation in the chip. But this consequence is of less relevance because due to its nature, taking correct temperature measurements in the chip of machined FRP is very difficult and was not considered under study.

Once the camera has measured the intensity of the radiation, it must be in-situ calibrated (figure 19) to deal with the additional radiations from reflects and atmosphere. This empirical calibration consisted on heating a blackbody (assumed to be of emissivity $\varepsilon = 1$) to a known temperature and measuring the radiation received. The process is repeated for several temperatures and later a fitting curve relating temperature and spectral radiance (similar to *Planck's law*) is obtained. Note that this empirical "*Planck's law*" is only valid for the measurements taken in the same conditions (recalling the importance of the external factor explained to paragraphs above). The empirical function (figure 19) is obtained from:

$$I = \frac{\lambda_1}{e^{\frac{\lambda_2}{T}} - \lambda_3} + \lambda_4$$

λ_1	λ_2	λ_3	λ_4
5.833x10^6	2.889x10^3	8.815x10	1.982x10^3

Table 6: Empirical calibration constants obtained

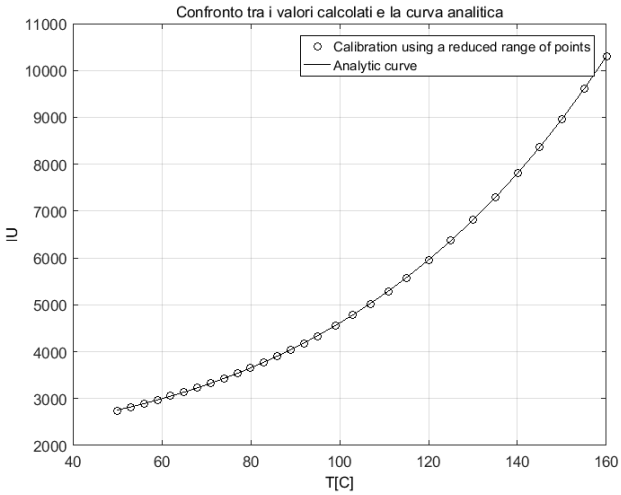

Figure 19: Experimental calibration curve

Figure 18: In-situ calibration

Note that this equation is only valid for blackbodies. To measure the temperature of a non-blackbody, the received spectral radiance, I, must be divided by the emissivity of the object. Finally, through this relation the temperature of the workpiece in areas of know emissivity, could be estimated.

3.8. Cutting procedure

Only 6 laminates were available to perform the 18 test (plus one failed test). The workpieces were wide enough to perform one test on each long edge of the workpiece. In this way, the material resources can be optimized.

Firstly, the workpiece is clamped to the orthogonal machine and the depth of the cut and cutting speed are adjusted. Several cuts without varying cutting conditions are performed, meanwhile force measurements are taken. This process is repeated until the force signal and a visual inspection demonstrate that the trimming process is uniform for the whole edge. In other words, that the force signal is stabilized. Figure20 shows the thrust for signal for a uniform trimming (2^{nd} cut) and non-uniform cut (1^{st} cut); it can be observed how the 1^{st} cut signal is slightly decreasing in the end. No less than 3 cuts were needed. In this way, it is assured that the induced mechanical damage is uniformly distributed and corresponds to several cuts; like in an industrial machining process. Once it is guaranteed that the following cut will be in the appropriate conditions, the infrared thermographic camera and the high-speed camera are ready to monitor the last test. When the entire set of tests for the first tool were launched (this would be the first round), the workpieces were subjected to damage inspection with a microscope and thermographic method (explained in section 3.10).

Since there were not enough laminates, the second round of test which corresponds to *tool2* was performed with the same specimens. The cutting conditions applied in a given workpiece's edge were the same as for the first round. This is, the machined edge at 200 m/min and feed = 0.2 mm with *tool1* was trimmed with the same cutting speed and depth but with *tool2* instead. In this way, the possible differences in fracture mechanisms between tests were minimized. Several cuts before monitoring with the infrared thermographic camera were performed; until the forces were stabilized. After completing all these cuts, it has been considered that the present internal damage was only induced by *tool2.*

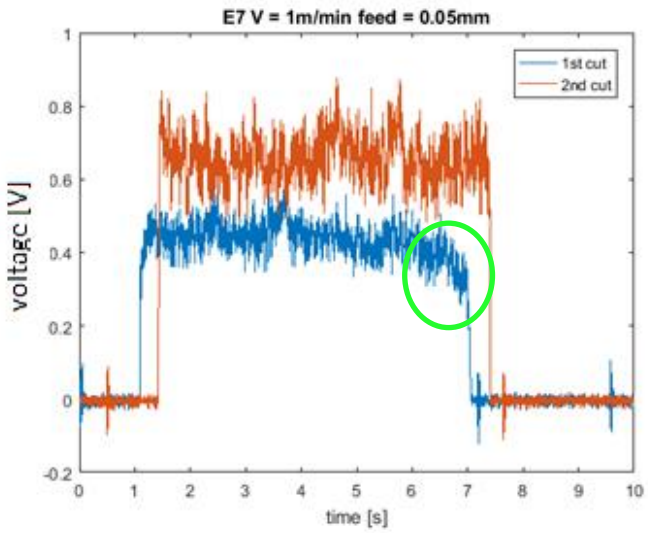

Figure 20: Force signal

Although it took 4 full-days to take all the measurements, the overall experimental time was around 1 week. This was due to the wide variety of problems that can be found when preparing the experiments. Moreover, the first results obtained concerning tool's damage were not satisfying and obliged to look for new objectives.

3.9. Temperature profiles while machining

Temperature was monitored during the machining process. For reason previously explained, the temperature analysis was limited to uniquely the workpiece. In the temperature field image, the contact point between tool and workpiece was taken as reference point. From that point, temperature measurements were taken along a 10 mm line in the cutting direction (X axis). At the end of this line, temperatures were also measured along a 5 mm vertical line. In order to do so, image pixel distances have been corrected with known distance in the image. In this way, temperature is always measured along real distances and results can be properly compared. Additionally, profiles were taken in the last frames of the cut so the profiles are temperature field are properly developed. Figure21 shows a characteristic temperature field during the machining process and the lines where temperature profiles were evaluated.

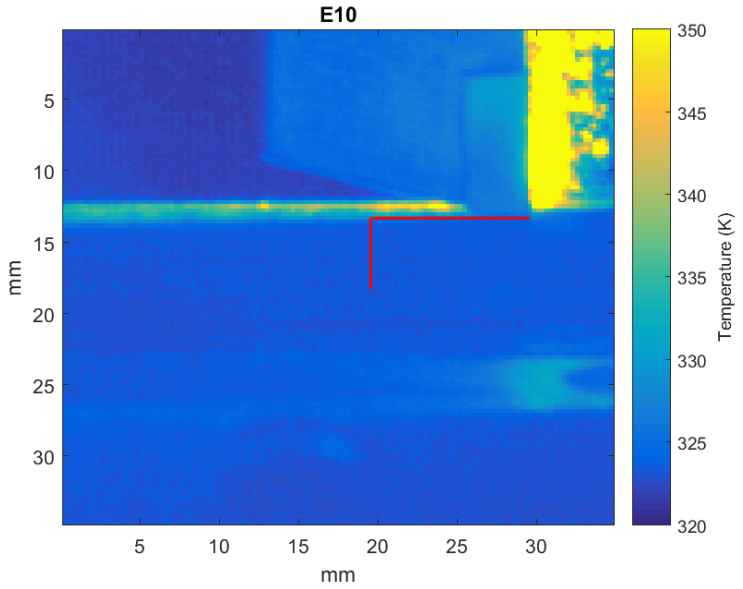

Figure 21: Temperature field image of the machining process. Test E10: Vc = 50m/min depth = 0.05mm

3.10. Non-destructive damage inspection procedure

To evaluate the quality of the orthogonal machining process, induced damage on tool and workpiece were studied. From an industrial point of view, tool's life is a determinant factor regarding productivity. Several photographs of the tool were taken with microscope to observe how it was deteriorated. However, the inconclusive results from the first round of experiments lead to focus more on workpiece's induced damage. In this way, an integrated external and internal damage study was accomplished.

External damage inspection was performed with a microscope and residual burr measurements were taken Figure22 The methodology followed to quantify the internal damage in the workpiece was based on thermographic non-destructive inspection. The workpiece was heat up to 85°C during 35 s and later the heat dissipation process was monitored during 15 s. The main idea of this method is to process the temperature measurements obtained with the purpose of looking for heat dissipation anomalies that evidences internal damages and defects. The methodology followed allowed to measure the depth of the internal defect.

Image tests	E1 to E10	E11 to E19 and undamaged test
Pixel length [mm]	0.2526	0.2471

Table 7: Temperature image pixel length for internal damaged workpiece

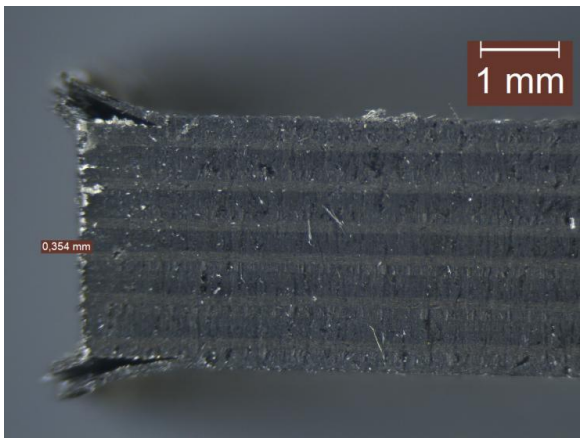

Figure 22: Front view of workpiece .Test E17: Vc = 200m/min, depth = 0.2mm

To accurately quantify the internal damage, firstly the location of the machined surface must be properly estimated in the temperature field image of the damaged workpiece Figure23. This is achieved by measuring the length of the burr on each test with the microscope and introducing it in the image. Note that each image has a characteristic pixel length to transform real dimensions into pixels. Table7 presents the pixel length of each image test.

Later, from the estimated location of the machined surface horizontal lines along each pixel row are drawn downwards, like the red and green lines of Figure23. Each of these lines corresponds to a pixel row and therefore marks a distance (in pixels) from the trimmed surface. Obviously, the pixel distance can be transformed into real distance (in mm) with the pixel length.

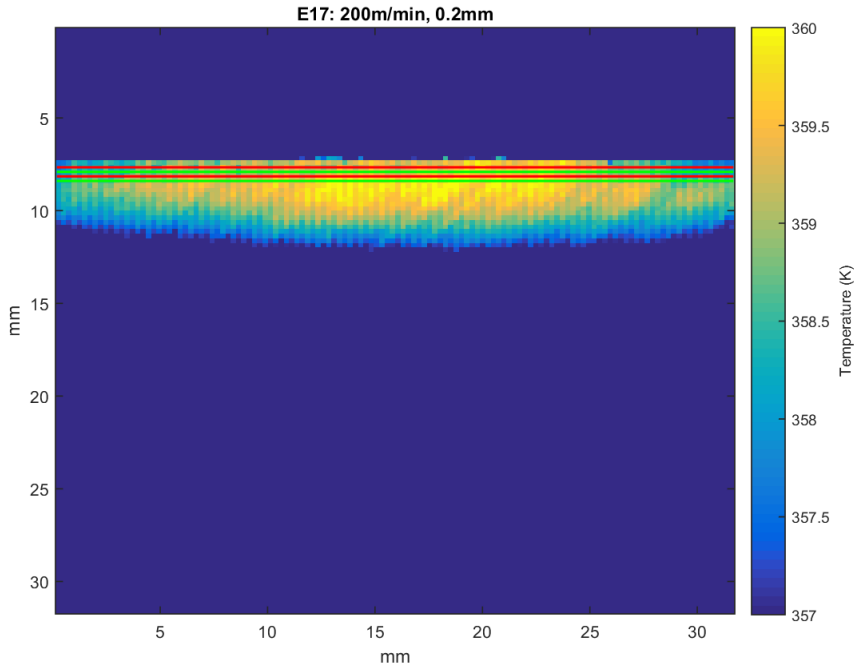

Figure 23: Temperaure field of workpiece. Test 17

In each of these lines, the temperature evolution is going to be plotted and analyzed looking for heat dissipation anomalies like in Figure24.

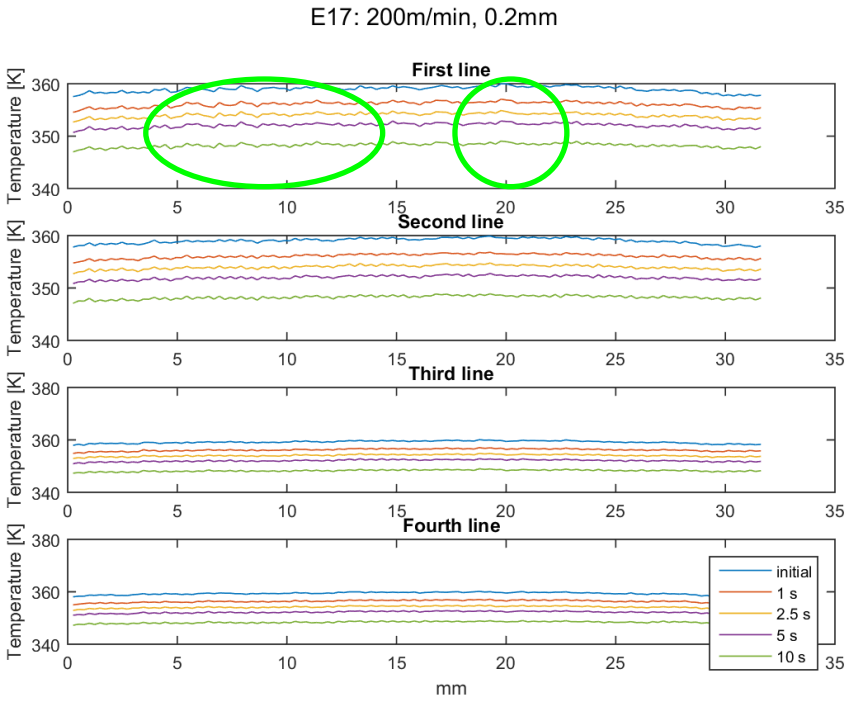

Figure 24: Temperature profiles of test 17

In this way, knowing until which line (or pixel row) are the heat dissipation anomalies present, allow us to quantify the depth of the internal damage.

Chapter 4: Results & discussions

The following content shows the most significant results obtained; the intermediate results are attached in the annexes.

4.1. Chip formation

The chip formation was monitored with the high-speed camera, in a similar way to metal cutting. However, the formation mechanism is so discontinuous that only dust mixed with broken fibers could be observed and no sound conclusions could be drawn. Moreover, the morphology of this kind of chip impedes to take appropriate temperature measurements, limiting the field of study of this project. Additionally, the small broken fibers released in the dust cloud can be easily breathed and are harmful for human's health. Figure25 shows a photogram of the trimming process for maxim feed and cutting speed.

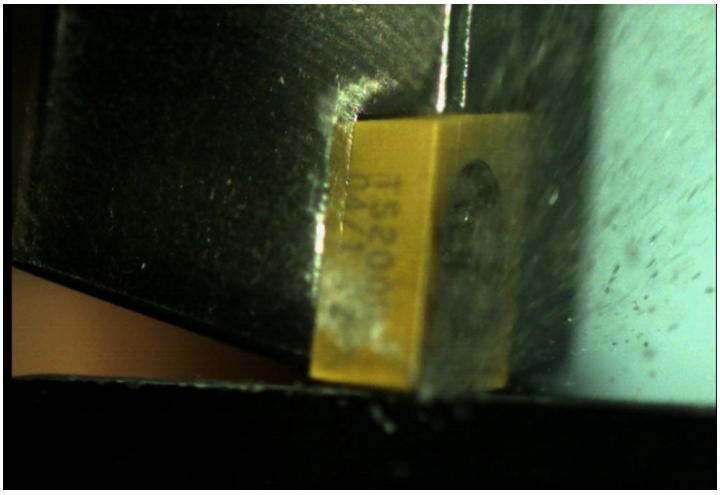

Figure 25: Chip formation image

4.2. Tool's damage

It was thought that some kind of damage could be observed on tool's cutting edge and relate it with the corresponding fiber orientations of each lamina (like in paper [22]). However, both tool's were so strong that they did not suffer any kind damage. As it can be seen in Figure26, no damage is observed for the most aggressive tool.

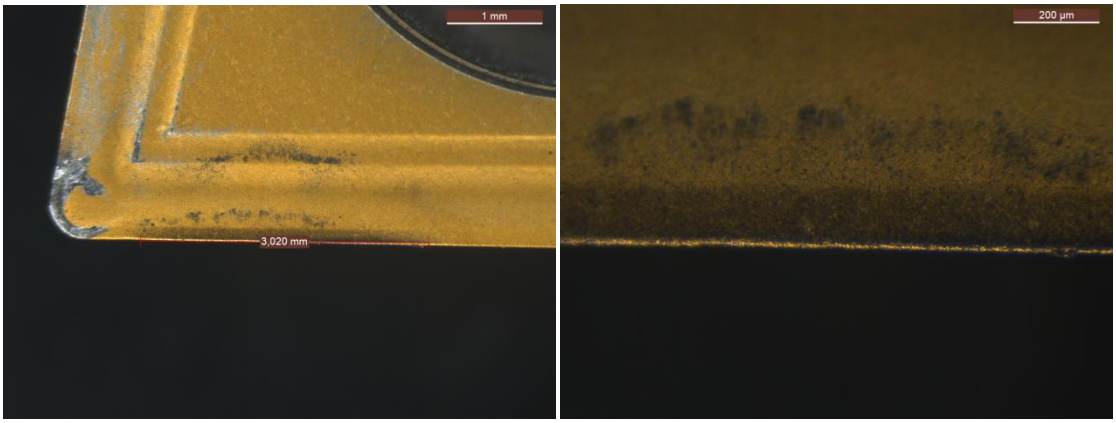

Figure 26: *Tool 1* damage

4.3. Forces

Principal and thrust cutting forces were measured. Some examples of the force profiles for different cutting speeds are presented below in Figures(27-29). As it can be observed, large magnitude and high frequency fluctuations in the signal are present. The behavior of these force profiles coincide with the results obtained by *D.H.Wang* and *M.Ramulu* [22] for similar cutting conditions on multidirectional FRP laminates. If we take a look to the literature about unidirectional FRP machining [4] or just to section 2.5, we will understand the nature of these high frequency fluctuations. They are characteristic of the 90° and positive (+) fiber orientations force signals measured in unidirectional laminates. However, the fracture mechanics of the multidirectional laminates does not need to be the same. Indeed, it must be considered that the multidirectional lay-up absolutely changes the rules of the game. The complex interactions between the different laminas orientations and the tool lead to synergy effects on induced damage. Basically that multidirectional laminates do not suffer as much as unidirectional laminates when machined. Note that the nature of these interactions is not under study in this project but their overall results on the workpiece.

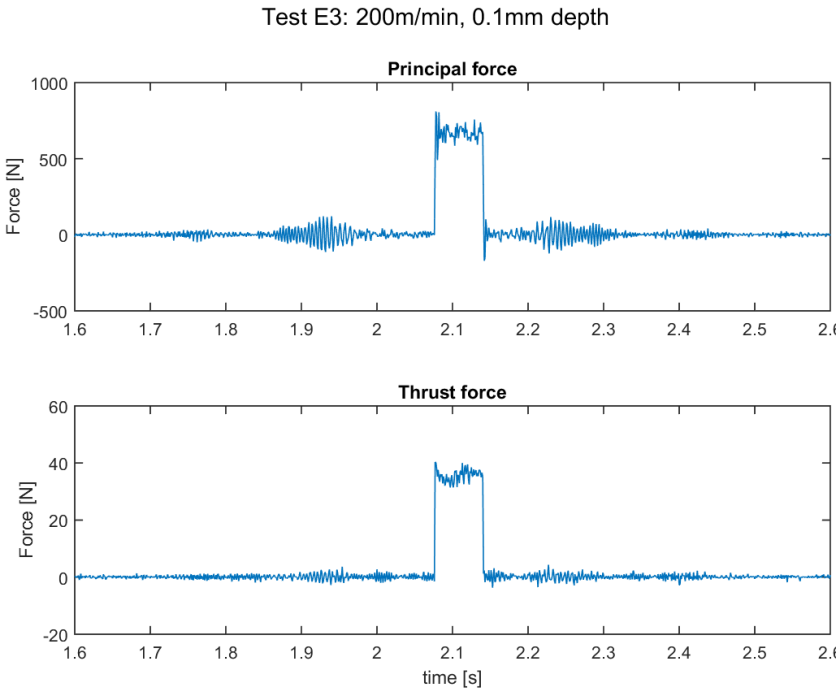

Figure 27: Force measurement for test E3

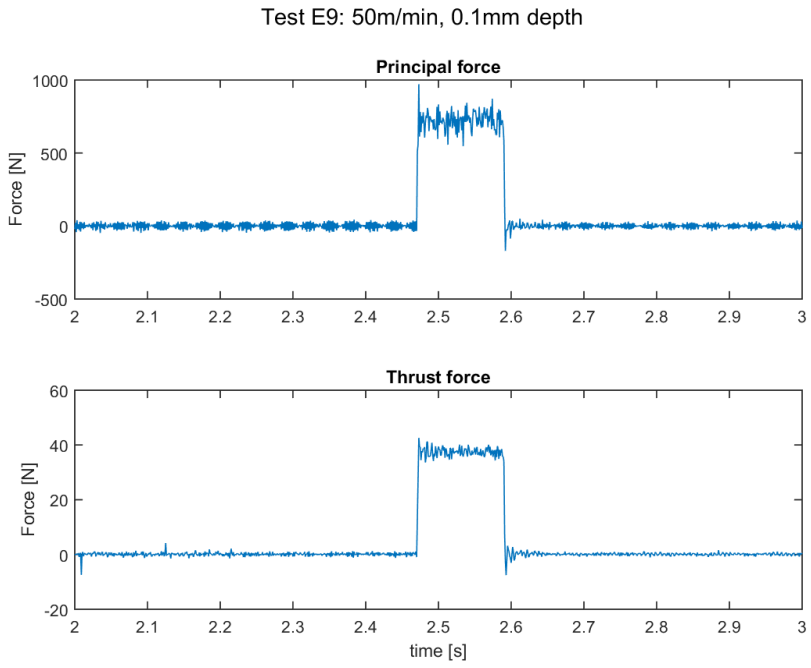

Figure 28: Force measurement for test E9

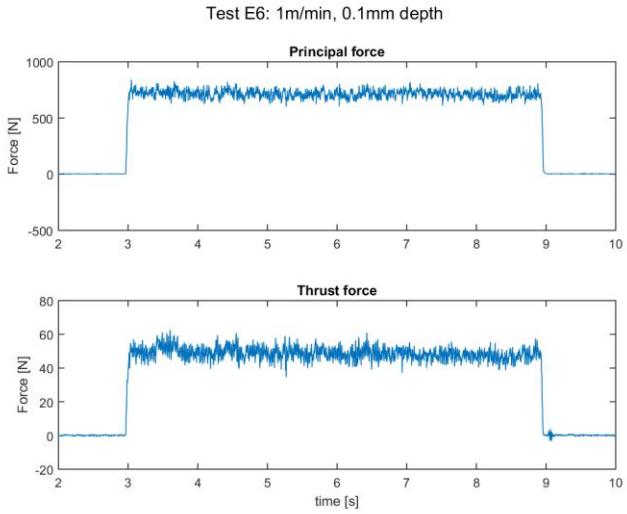

Figure 29: Force measurement for test E6

Additionally, for high cutting speeds, it was observed that behavior of the cutting force signal is similar to an impact. Indeed, for all cases of 200 and 50 m/min it could be appreciated that there is an initial peak at the beginning of the cut in the principal force signal.

Table 8 contains the resulting mean value of the cutting forces on each test. To have a better visualization of these results, forces have been plotted in a bar diagram (Figure(30-32) for the same cutting speeds.

	Workpiece		**Condition**			**Results**	
Test	Laminate	laminate edge	tool	Vc (m/min)	feed(mm)	Principal force (N)	Thrust force (N)
E1	1	1	tool1	200	0.2	687.37	60.26
E2	1	2	tool1	200	??	FAILED	FAILED
E3	2	1	tool1	200	0.1	667.03	35.78
E4	2	2	tool1	200	0.05	653.41	19.41
E5	3	1	tool1	1	0.2	829.45	86.33
E6	3	2	tool1	1	0.1	715.37	48.86
E7	4	1	tool1	1	0.05	631.12	26.30
E8	4	2	tool1	50	0.2	727.80	69.93
E9	5	1	tool1	50	0.1	719.99	37.48
E10	5	2	tool1	50	0.05	665.49	19.26
E11	3	1	tool2	1	0.2	823.29	95.17
E12	3	2	tool2	1	0.1	711.34	63.40
E13	4	1	tool2	1	0.05	668.62	49.07
E14	4	2	tool2	50	0.2	725.57	77.30
E15	5	1	tool2	50	0.1	674.88	60.04
E16	5	2	tool2	50	0.05	631.86	43.98
E17	6	1	tool2	200	0.2	736.28	107.70
E18	2	1	tool2	200	0.1	707.36	47.82
E19	2	2	tool2	200	0.05	643.24	29.55

Table 8: Forces results

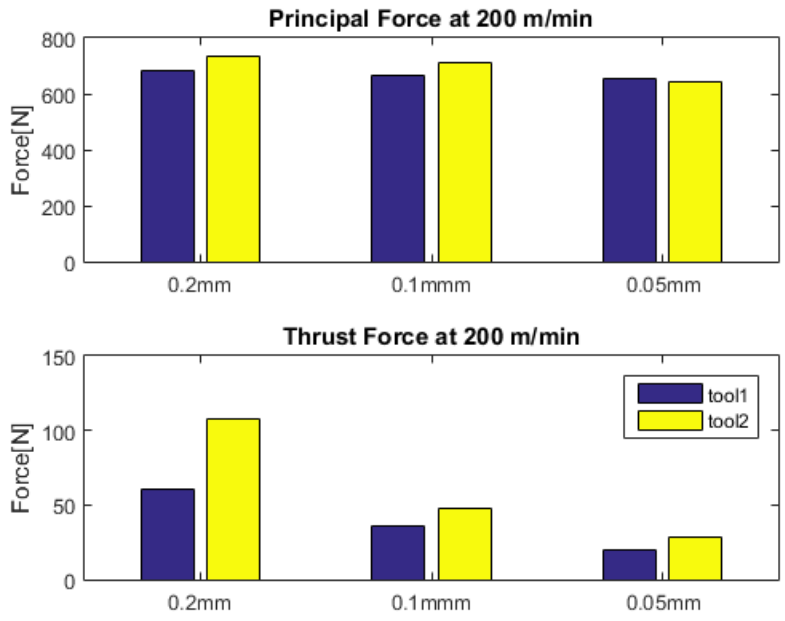

Figure 30: Mean forces for 200 m/min test

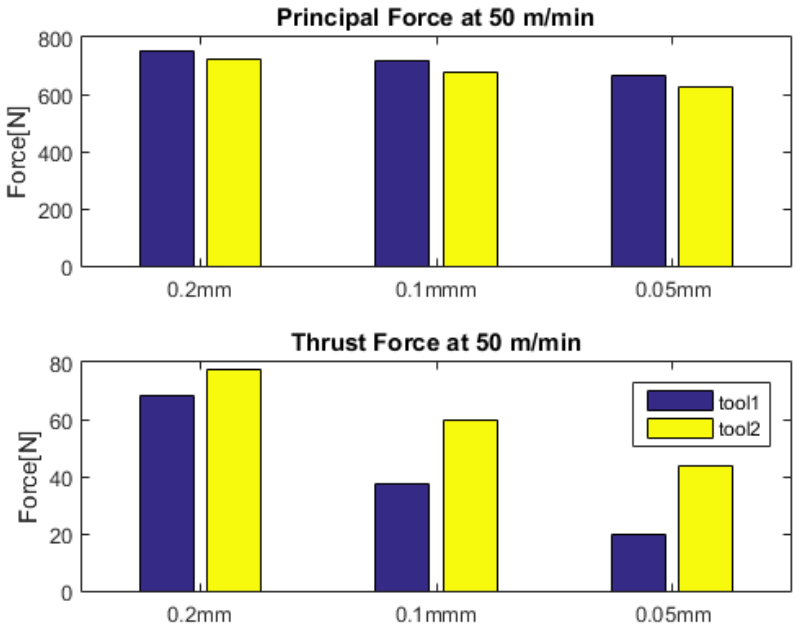

Figure 31: Mean forces for 50 m/min test

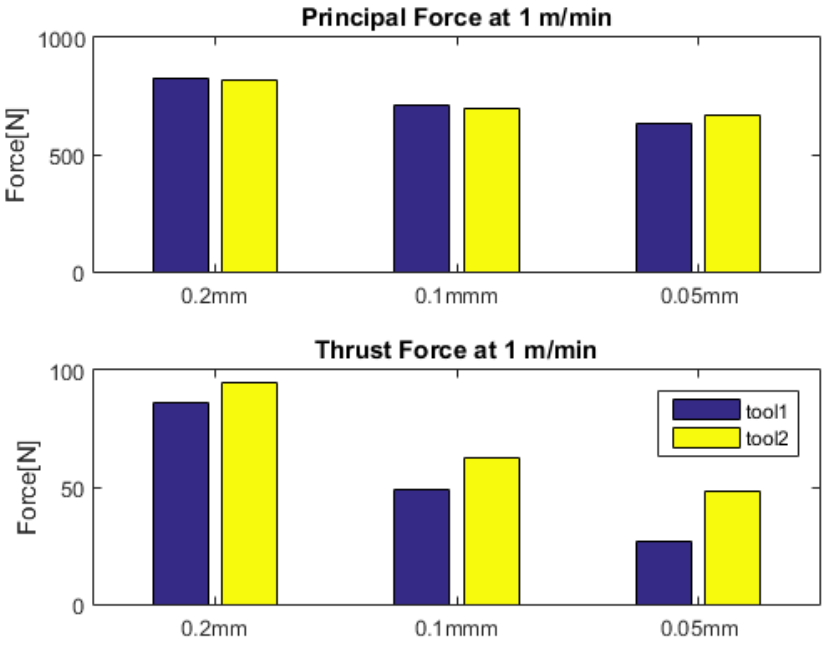

Figure 32: Mean forces for 1 m/min test

From these results, there is no doubt that forces are highly dependent on cutting speed and depth of the cut. As it can be appreciated, maximum forces are obtained for minimum speed and maximum feed ($V_c = 1m/min$ and 0.2mm feed). Cutting forces are reduced as speed is increased or the feed is shortened. This force tendency must be taken into account when seeking tool's life optimization. Concerning the different tool effects, it has been observed that the thrust force for *tool2* is always bigger, no matter the cutting conditions. This evidences that in some way, the less aggressive cutting edge tool exerts a higher force on the workpiece. Additionally, notice that there is almost no significant difference in principal force for 1m/min cutting speed regarding tool's effect. However for 50m/min tests, the principal cutting force corresponding to *tool1* is bigger than *tool2* and for 200m/min is the other way around. So based on this results the aggressive tool, *tool1*, is only effective in reducing cutting forces at very high speed machining processes. Nevertheless, at this speed the *tool1's* effect is reduced for 0.05 mm depth.

4.4. Temperature profiles during machining

Next, some illustrative results regarding temperature distribution during the process are presented Figures(33-36). The lines where temperature profiles are taken are also showed in red. The horizontal one is along the X direction, and the vertical one is along the Y direction.

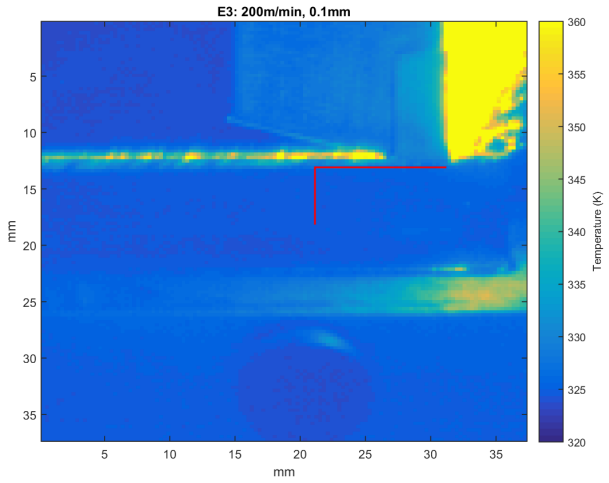

Figure 33: Temperature field in the cutting proccess. Test E3

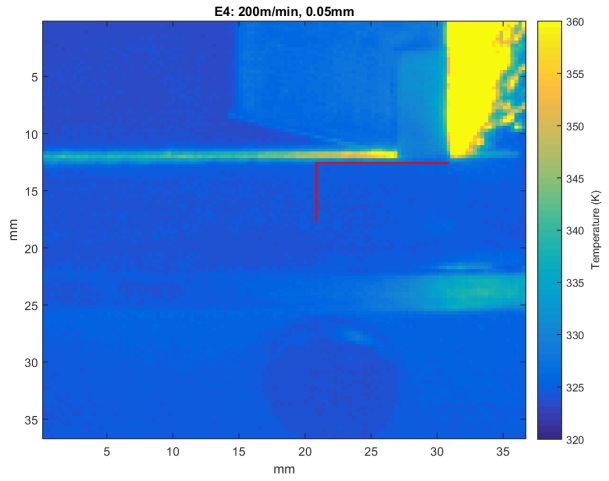

Figure 34: Temperature field in the cutting proccess. Test E4

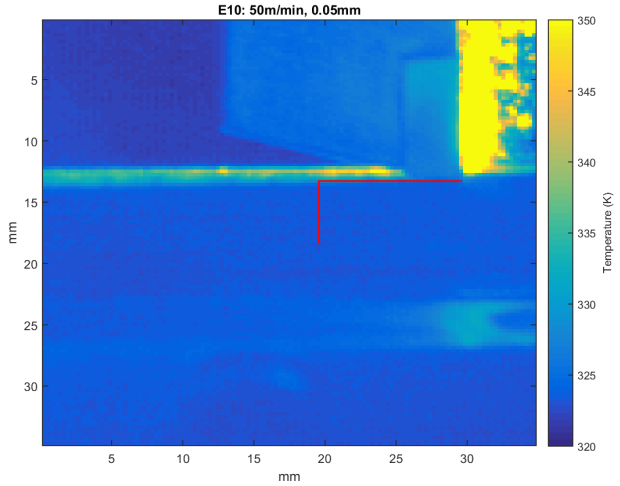

Figure 35: Temperature field in the cutting proccess. Test E10

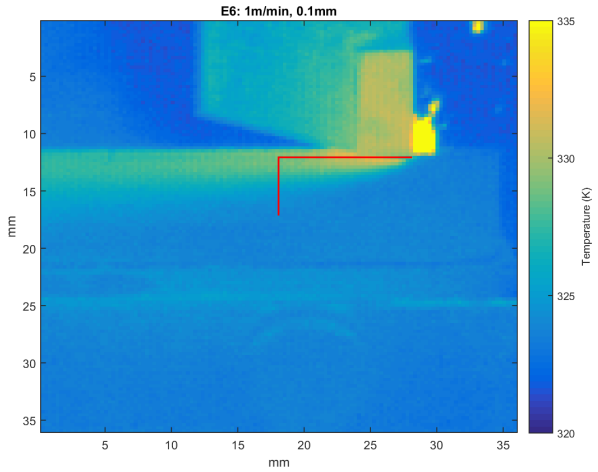

Figure 36: Temperature field in the cutting proccess. Test E6

It is evident that the high temperature values of *dust chip* saturates the image. Although precise temperature measurements cannot be taken in this region of the image, it is clearly appreciated that chip is the main medium by which the heat generated during the process is evacuated. It has been observed that the predominant cutting parameter in heat transfer is the cutting speed. As it can be noted, the temperature distribution on the workpiece for 1m/min is significantly different to 50 or 200 m/min cases. For these last cases (medium and high speed trimming) , the heat is mainly evacuated through the chip and the rest remains concentrated in a small region near the machined surface. But on the other hand, for the low speed tests it takes enough time for the heat to transfer to the entire workpiece. For this reason an extended and smoother temperature distribution is observed in the workpiece.

For a better visualization of the temperature distribution, Figures(37-42) show the temperature for different cutting velocities along horizontal and vertical lines of 10 and 5 mm length respectively.

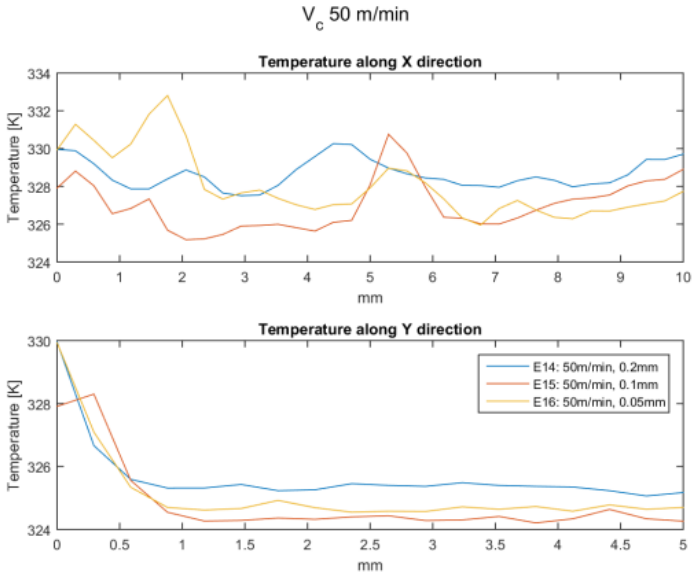

Figure 37: Temperature profiles. Test E14, E15, E16

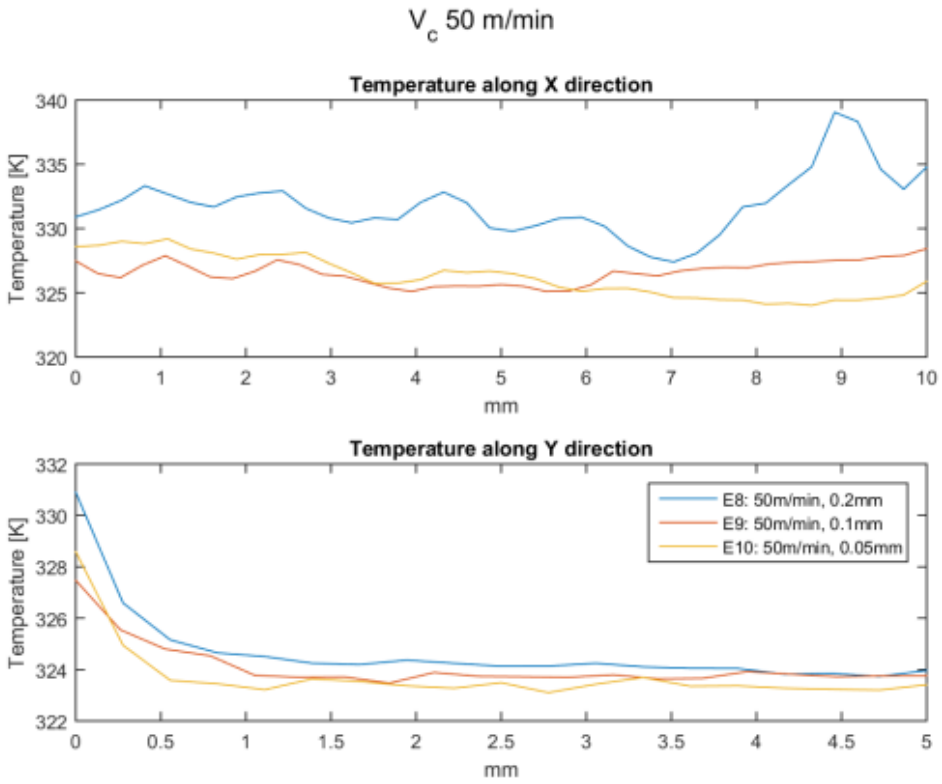

Figure 38: Temperature profiles. Test E8,E 9, E10

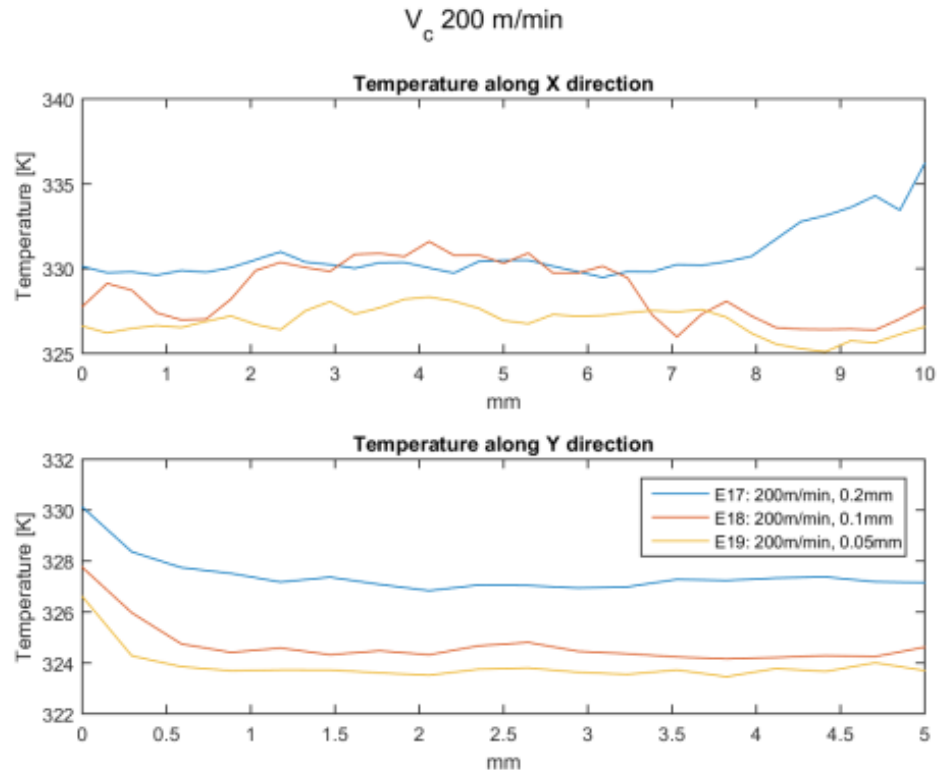

Figure 39: Temperature profiles. Test E17, E18, E19

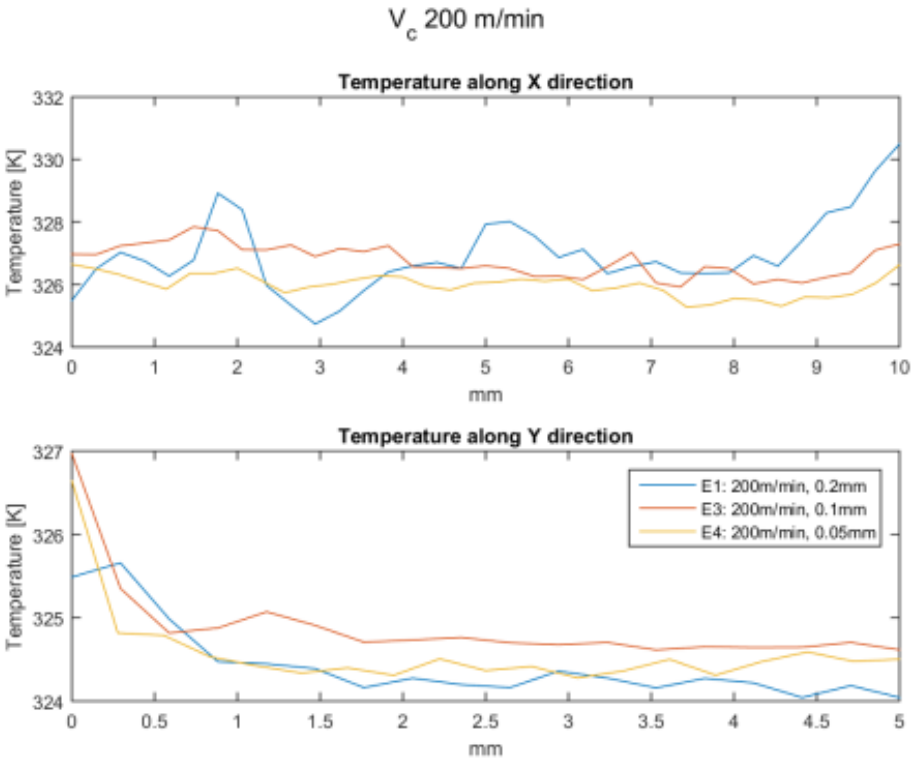

Figure 40: Temperature profiles. Test E1, E3, E4

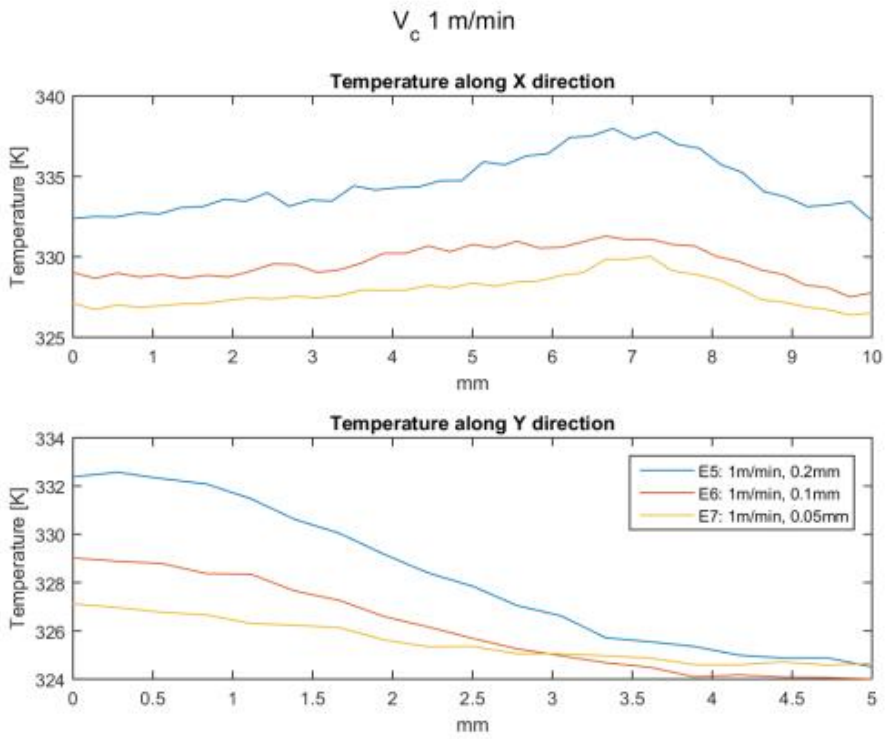

Figure 41: Temperature profiles. Test E5, E6, E7

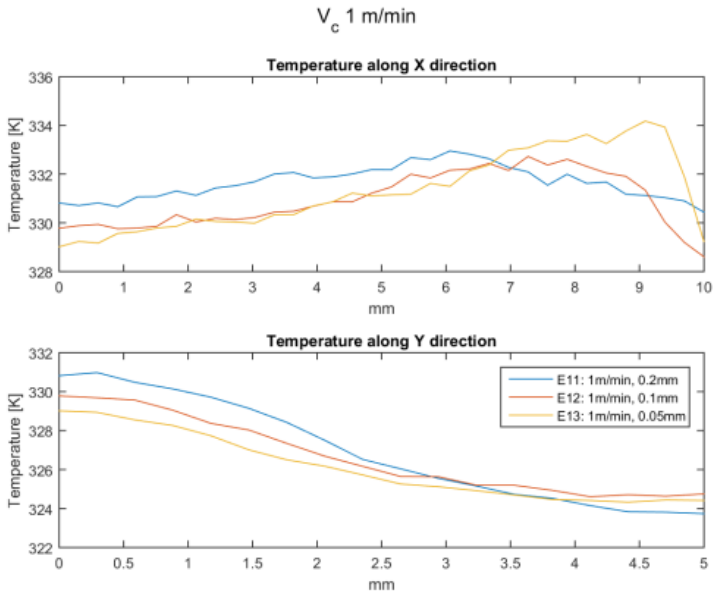

Figure 42: Temperature profiles. Test 11, 12, 13

Since the line along the X direction was selected very closely to the trimmed edge, the random fluctuations on the corresponding temperature plots are probably due to fiber pull-out and local delaminations of the last lamina of the composite. It is also important to take into account that the low resolution of the image (128x128 pixels) implies some uncertainty when selecting the horizontal line; it is not very well defined where is the trimmed edge. This error becomes relatively high when dealing with small temperature fields like in 50 and 200 m/min tests. Therefore, no sound conclusions can be drawn from temperature along the X for medium and high speed test. However for the low speed test (1m/min), the horizontal temperature profile is clearly defined and shows that temperature reaches a maximum immediately behind the tool-workpiece contact point.

On the other hand, vertical profiles along the Y direction show the depth of the thermal effects at the end of the cutting process. For low cutting speeds, heat has been transferred to the workpiece reaching depths of 3-4 mm. The corresponding plots are very smooth and are evidently that heat transfer has reached a steady state. The vertical profiles for medium and high speed show that the thermal effects are not very extensive during the cutting process (no more than 1.5 mm). The main reason why is because the temperature profile is not totally developed like in low speed tests. The combination of the high speed cutting process together with the low thermal conductivity of the resin result in plotted temperature profiles that correspond to a heat transfer transient state.

The maximum temperatures reached are more or less similar for all cutting conditions, no more than 340 K. If we consider a glass transition temperature, T_g of the order of 480K , for Carbon/epoxy laminate like in [6], these machining tests are far away from suffer induced thermal damage.

The temperature profiles also show the sensitivity to the depth of the cut. The higher the depths of the cut, the higher are the induced temperatures. This is obvious since more energy is needed to remove more material.

4.5. Workpiece induced damage

For the visual the external inspection photographs of the front and side view of the laminate were taken like in Figures(43-45).

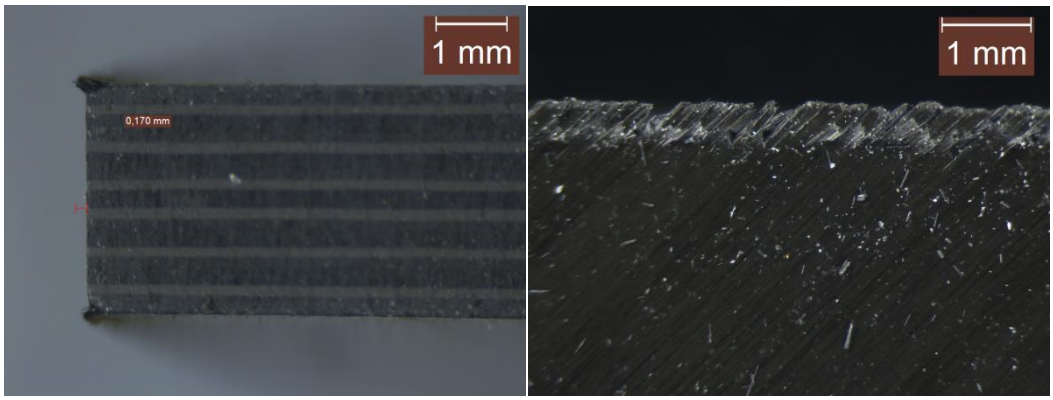

Figure 43: External Damage Workpiece. Test 10

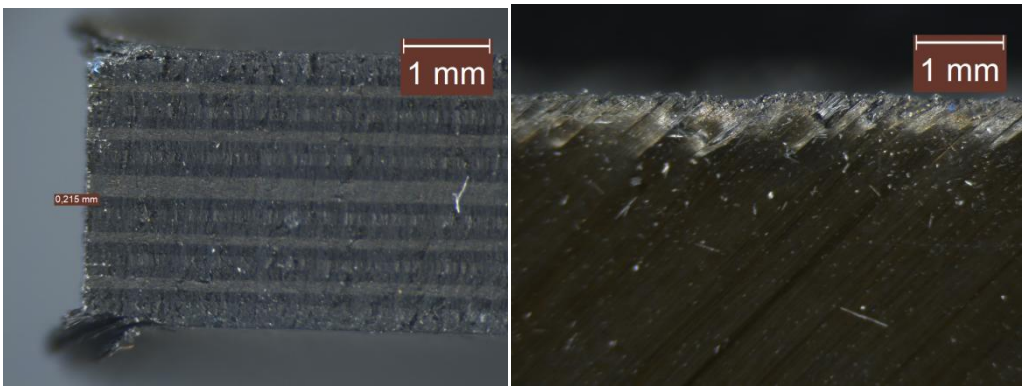

Figure 44: External Damage Workpiece. Test 12

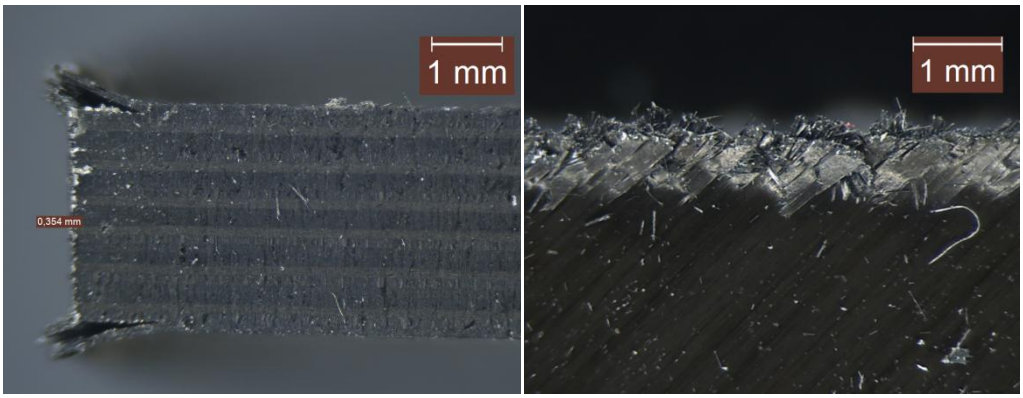

Figure 45: External Damage Workpiece. Test 17

The main external defect observed for all specimens was the fiber pullout of the first and last laminas; it can be easily appreciated in the front view photographs. When the cut is performed the material is not totally removed, leaving a burr that worsens the surface quality. Not only the burr deteriorates the machined quality of the workpiece but also, and more important, it is accompanied by delaminations of the first and last laminas that are extended into the workpiece. The most logical explanation for these results is that there is a local instability. The compressive loads of the tool bend the laminas and separate them from the rest of the laminate. The sketch in Figure46 represents this behavior.

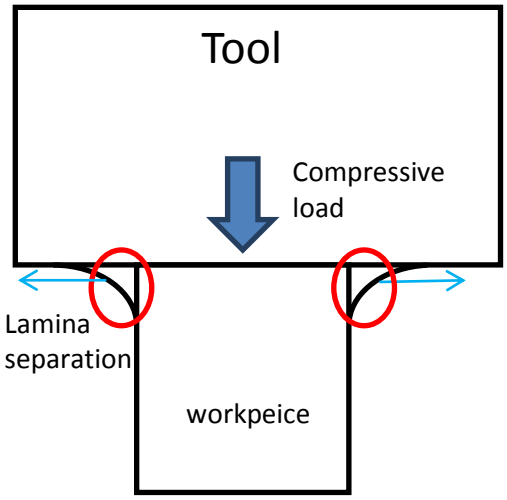

Figure 46: External damage mechanics scheme

It has been noticed that the external delaminations are "proportionally" related to the length of the burr. In this way, measuring the length of the burr has been considered as a good parameter to evaluate the machined quality.

The quality of the burr has been analyzed. From Figures(43-45) it can be clearly observed that the quality is reduced with increasing feed. For same feed and different speed it can be appreciated that the burr quality of the low speed test (Figure47 up-left) is significantly better than at high speed tests (Figure47 up-right). However, when the depth was minimized (0.05 mm) the cutting speed effects were almost negligible Figure47(down-left and down-right).

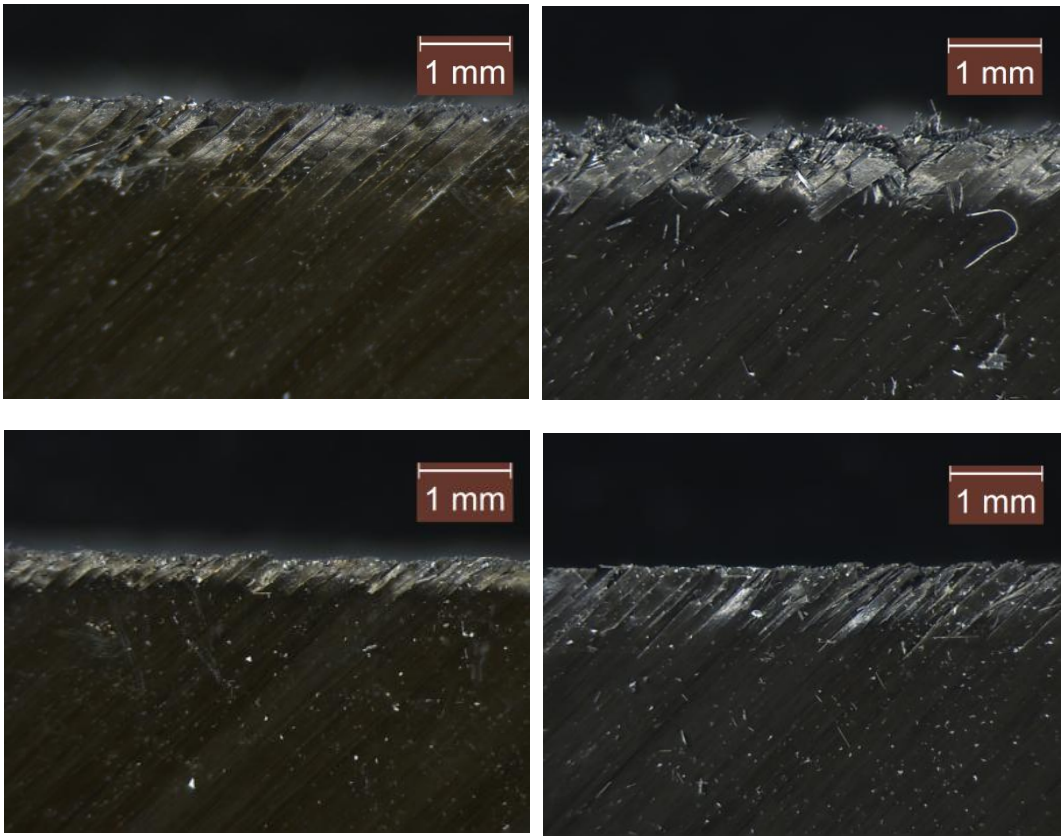

Figure 47: Burr quality inspection. Test 11 (up left) Test 17 (up right) Test 13 (down left) Test 19 (down right)

Concerning internal damage some illustrative heat dissipation results are presented in Figures(48-52) to show how internal defects looks like compared with the undamaged specimen.

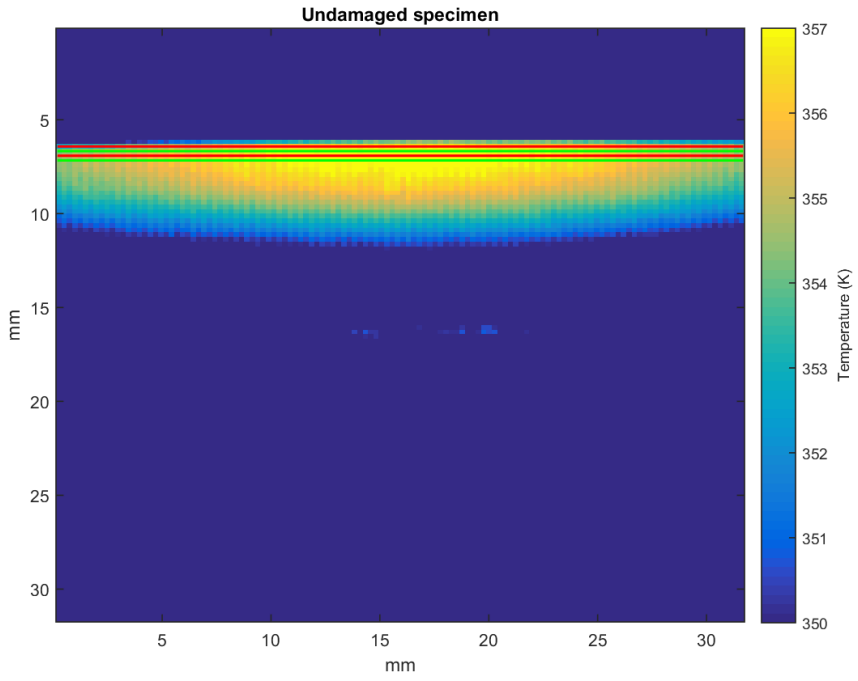

Figure 48: Temperature field undamaged workpiece

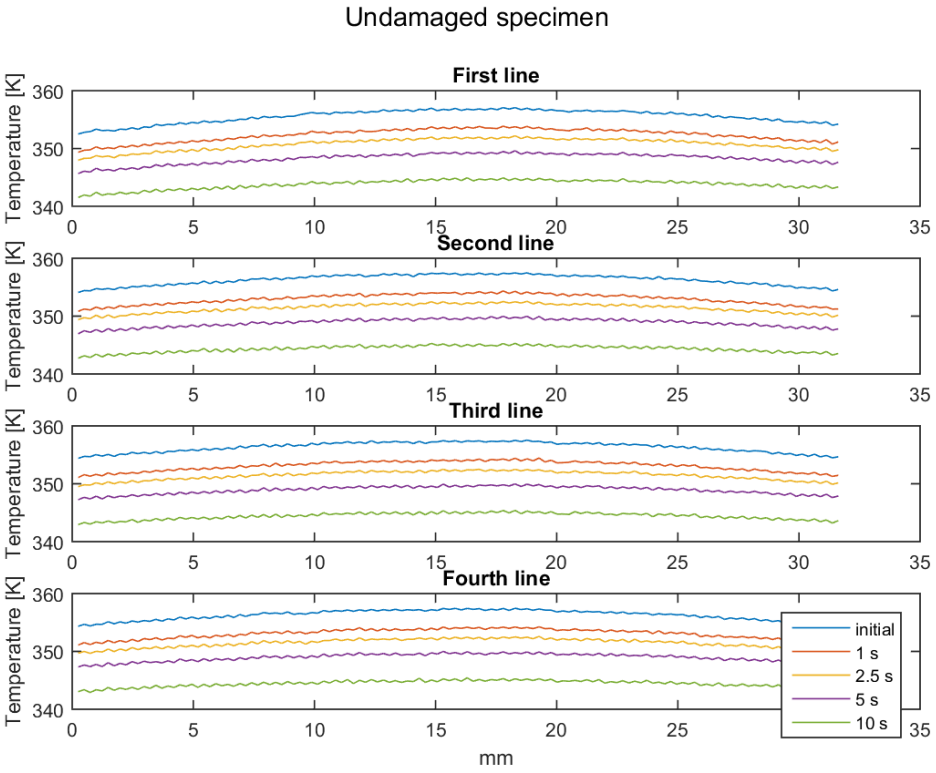

Figure 49: Undamaged temperature profiles

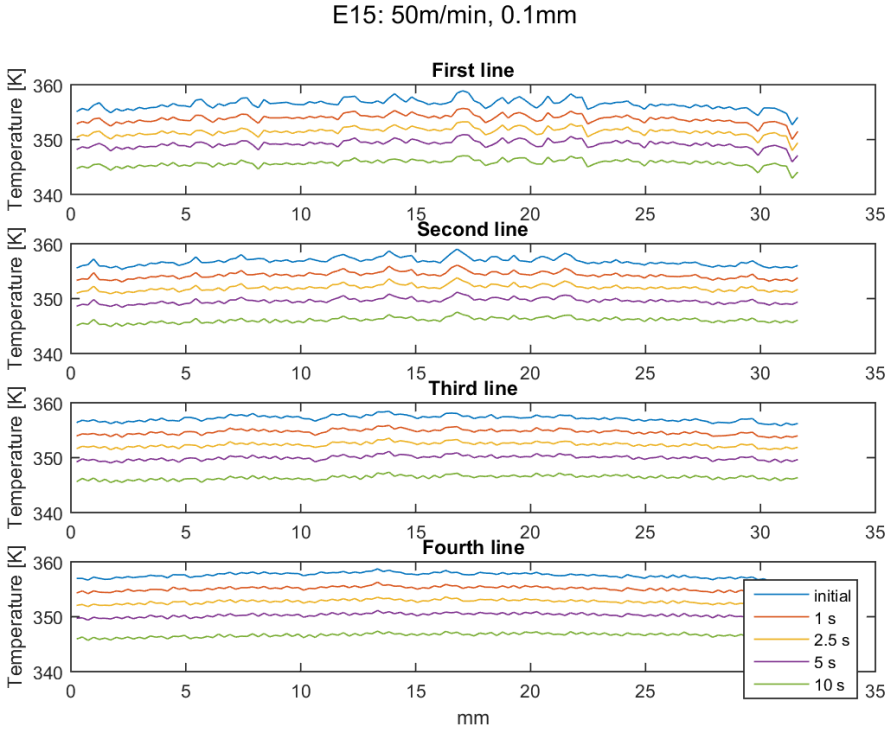

Figure 50: Undamaged temperature profiles. Test E15

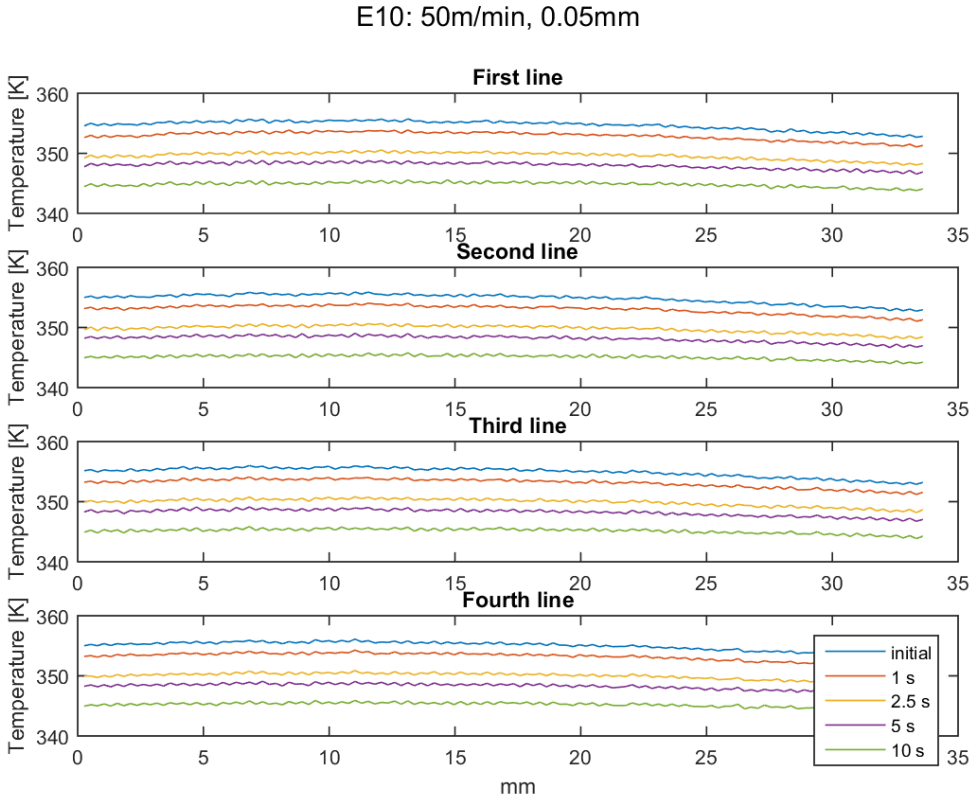

Figure 51: Undamaged temperature profiles. Test E10

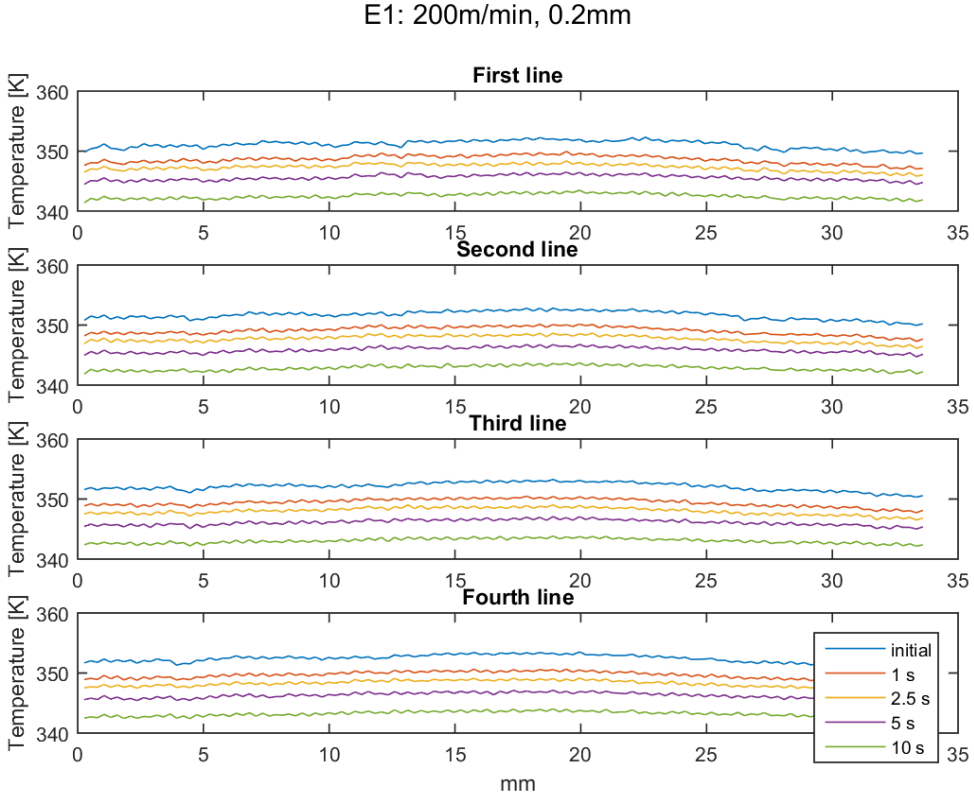

Figure 52: Undamaged temperature profiles. Test E1

It can be appreciated that there is a smooth distribution and evolution of the temperatures on the undamaged workpiece (Figure49)along the four lines, without any kind of anomaly. The E15 temperature profiles (Figure50) evidence a huge induced internal damage due to the high temperature fluctuations shown. E10 measurements (Figure51)show no induced damage and E1 (Figure52)show the typical profiles of internal damage. Remember that depending on the test, each line denotes a distance from the machined surface due to the varying pixel length Table 7.

Additionally, comment that it was found and internal fabrication defect on the workpiece used for test E1. In the temperature profiles of Figure52 there is a small anomaly near the 5 mm that is not present in the most external line. If we take a look to the temperature field image of the workpiece Figure53, a huge defect can be noticed and for sure that it has not been induced by the orthogonal machining.

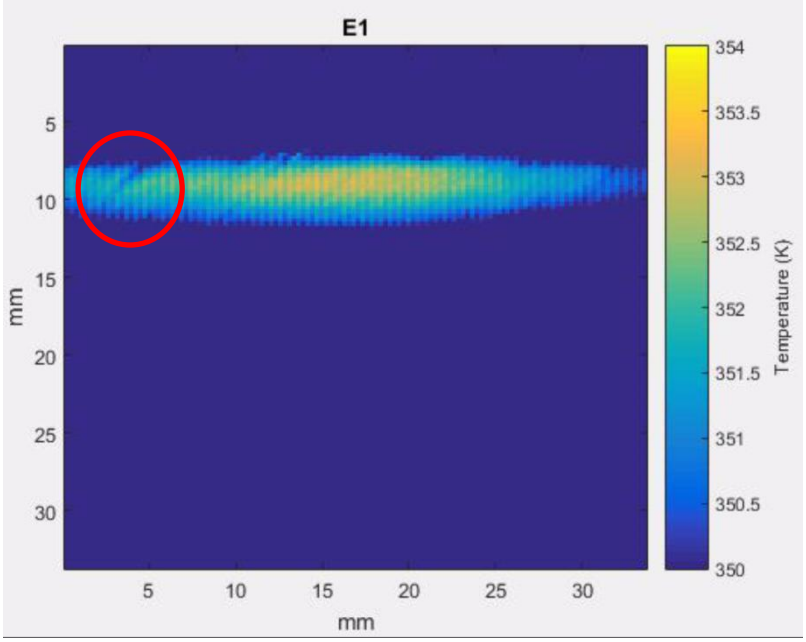

Figure 53: Temperature field workpiece test 1

Next, Table9 collects the quantitative results of the parameters used to evaluate workpiece's quality. These parameters are the burr length and the depth of the internal induced damage. Also they have been depicted in bar diagrams in Figures(54,55).

	Workpiece		Condition			Results	
Test	Laminate	laminate edge	tool	Vc (m/min)	feed(mm)	Burr length (mm)	Internal damage depth (mm)
E1	1	1	tool1	200	0.2	1.25	0.53
E2	1	2	tool1	200	??	FAILED	FAILED
E3	2	1	tool1	200	0.1	0.15	0.00
E4	2	2	tool1	200	0.05	0	0.00
E5	3	1	tool1	1	0.2	0.47	0.00
E6	3	2	tool1	1	0.1	0.27	0.26
E7	4	1	tool1	1	0.05	0.14	0.26
E8	4	2	tool1	50	0.2	0.37	0.53
E9	5	1	tool1	50	0.1	0.21	0.26
E10	5	2	tool1	50	0.05	0.17	0.00
E11	3	1	tool2	1	0.2	0.35	0.25
E12	3	2	tool2	1	0.1	0.215	0.25
E13	4	1	tool2	1	0.05	0.11	0.00
E14	4	2	tool2	50	0.2	0.68	0.49
E15	5	1	tool2	50	0.1	0.298	1.05
E16	5	2	tool2	50	0.05	0.134	0.25
E17	6	1	tool2	200	0.2	0.354	0.49
E18	2	1	tool2	200	0.1	0.417	0.25
E19	2	2	tool2	200	0.05	0.2	0.00

Table 9: Damage results

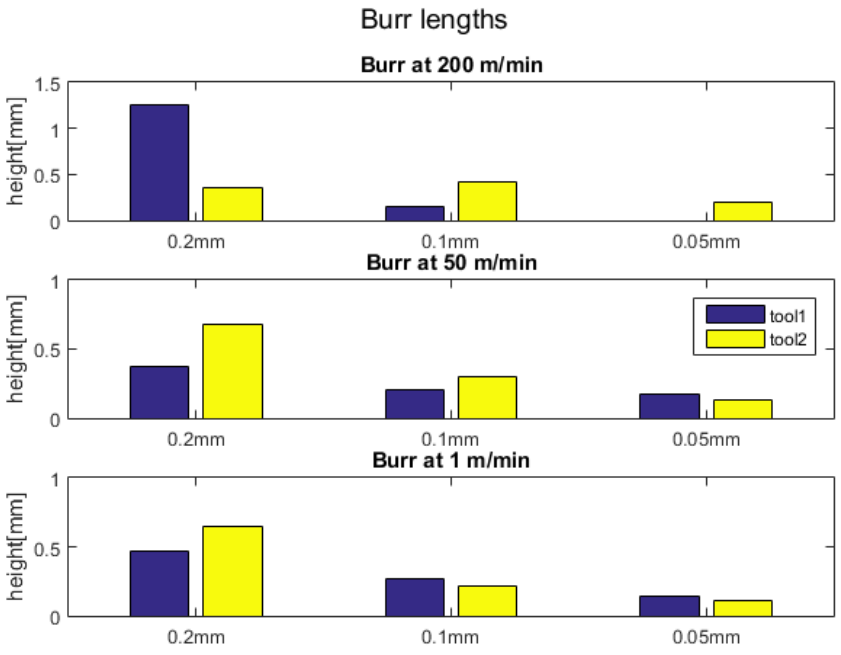

Figure 54: Burr lenghts

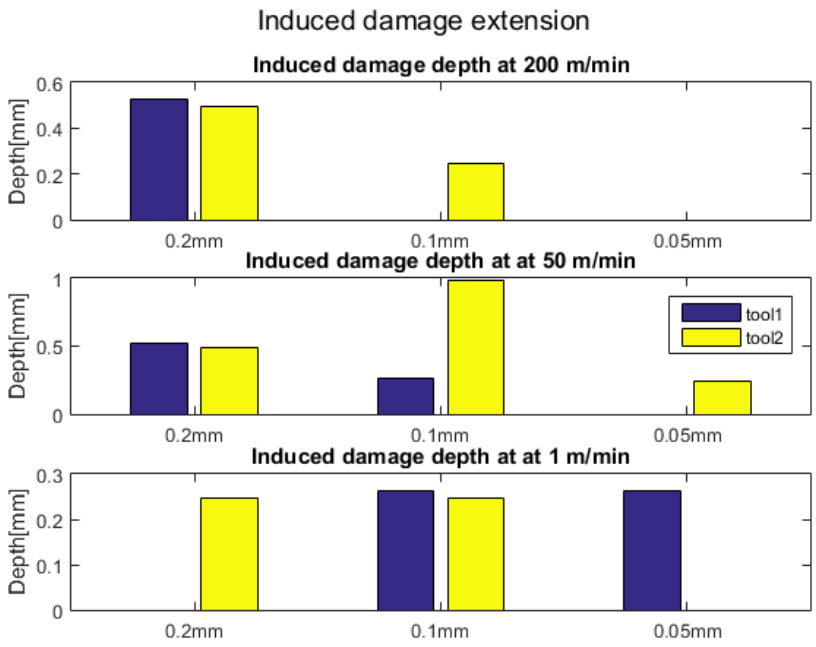

Figure 55: induced damage extension

It can be appreciated that the burr's length strongly depends on the feed of the cut. Increasing the feed significantly worsen the machined quality of the resultant workpiece. The cutting speed effect on burr's length is less determinant for both tools. Nevertheless it can be considered that at low feeds, the higher the speed, the better the quality. Regarding tool effect on burr's length, it is highly dependent on the cutting conditions although generally *tool2* results in larger burrs compared with *tool1*. Recalling force measurements, this statement is probably because thrust force exerted by *tool2* is always bigger, and therefore the compressive loads that induces the external delamination are also bigger.

Concerning induced internal damage, no clear relations between cutting parameters and the results obtained are observed. The sensitivity to the cutting parameters in FRP trimming is not so evident as for metal cutting. Nevertheless, for some given cutting conditions the induced damage results attract attention:

- For the minimum feed and the highest cutting speed (0.05mm and 200 m/min) results show that the induced internal damage is negligible for both tools.
- For the greatest feed and cutting speed (0.2 mm and 200m/min) the workpiece is significantly damage with both tools.
- For the same feed but the lowest velocity (0.2 mm and 1m/min) the workpiece does not seem to suffer in the same way.

Additionally, it seems that *tool2* induces more internal damage on the workpieces.

The fact that no clear tendencies are presented in the induced internal damage results is due to the complex behavior of FRP when they are machined. When evaluating the induced

mechanical damage on these workpieces, general conclusion (like with force measurements or temperature profiles) cannot be drawn because the complexity of the fracture mechanics involved is very high. Consequently, the cause-effect relations are not trivial. Basically, the mathematical statement: $if\ a+b>c; d>a\ \ and\ e>d;\ then\ d+e>c$ is not fulfilled in the FRP machining world. Understanding the interaction between multidirectional laminates and the tool is a nowadays problem that researchers still willing to solve. However, specific conclusions can be drawn from some cutting conditions. For example, determining the cutting condition that minimize the internal damage is very useful in the industrial sector.

Chapter 5: Economic and legal framework

5.1. Budget

The approximate budget for the realization of this Bacherlor's Thesis is presented in the following table:

Personnel	
total engineer hours (h)	300
engineer cost per hour (€/h)	30
Lincenses	
Matlab (3 months)	8000€/year
Materials	
2 set of tools (€)	30
a set of 6 workpieces (€)	60
Instruments	
orthogonal cutting machine (2 weeks)	6000€/year
force measurement equipment (2 weeks)	2000€/year
thermographic camera (2weeks)	8000€/year
high-speed camera (2 weeks)	6000€/year
Total	**11.966,15 €**

Table 10: Budget

All resources were provided by the university and the approximated cost was 12000€.

5.2. Legal framework

Concerning the legal framework, during the entire experimental procedure the BOE-A-1995-24292 [22]has been followed. In this way, security and health is guaranteed by minimizing labor risks. This framework defines some guidelines to avoid harmful risks like breathing the small broken fibers released during the cutting processes.

Moreover, the European standard ECSS-E-HB-32-20 Part 4A [24] about composite machining for aerospace applications has also been applied in this project. It defines some guidelines to guarantee quality results.

Chapter 6: Conclusions & future researches

6.1. Conclusions

Orthogonal cutting on multidirectional Carbon FRP laminates was experimentally investigated as simplified machining method. The parametric study has been performed aiming to optimize the industrial machining process of Carbon FRP. Different tools and cutting parameters were analyzed and based on the results obtained, the following conclusions were made:

- Forces. They are factors that definitely determine the machined quality of the final workpiece. A strong dependence on cutting speed and feed was found. It was observed that *tool2* always exerted a higher thrust force on the workpiece.
- Thermal effects. It has been observed that heat transfer mechanism is strongly dependent on the cutting speed. Additionally, it has been observed that heat is mainly evacuated through the "chip", a small amount is transferred to the workpiece. The maximum temperature reached in all test were significantly below glass transition temperatures, T_g, of similar FRP composites. Consequently there is no risk of thermal damage in these cutting conditions.
- External damage. It was found to be closely related with the thrust forces. Compressive loads during the machining process induce local instabilities in the external laminas causing burr and delaminations. Burr's length was found to be a good parameter to evaluate the quality of the machined workpiece because it is strongly related with external delaminations. Burr's length is minimized with decreasing feed. Moreover, it could be appreciated how the higher thrust forces exerted by *tool2* resulted in poorer machined workpiece.
- Internal damage. No general conclusions could be drawn. But it was observed that the induced mechanical damage was minimized for the maximum cutting speed and minimum feed independently of the tool used. Moreover, it was also appreciated that *tool2* induced more internal damage on workpieces.
- Chip formation. It is almost impossible to study its mechanism or morphology in high speed trimming because only a huge amount of dust and small particles are released.
- Tool's damage. The tool's materials (Carbide-Cermet) used in the cutting process were so strong that no damage was evidenced on tool's surface. Consequently, no conclusion could be drawn regarding tool's life expectancy.

After analyzing all the cutting conditions and their effects on the overall performance of orthogonal FRP machining, the optimum cutting condition selected was 200 m/min cutting speed, 0.05 mm feed with *tool1*. For this condition:

- Low forces are obtained because of the small feed although they are not the lowest ones.
- A low amount of heat is transferred to the workpiece.

- The compressive loads applied on the workpiece by *tool1* are the minimum and therefore, as results show, the burr and the external damage are minimized.
- Results show that internal mechanical damage was also minimized for these cutting conditions.

In this way, quality machined workpieces are guaranteed.

6.2. Future works

Next, some ideas for future works are presented with the objective of going further in the FPR machining field:

- Work on the non-destructive inspection methods. It would be interesting to know the exact location of the induced damage inside the workpiece. Not only in the vertical plan, but also in the horizontal one.
- To elaborate a 3D numerical model that simulates multidirectional FRP laminates machining. It is a very difficult task but it can be complemented with the results obtained during this project.
- To perform a frequency analysis on the force signal. With this task, it will be tried to decompose the signal and see if the breaking fiber mechanism is reflected in the analysis.
- To study experimentally thermal damage on orthogonal trimming of FRP. It is proposed to heat up the tools and evaluate if the mechanical performance of the entire workpiece is deteriorated.
- To perform the same parametric study on different machining process like drilling or milling.

References

[1] B. Harris and o. M. Institute, *Engineering Composite Materials.* IOM, 1999Available: https://books.google.es/books?id=9MVRAAAAMAAJ

[2] L. C. LANCASTER, *Concrete Vaulted Construction in Imperial Rome.* Cambridge: Cambridge University Press, 2005.

[3] G. H. Staab, "1 - introduction to composite materials," in *Laminar Composites (Second Edition)*, G. H. Staab, Ed. Butterworth-Heinemann, 2015, pp. 1-16. DOI: https://doi.org/10.1016/B978-0-12-802400-3.00001-5.

[4]. D. H. Wang, M. Ramulu and D. Arola, "Orthogonal cutting mechanisms of graphite/epoxy composite. Part I: unidirectional laminate," *International Journal of Machine Tools and Manufacture,* vol. 35, *(12),* pp. 1623-1638, December 1995, 1995. . DOI: https://doi.org/10.1016/0890-6955(95)00014-O.

[5] E. Uhlmann, S. Richarz, F. Sammler and R. Hufschmied, "High Speed Cutting of Carbon Fibre Reinforced Plastics," *Procedia Manufacturing,* vol. 6, *(Supplement C),* pp. 113-123, 2016, 2016. . DOI: https://doi.org/10.1016/j.promfg.2016.11.015.

[6] G. Mullier and J. F. Chatelain, "Influence of thermal damage on the mechanical strength of trimmed CFRP," *World Academy of Science, Engineering and Technology, International Journal of Mechanical, Aerospace, Industrial, Mechatronic and Manufacturing Engineering,* vol. 9, *(8),* pp. 1559-1566, 2015.

[7] N. Li, Y. Li, J. Zhou, Y. He and X. Hao, "Drilling delamination and thermal damage of carbon nanotube/carbon fiber reinforced epoxy composites processed by microwave curing," *International Journal of Machine Tools and Manufacture,* vol. 97, *(Supplement C),* pp. 11-17, October 2015, 2015. . DOI: https://doi.org/10.1016/j.ijmachtools.2015.06.005.

[8] K. K. Panchagnula and K. Palaniyandi, "Drilling on fiber reinforced polymer/nanopolymer composite laminates: a review," *Journal of Materials Research and Technology,* Available online 12 August 2017, 2017. . DOI: https://doi.org/10.1016/j.jmrt.2017.06.003.

[9] N. Bhatnagar, D. Nayak, I. Singh, H. Chouhan and P. Mahajan, "Determination of Machining-Induced Damage Characteristics of Fiber Reinforced Plastic Composite Laminates," *Mater. Manuf. Process.,* vol. 19, *(6),* pp. 1009-1023, 12/31, 2004. Available: http://dx.doi.org/10.1081/AMP-200035177. DOI: 10.1081/AMP-200035177.

[10] A. Koplev, A. Lystrup and T. Vorm, "The cutting process, chips, and cutting forces in machining CFRP," *Composites,* vol. 14, *(4),* pp. 371-376, October 1983, 1983. . DOI: https://doi.org/10.1016/0010-4361(83)90157-X.

[11] V. Lopresto, A. Langella, G. Caprino, M. Durante and L. Santo, "Conventional Orthogonal Cutting Machining on Unidirectional Fibre Reinforced Plastics," *Procedia CIRP,* vol. 62, *(Supplement C),* pp. 9-14, 2017, 2017. . DOI: https://doi.org/10.1016/j.procir.2016.07.036.

[12] N. A. Abukhshim, P. T. Mativenga and M. A. Sheikh, "Heat generation and temperature prediction in metal cutting: A review and implications for high speed machining," *International Journal of Machine Tools and Manufacture,* vol. 46, *(7),* pp. 782-800, June 2006, 2006. . DOI: https://doi.org/10.1016/j.ijmachtools.2005.07.024.

[13] L. Sorrentino, S. Turchetta, L. Colella and C. Bellini, "Analysis of Thermal Damage in FRP Drilling," *Procedia Engineering,* vol. 167, *(Supplement C),* pp. 206-215, 2016, 2016. . DOI: https://doi.org/10.1016/j.proeng.2016.11.689.

[14] G. J. Tattersall, "Infrared thermography: A non-invasive window into thermal physiology," *Comparative Biochemistry and Physiology Part A: Molecular & Integrative Physiology,* vol. 202, *(Supplement C),* pp. 78-98, December 2016, 2016. . DOI: https://doi.org/10.1016/j.cbpa.2016.02.022.

[15] E. Whitenton, "An introduction for machining researchers to measurement uncertainty sources in thermal images of metal cutting," vol. 12, *(International Journal of Machining and Machinability of Materials),* July. 31, 2012.

[16] A. Khomenko, O. Karpenko, E. G. Koricho, M. Haq, G. L. Cloud and L. Udpa, "Quantitative comparison of optical transmission scanning with conventional techniques for NDE of impact damage in GFRP composites," *Composites Part B: Engineering,* vol. 123, *(Supplement C),* pp. 92-104, 15 August 2017, 2017. . DOI: https://doi.org/10.1016/j.compositesb.2017.05.008.

[17] Y. Zhao, L. Tinsley, S. Addepalli, J. Mehnen and R. Roy, "A coefficient clustering analysis for damage assessment of composites based on pulsed thermographic inspection," *NDT & E International,* vol. 83, *(Supplement C),* pp. 59-67, October 2016, 2016. . DOI: https://doi.org/10.1016/j.ndteint.2016.06.003.

[18] S. Moustakidis, A. Anagnostis, P. Karlsson and K. Hrissagis, "Non-destructive inspection of aircraft composite materials using triple IR imaging," *Ifac-Papersonline,* vol. 49, *(28),* pp. 291-296, 2016, 2016. . DOI: https://doi.org/10.1016/j.ifacol.2016.11.050.

[19] (2009). *Data sheet, Type 9257B*. Available: https://www.kistler.com/?type=669&fid=51226.

[20] J. A. Hubbard, A. L. Brown, A. Dodd, S. Gomez-Vasquez and C. Ramirez, "Carbon fiber composite characterization in adverse thermal environments," Albuquerque New Mexico, Tech. Rep. SAND2011-2833, May. 2011.

[21] J. L. Cantero, J. Díaz-Álvarez, M. H. Miguélez and N. C. Marín, "Analysis of tool wear patterns in finishing turning of Inconel 718," *Wear,* vol. 297, *(1),* pp. 885-894, 15 January 2013, 2013. . DOI: https://doi.org/10.1016/j.wear.2012.11.004.

[22] D. H. Wang, M. Ramulu and D. Arola, "Orthogonal cutting mechanisms of graphite/epoxy composite. Part II: multi-directional laminate," *International Journal of Machine Tools and Manufacture,* vol. 35, *(12),* pp. 1639-1648, December 1995, 1995. . DOI: https://doi.org/10.1016/0890-6955(95)00015-P.

[23] Ley 31/1995, de 8 de noviembre, de prevención de Riesgos Laborales. núm. 269, de 10/11/1995. https://www.boe.es/buscar/pdf/1995/BOE-A-1995-24292-consolidado.pdf

[24] ESA Requirements and Standards Division, ECSS-E-HB-32-20 Part 1A. *Structural materials handbook - Part 1: Overview and material properties and applications*. 20 March 2011. http://www.ecss.nl/wp-content/uploads/handbooks/ecss-e-hb/ECSS-E-HB-32-20_Part1A.pdf

Bibliography

1] D. Aleksendrić and P. Carlone, "1 - introduction to composite materials," in *Soft Computing in the Design and Manufacturing of Composite Materials*, D. Aleksendrić, and P. Carlone, Eds. Oxford: Woodhead Publishing, 2015, pp. 1-5.
DOI: https://doi.org/10.1533/9781782421801.1.

[2] S. Gururaja and M. Ramulu, "Analytical formulation of subsurface stresses during orthogonal cutting of FRPs," *Composites Part A: Applied Science and Manufacturing,* vol. 41, *(9),* pp. 1164-1173, September 2010, 2010. .
DOI: https://doi.org/10.1016/j.compositesa.2010.04.016.

[3] K. R. Knowles, J. Tu and J. S. Wiggins, "Thermal and volumetric property analysis of polymer networks and composites using elevated temperature digital image correlation," *Polymer Testing,* vol. 58, *(Supplement C),* pp. 48-53, April 2017, 2017. .
DOI: https://doi.org/10.1016/j.polymertesting.2016.12.013.

[4] B. Lane, E. Whitenton, V. Madhavan and M. Donmez, *Uncertainty in Measurement of the Maximum Cutting Tool Temperature by Infrared Thermography.* 201442.

[5] S. Moustakidis, A. Anagnostis, P. Karlsson and K. Hrissagis, "Non-destructive inspection of aircraft composite materials using triple IR imaging," *Ifac-Papersonline,* vol. 49, *(28),* pp. 291-296, 2016, 2016. . DOI: https://doi.org/10.1016/j.ifacol.2016.11.050.

[6] I. S. N. V. R. Prashanth, D. V. R. Shankar, M. M. Hussain and D. R. Reddy, "Performances of different mill cutters in machining of GFRP Composite Laminates," *Materials Today: Proceedings,* vol. 4, *(2, Part A),* pp. 2800-2805, 2017, 2017. .
DOI: https://doi.org/10.1016/j.matpr.2017.02.159.

[7] D. Pulungan, G. Lubineau, A. Yudhanto, R. Yaldiz and W. Schijve, "Identifying design parameters controlling damage behaviors of continuous fiber-reinforced thermoplastic composites using micromechanics as a virtual testing tool," *International Journal of Solids and Structures,* vol. 117, *(Supplement C),* pp. 177-190, 15 June 2017, 2017. .
DOI: https://doi.org/10.1016/j.ijsolstr.2017.03.026.

[8] M. Ramulu, D. Kim and G. Choi, "Frequency analysis and characterization in orthogonal cutting of glass fiber reinforced composites," *Composites Part A: Applied Science and Manufacturing,* vol. 34, *(10),* pp. 949-962, October 2003, 2003. .
DOI: https://doi.org/10.1016/S1359-835X(03)00203-3.

[9] G. V. G. Rao, P. Mahajan and N. Bhatnagar, "Micro-mechanical modeling of machining of FRP composites – Cutting force analysis," *Composites Science and Technology,* vol. 67, *(3),* pp. 579-593, March 2007, 2007. .
DOI: https://doi.org/10.1016/j.compscitech.2006.08.010.

[10] C. Schmidt, B. Denkena, K. Völtzer and T. Hocke, "Thermal Image-based Monitoring for the Automated Fiber Placement Process," *Procedia CIRP,* vol. 62, *(Supplement C),* pp. 27-32, 2017, 2017. . DOI: https://doi.org/10.1016/j.procir.2016.06.058.

[11] X. Soldani, C. Santiuste, A. Muñoz-Sánchez and M. H. Miguélez, "Influence of tool geometry and numerical parameters when modeling orthogonal cutting of LFRP composites," *Composites Part A: Applied Science and Manufacturing,* vol. 42, *(9),* pp. 1205-1216, September 2011, 2011. . DOI: https://doi.org/10.1016/j.compositesa.2011.04.023.

[12] L. Sorrentino, S. Turchetta, L. Colella and C. Bellini, "Analysis of Thermal Damage in FRP Drilling," *Procedia Engineering,* vol. 167, *(Supplement C),* pp. 206-215, 2016, 2016. .
DOI: https://doi.org/10.1016/j.proeng.2016.11.689.

Appendixes

Temperature field during the machining processes

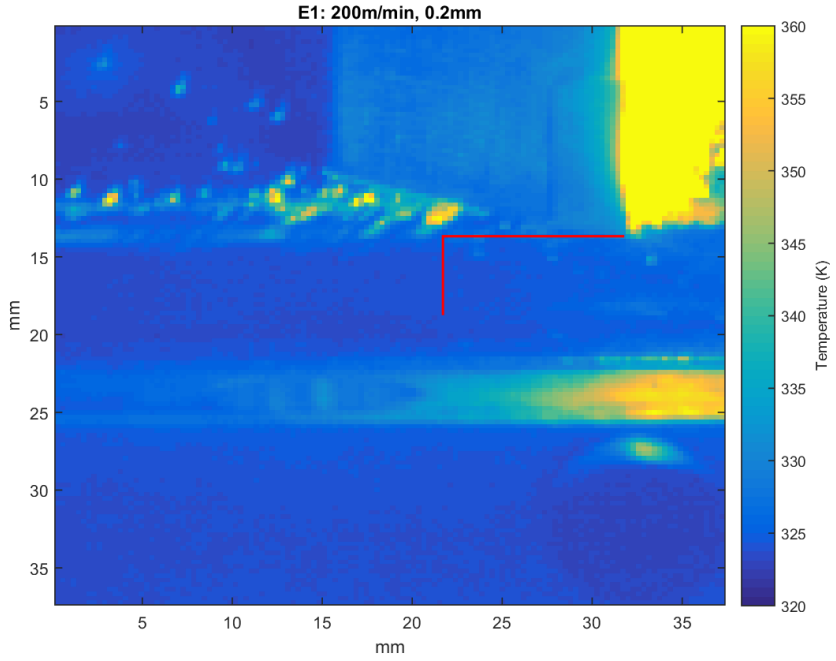

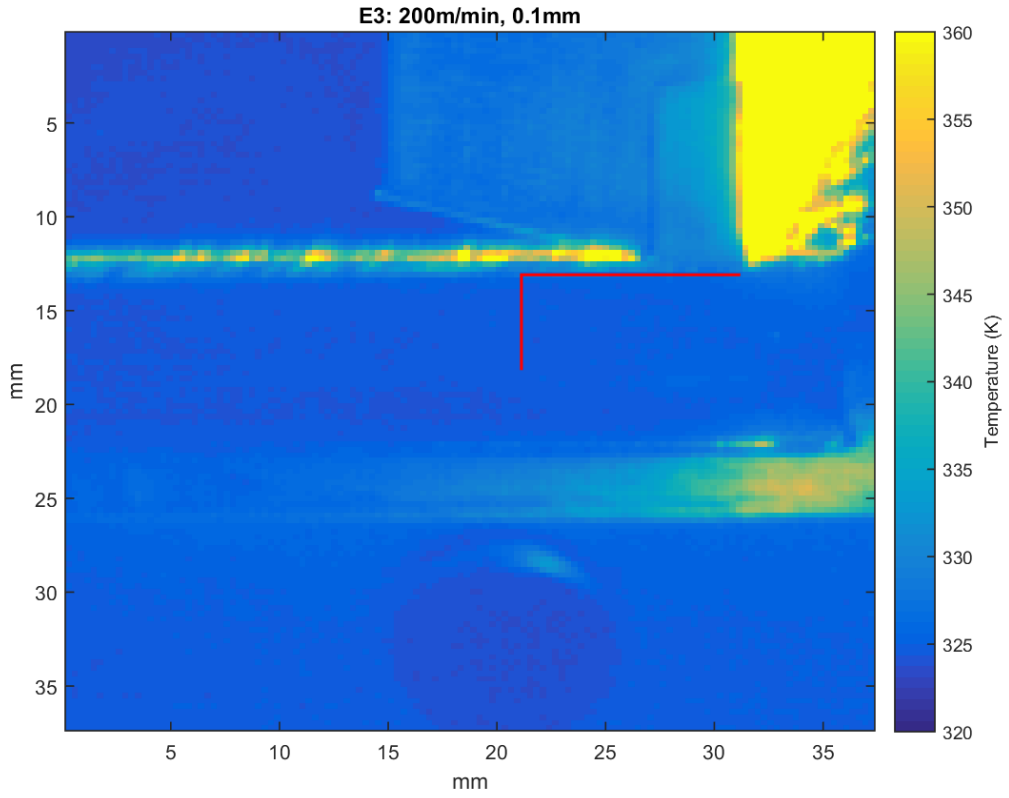

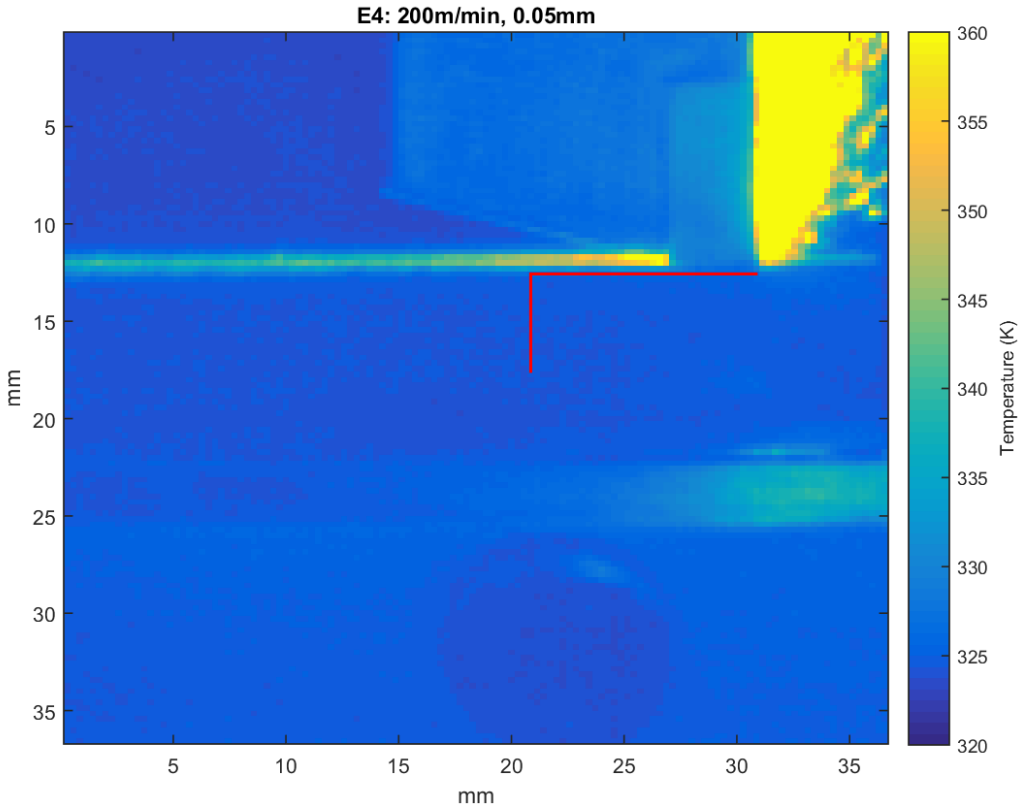
E4: 200m/min, 0.05mm
mm
mm
Temperature (K)
5
10
15
20
25
30
35
360
355
350
345
340
335
330
325
320

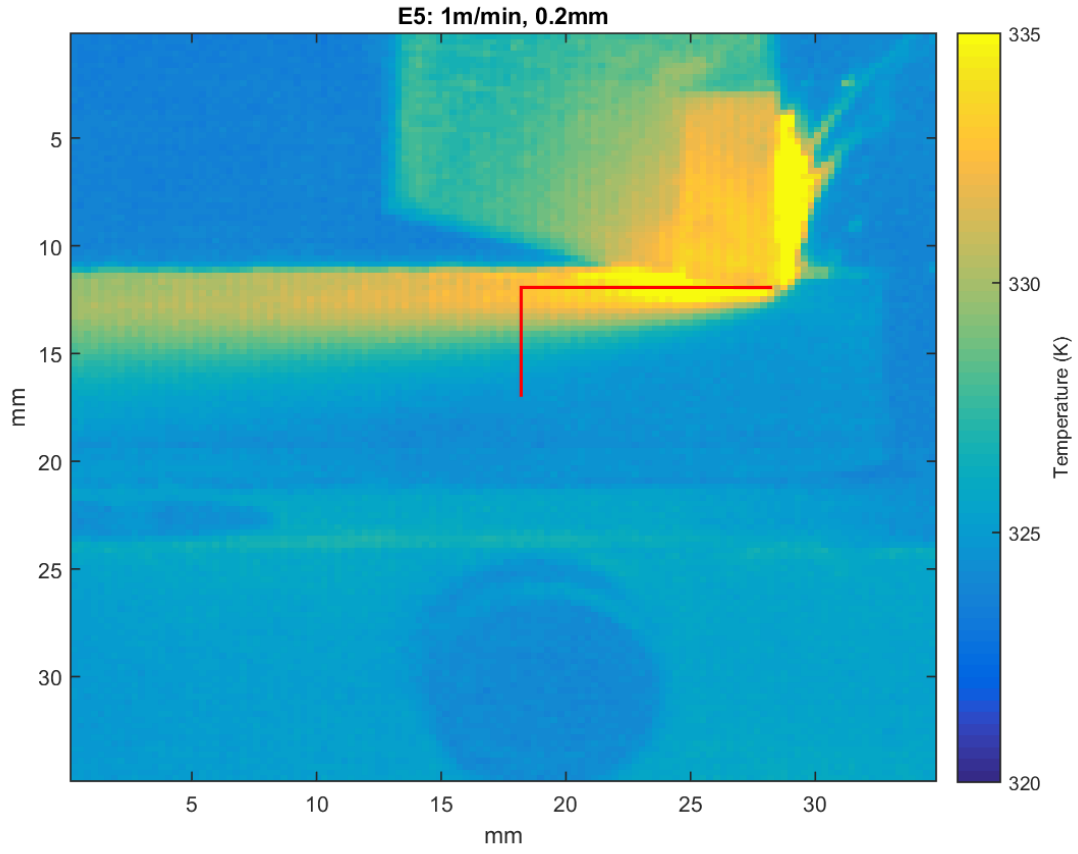
E5: 1m/min, 0.2mm
mm
mm
Temperature (K)
5
10
15
20
25
30
335
330
325
320

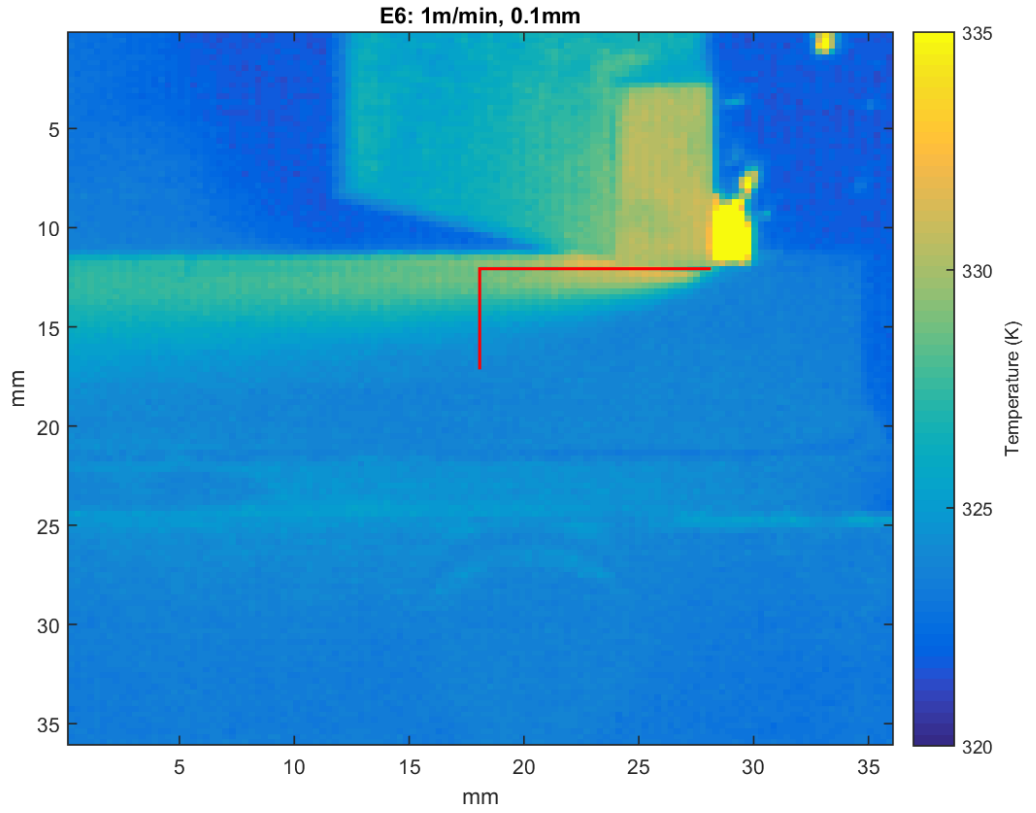
E6: 1m/min, 0.1mm
mm
mm
Temperature (K)
5
10
15
20
25
30
35
320
325
330
335

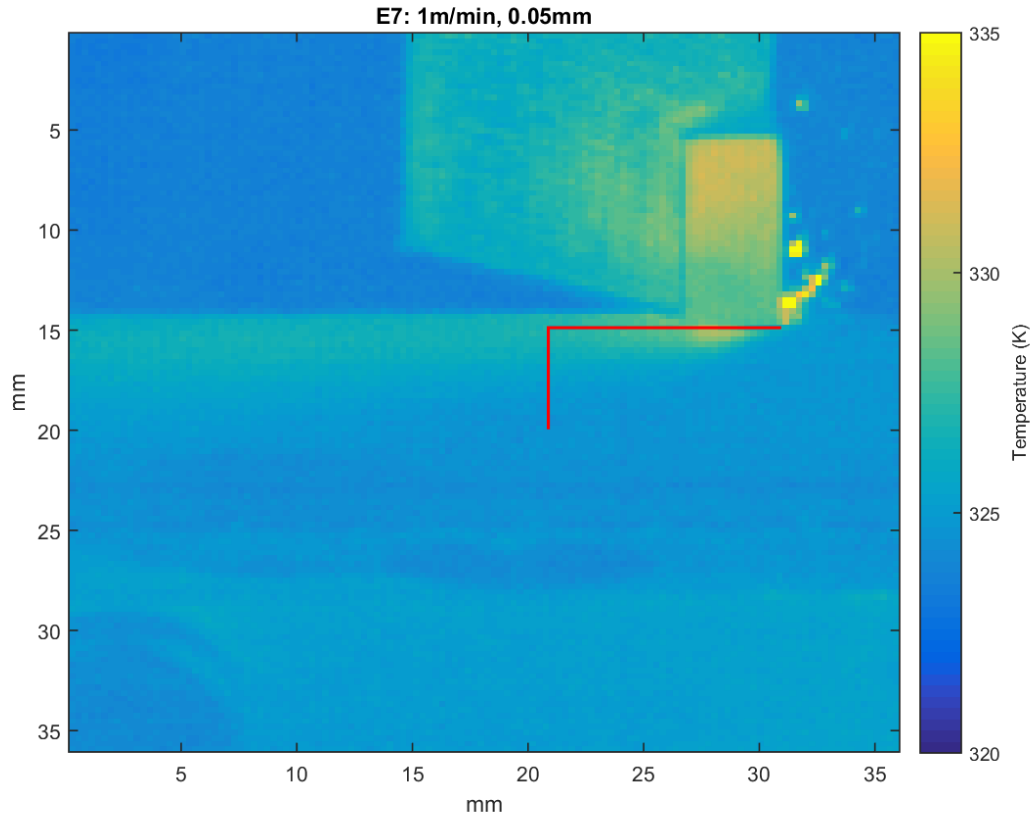
E7: 1m/min, 0.05mm
mm
mm
Temperature (K)
5
10
15
20
25
30
35
320
325
330
335

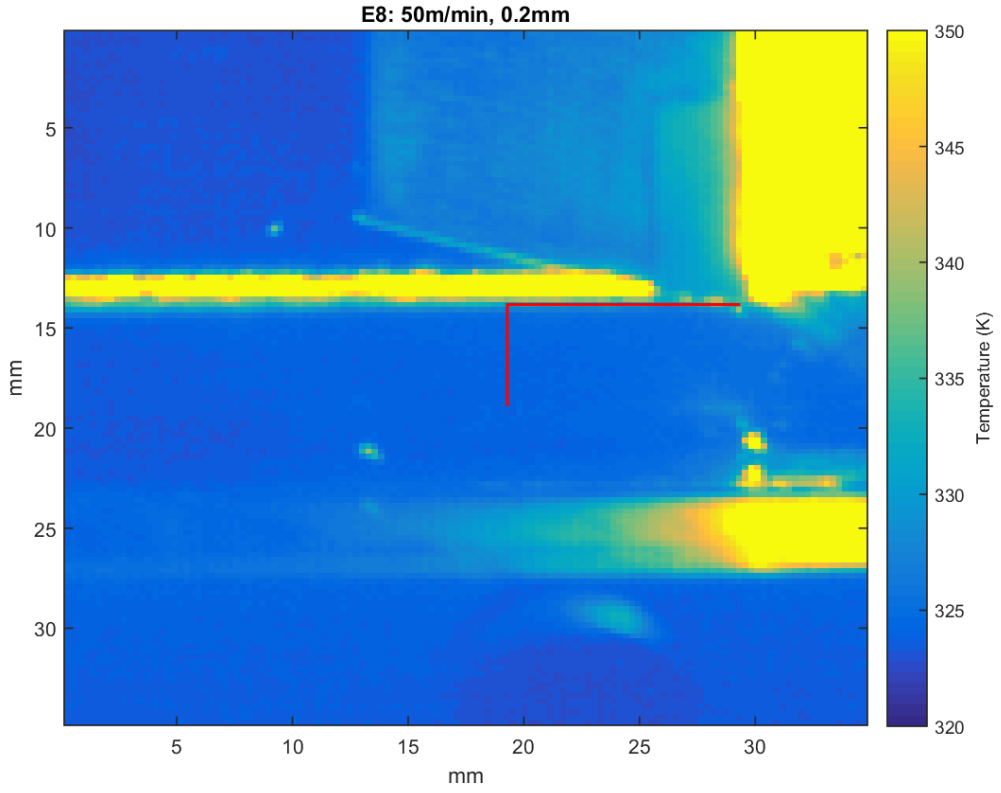
E8: 50m/min, 0.2mm
mm
mm
Temperature (K)
5
10
15
20
25
30
320
325
330
335
340
345
350

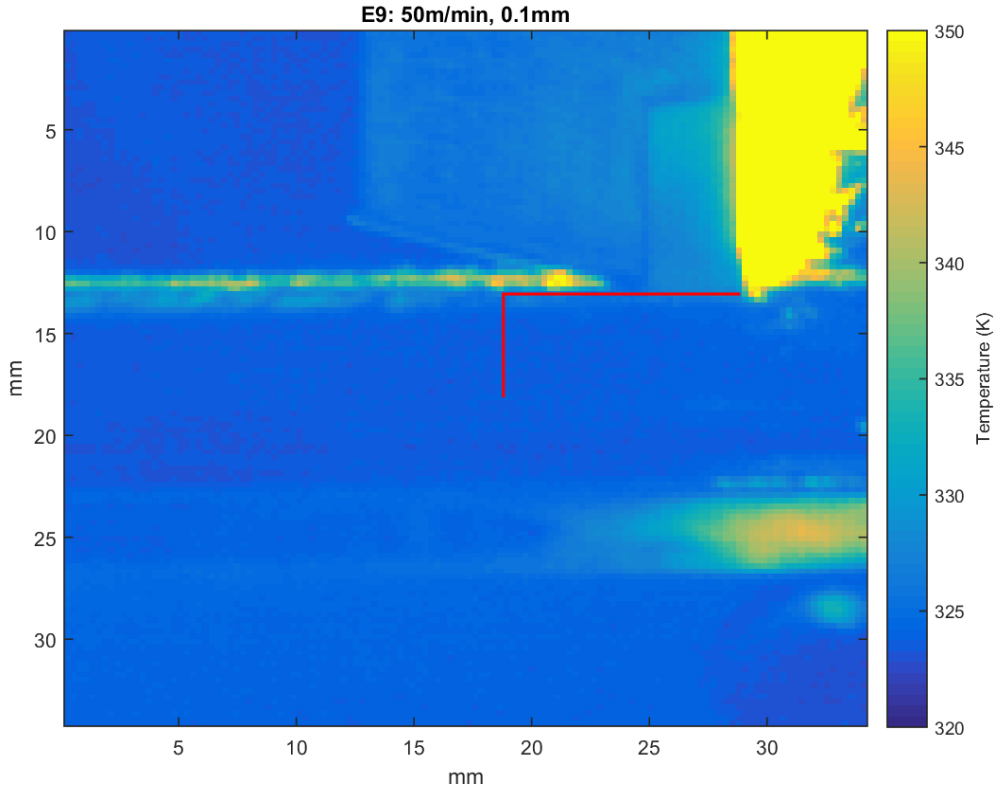
E9: 50m/min, 0.1mm
mm
mm
Temperature (K)
5
10
15
20
25
30
320
325
330
335
340
345
350

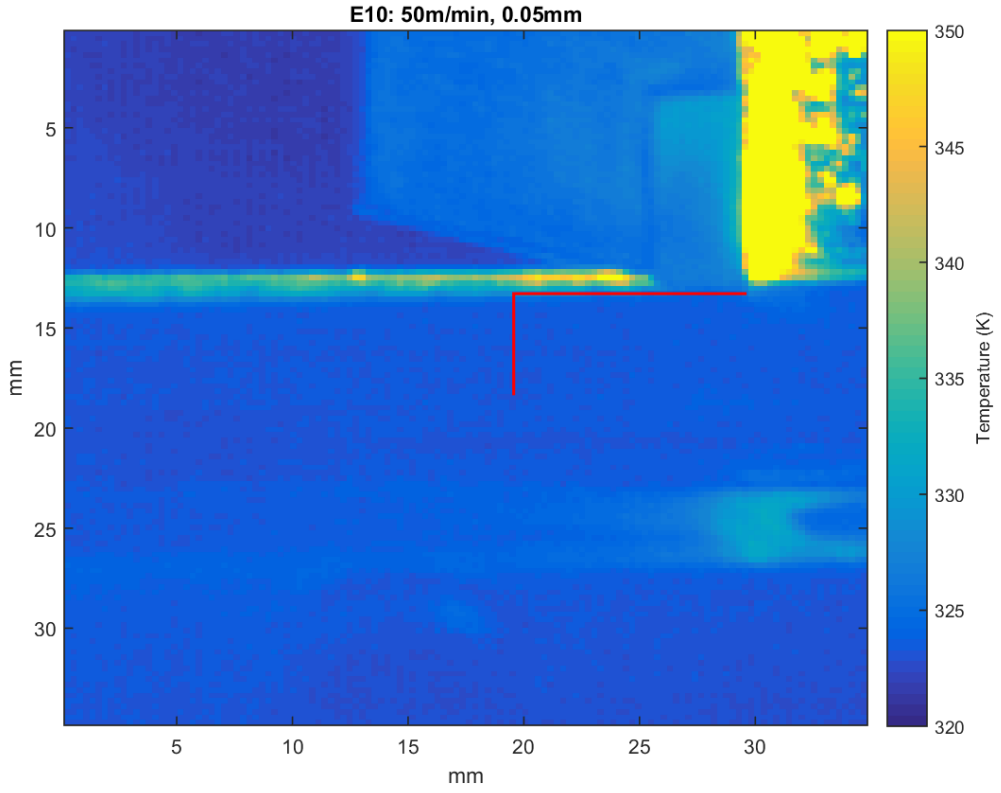
E10: 50m/min, 0.05mm
mm
mm
Temperature (K)
5
10
15
20
25
30
320
325
330
335
340
345
350

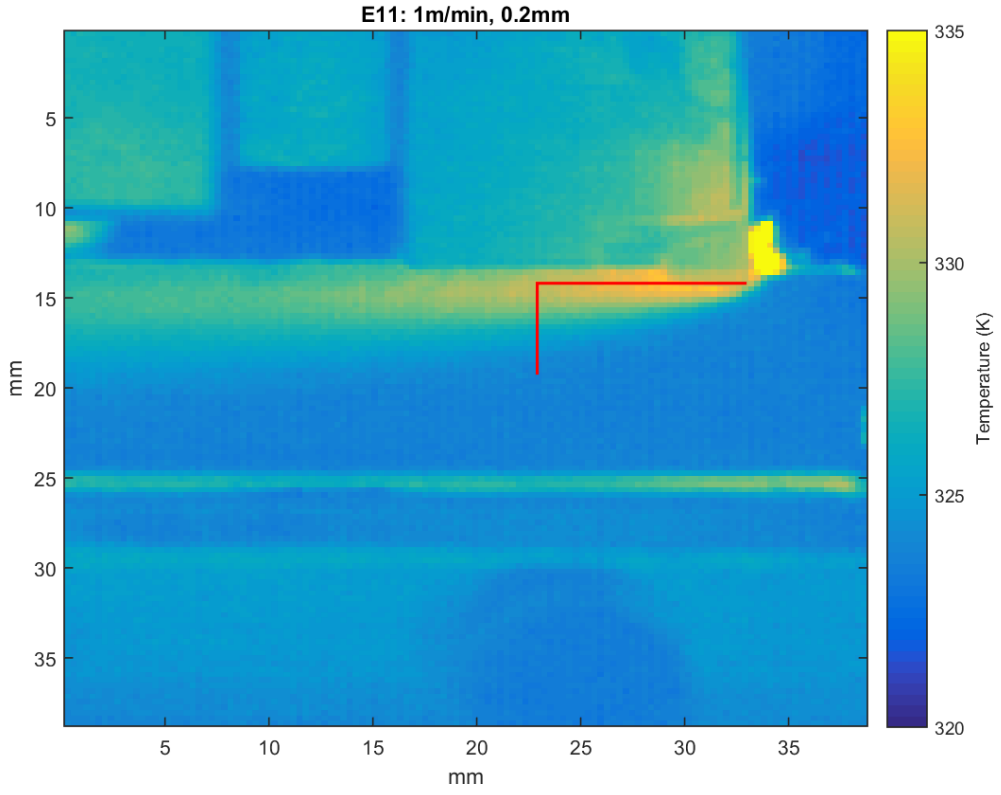
E11: 1m/min, 0.2mm
mm
mm
Temperature (K)
5
10
15
20
25
30
35
320
325
330
335

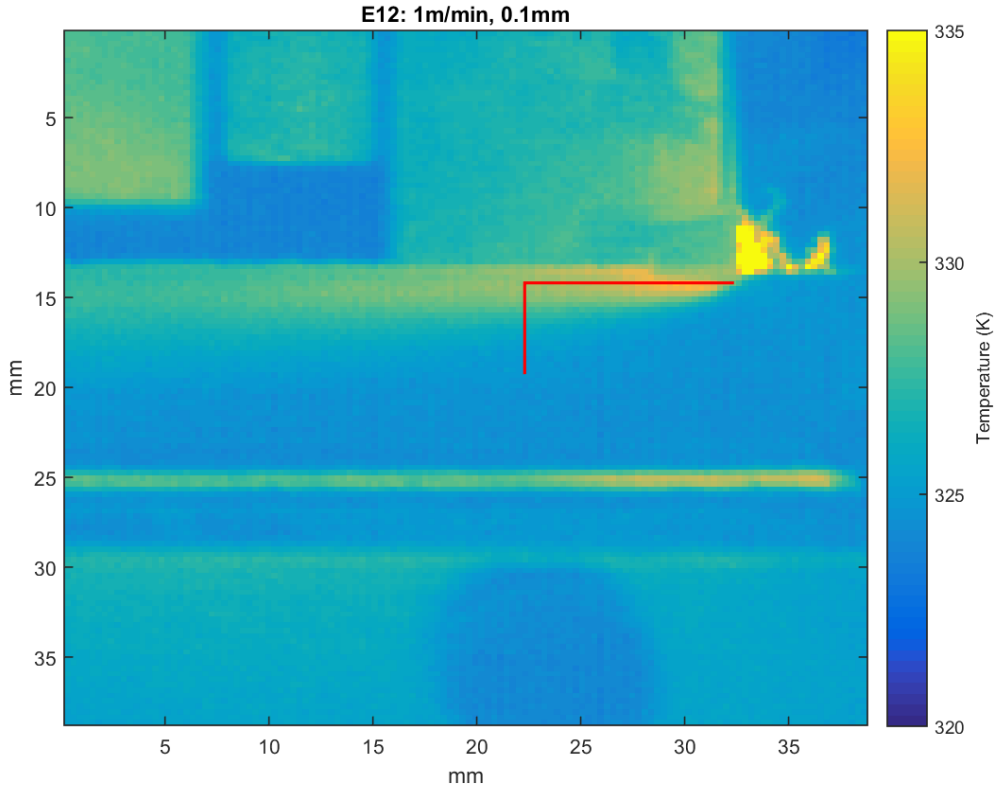
E12: 1m/min, 0.1mm
mm
mm
Temperature (K)
5
10
15
20
25
30
35
320
325
330
335

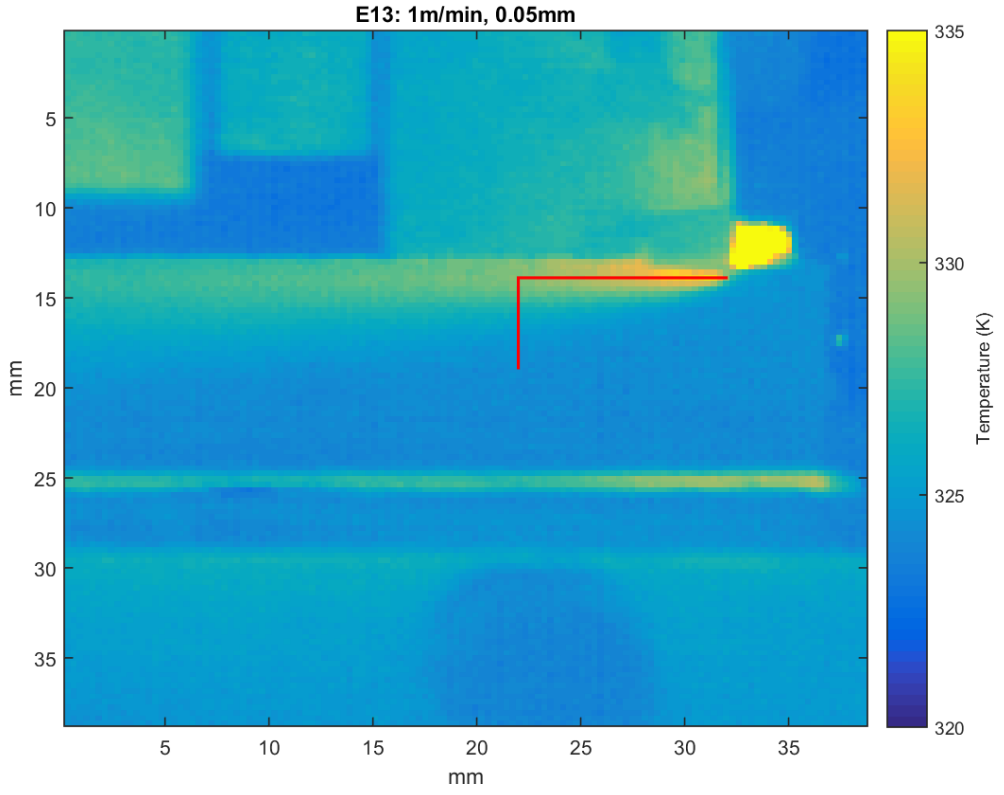
E13: 1m/min, 0.05mm
mm
mm
Temperature (K)
5
10
15
20
25
30
35
320
325
330
335

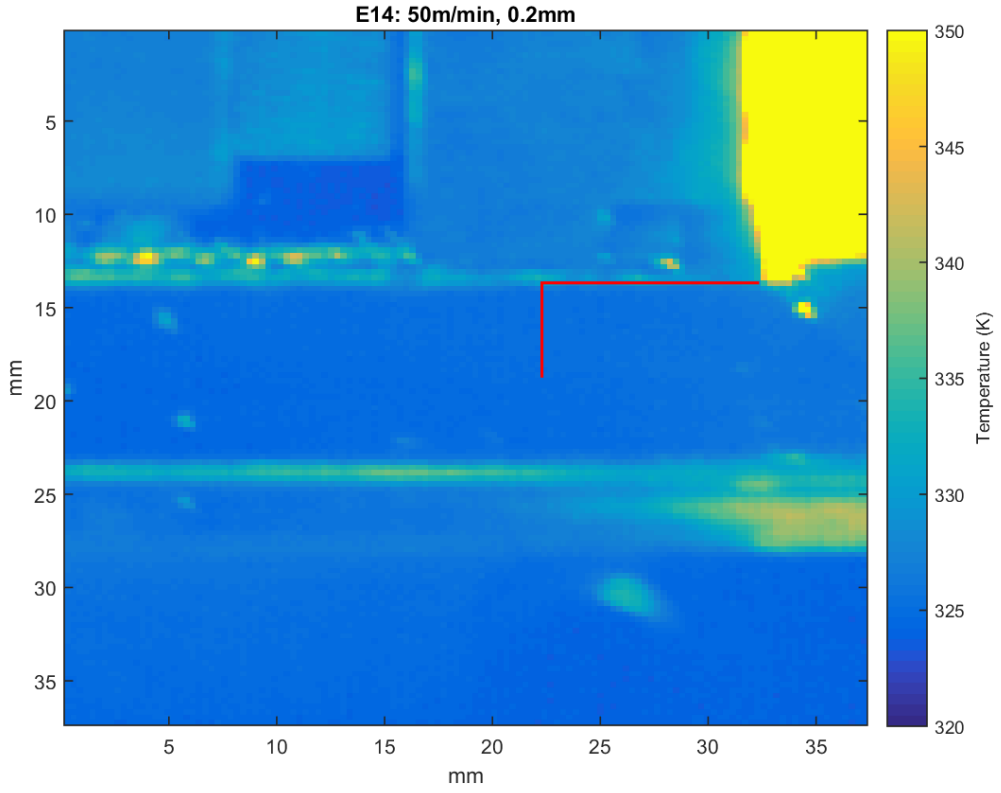
E14: 50m/min, 0.2mm
mm
mm
Temperature (K)
5
10
15
20
25
30
35
320
325
330
335
340
345
350

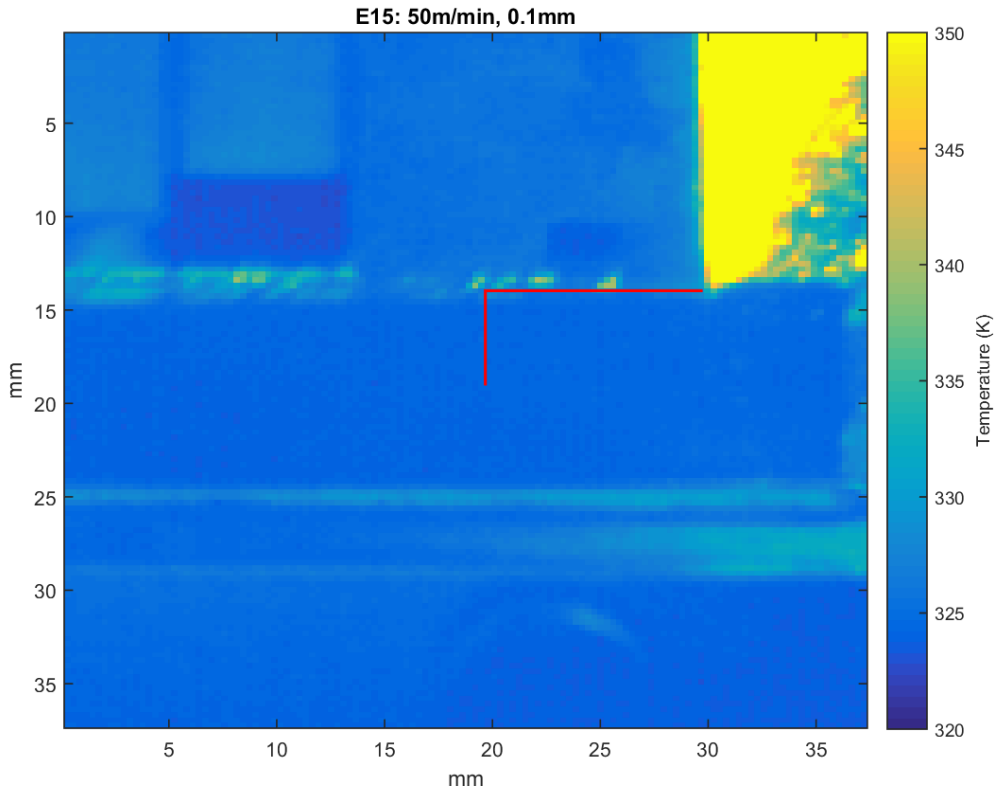
E15: 50m/min, 0.1mm
mm
mm
Temperature (K)
5
10
15
20
25
30
35
320
325
330
335
340
345
350

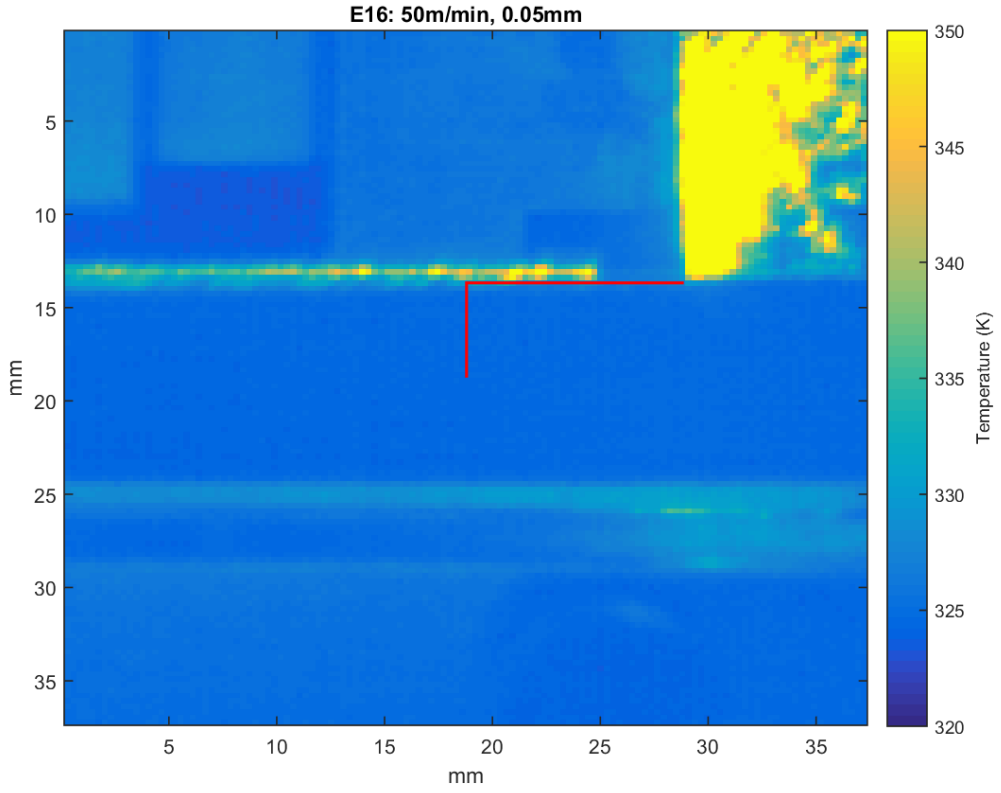
E16: 50m/min, 0.05mm
mm
mm
Temperature (K)
5
10
15
20
25
30
35
320
325
330
335
340
345
350

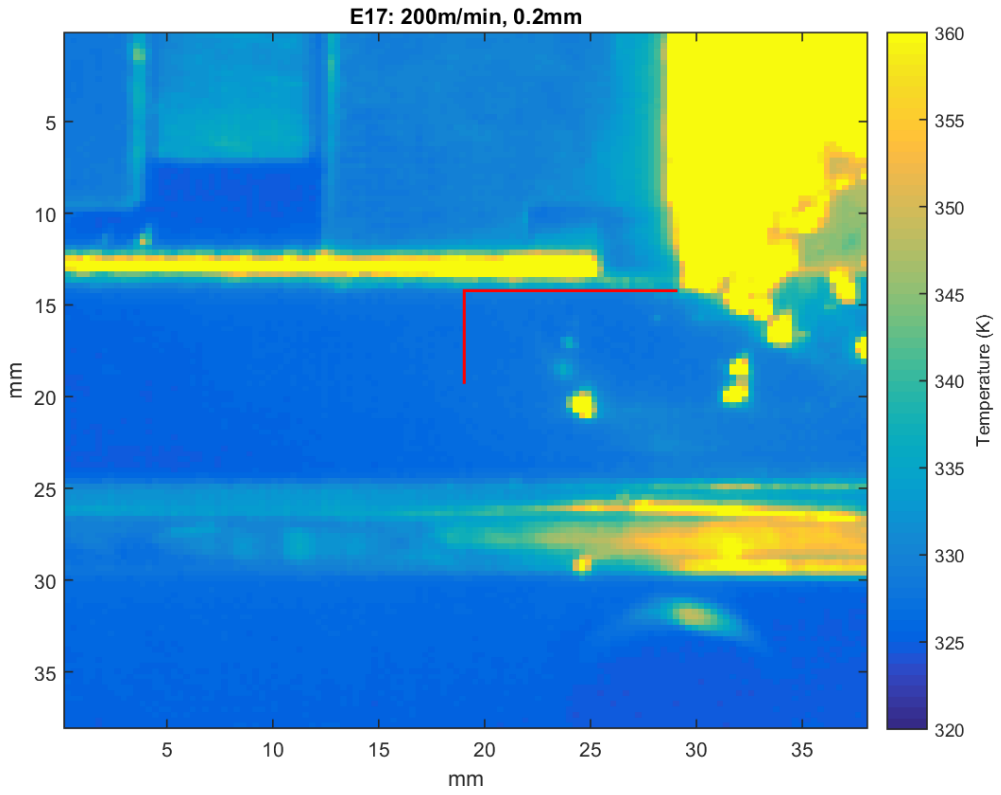
E17: 200m/min, 0.2mm
mm
mm
Temperature (K)
5
10
15
20
25
30
35
320
325
330
335
340
345
350
355
360

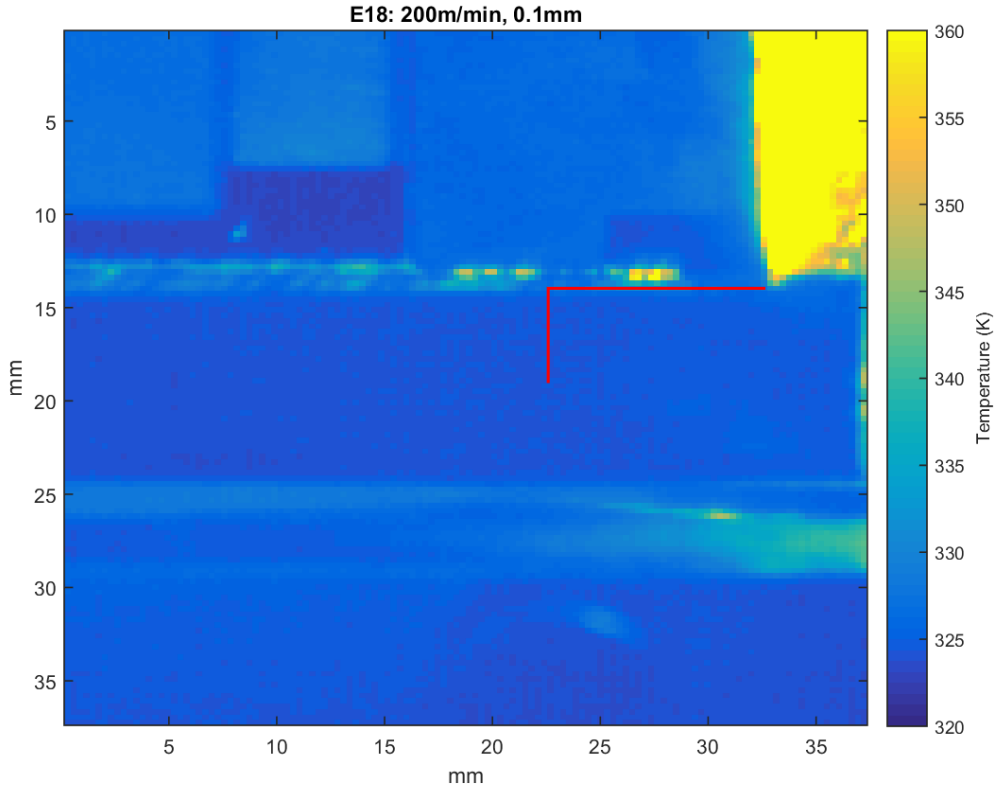
E18: 200m/min, 0.1mm
mm
mm
Temperature (K)
5
10
15
20
25
30
35
320
325
330
335
340
345
350
355
360

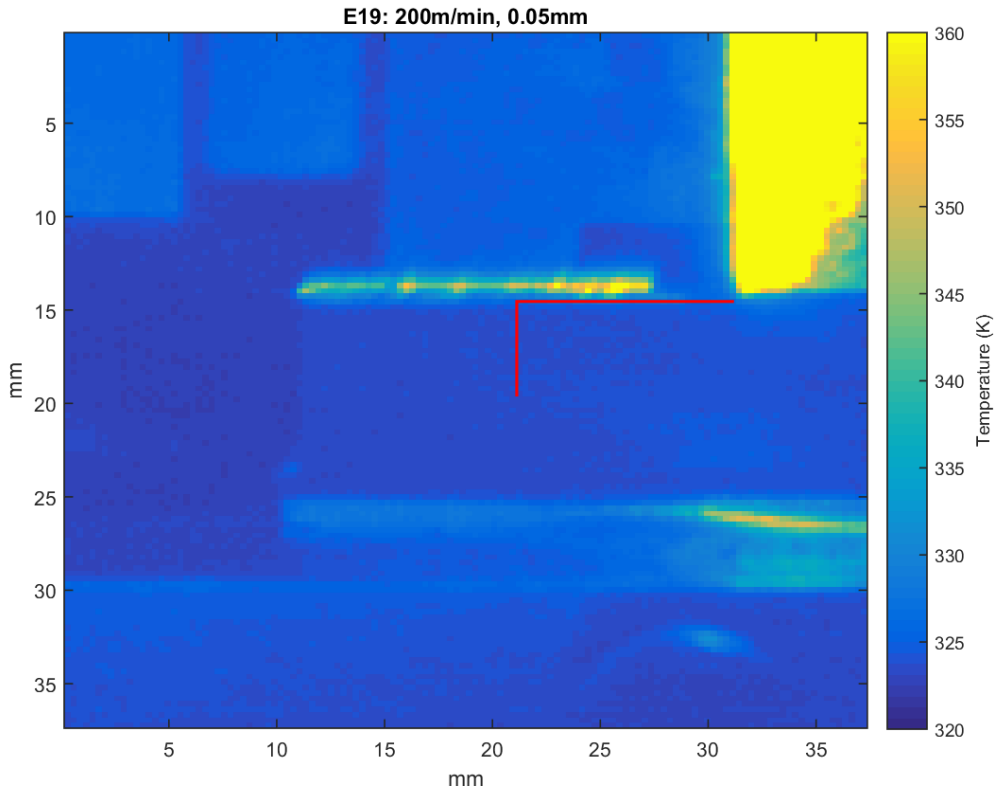
E19: 200m/min, 0.05mm
mm
mm
Temperature (K)
5
10
15
20
25
30
35
320
325
330
335
340
345
350
355
360

Profile temperature along the 4 lines to determine the internal damage

E1: 200m/min, 0.2mm

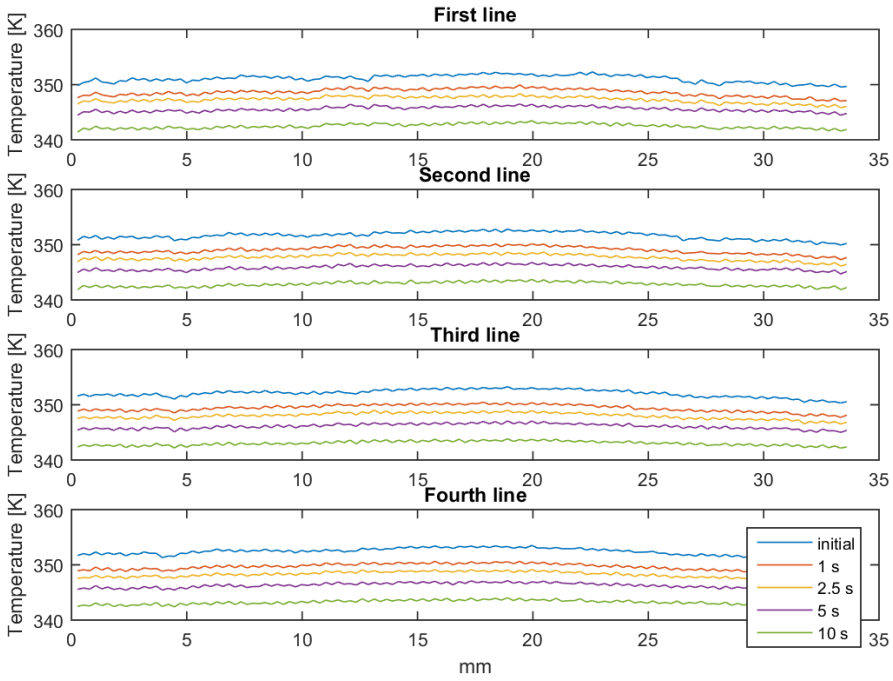

E3: 200m/min, 0.1mm

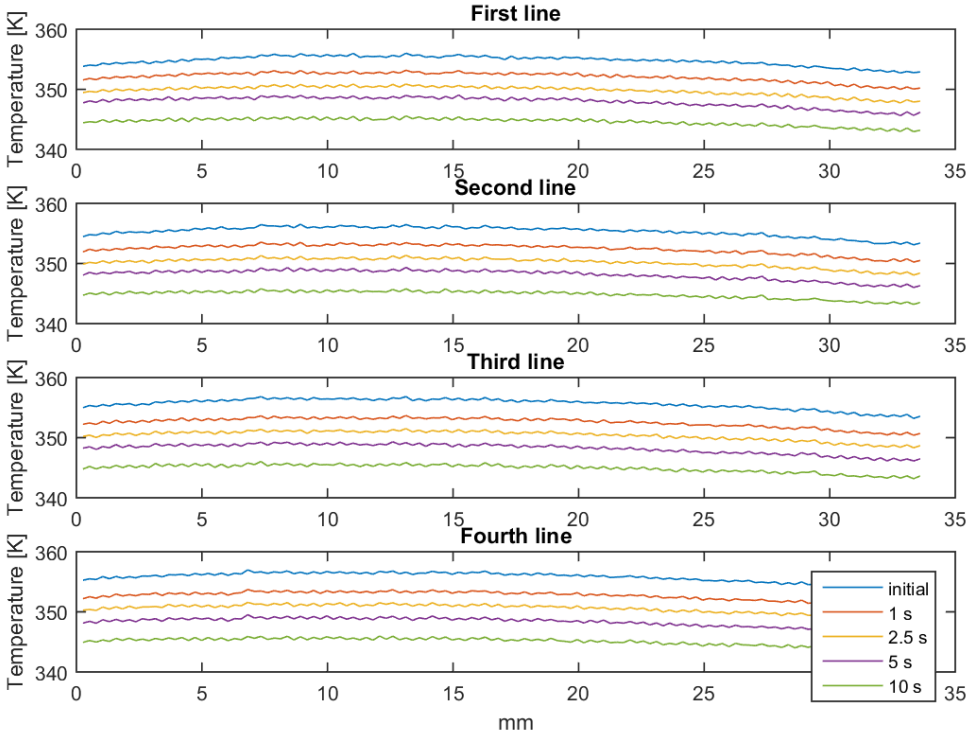

E4: 200m/min, 0.05mm

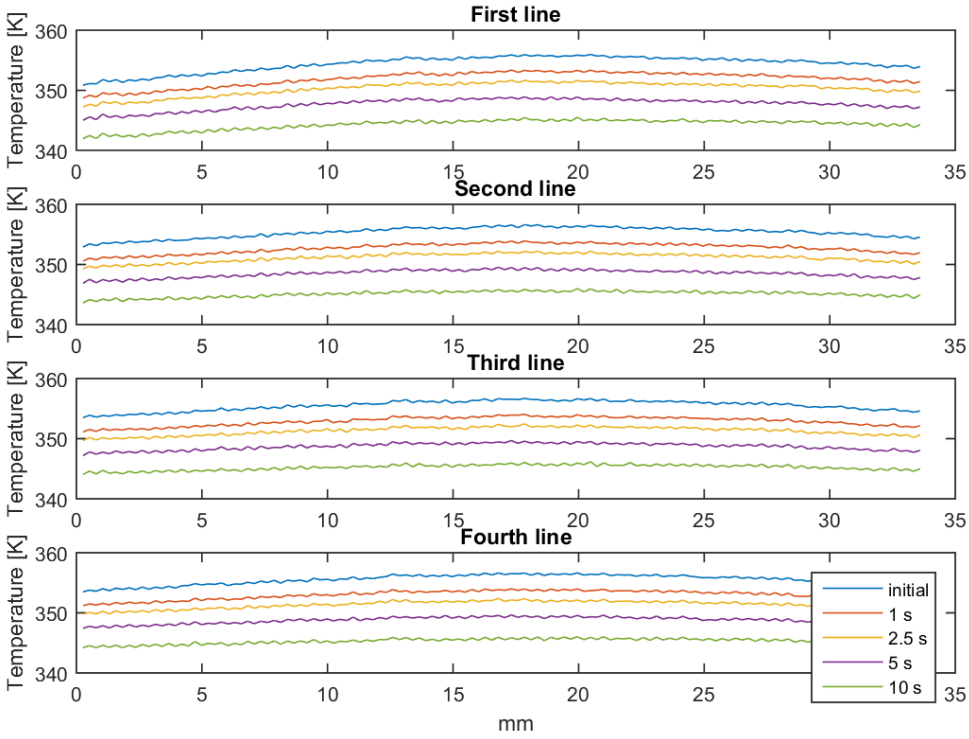

E5: 1m/min, 0.2mm

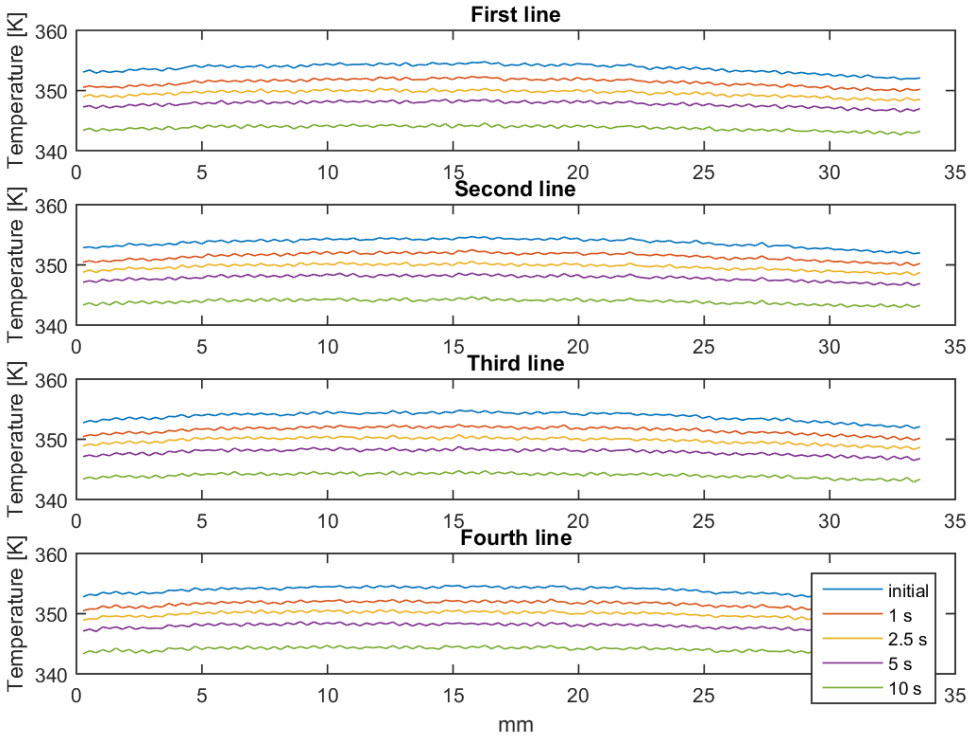

E6: 1m/min, 0.1mm

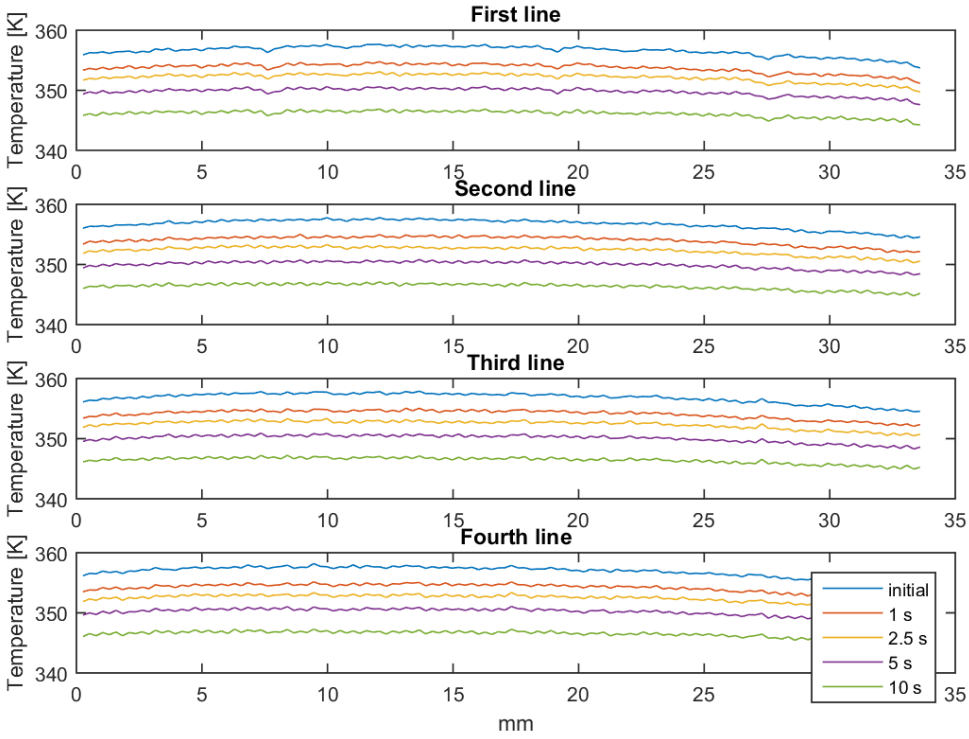

E7: 1m/min, 0.05mm

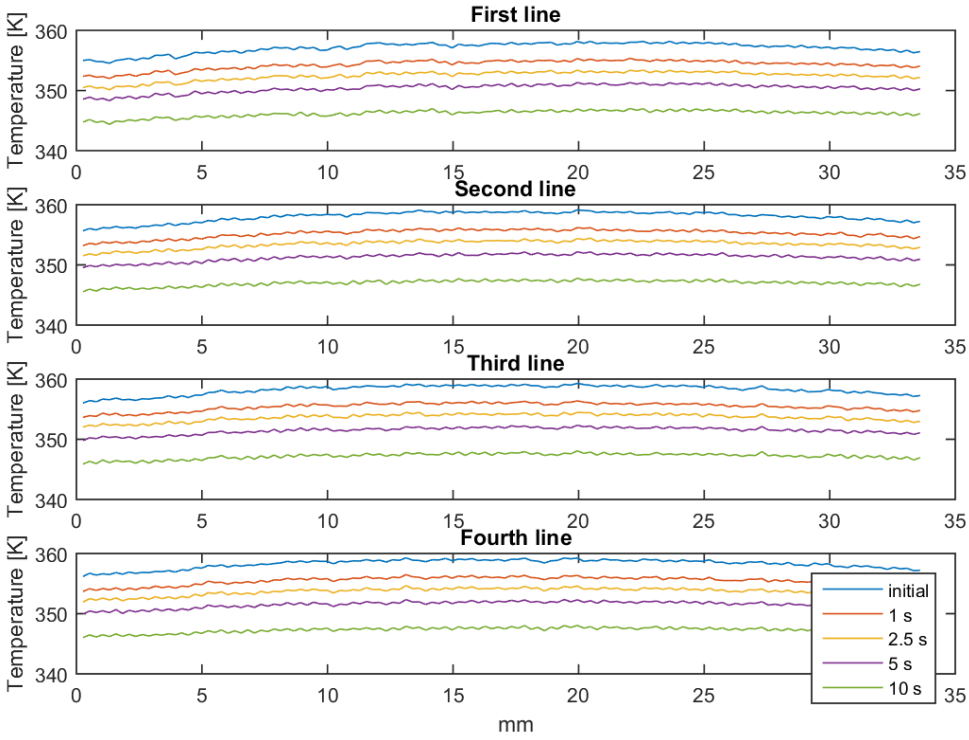

E8: 50m/min, 0.2mm

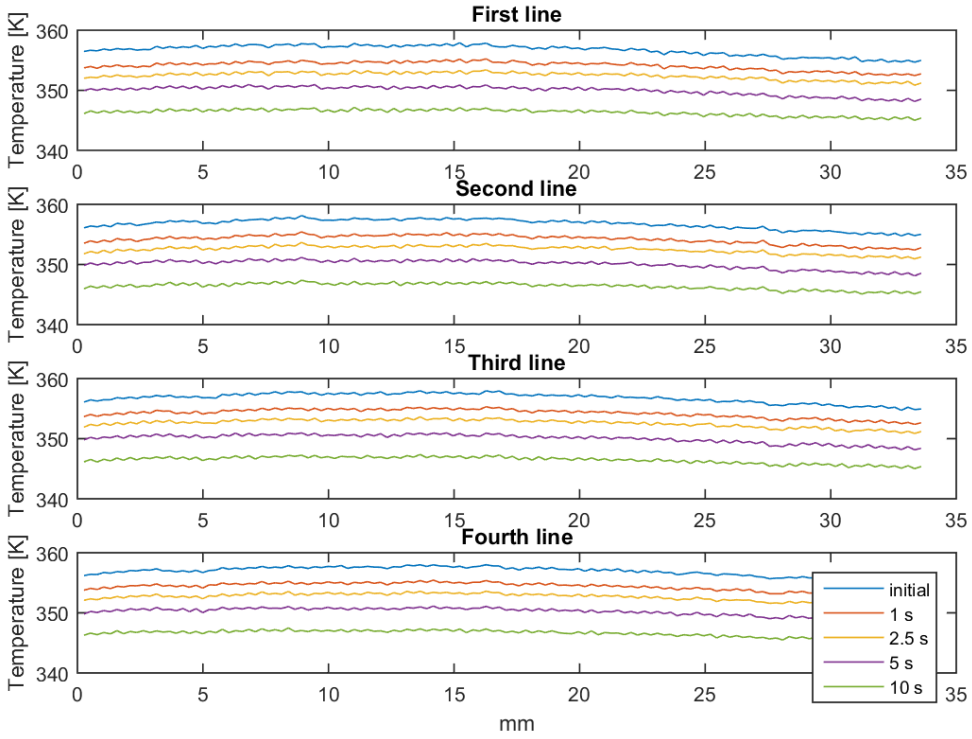

E9: 50m/min, 0.1mm

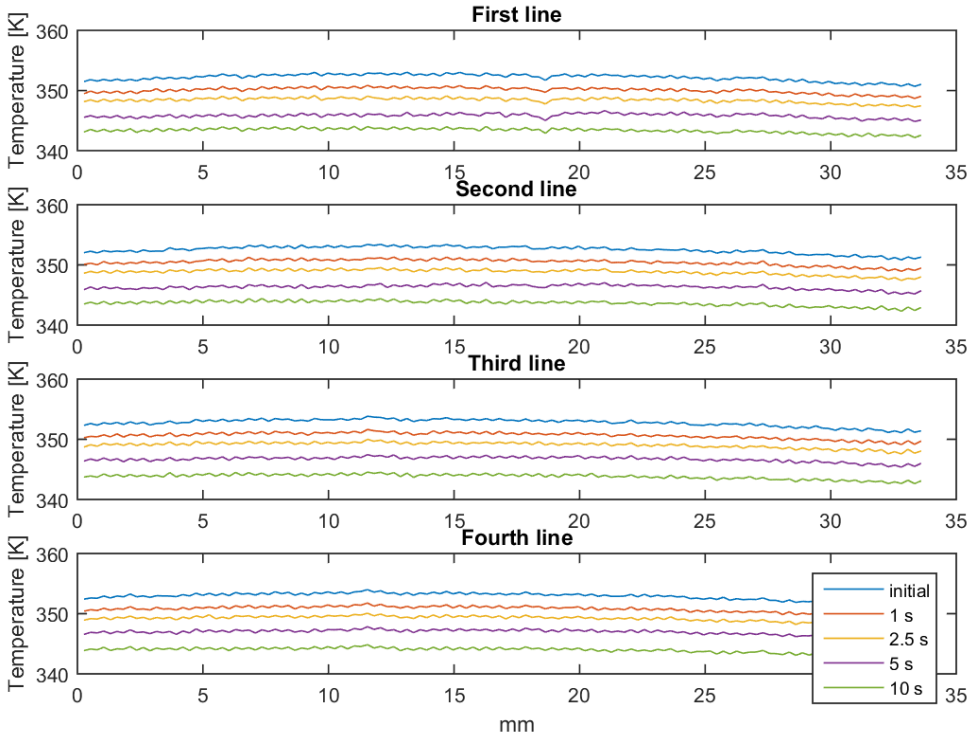

E10: 50m/min, 0.05mm

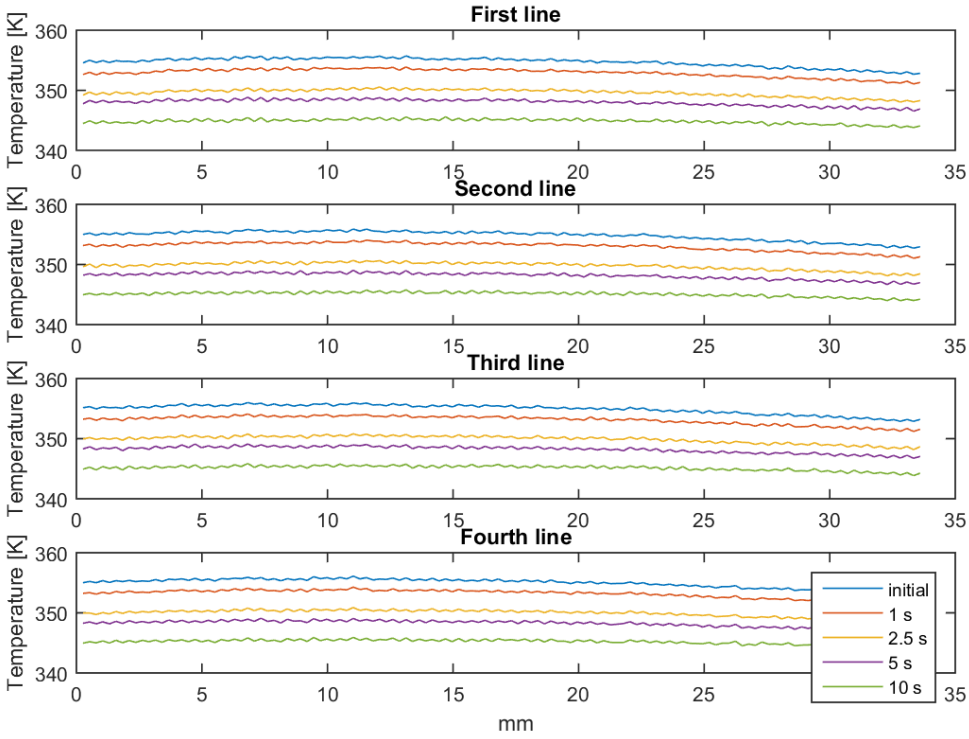

E11: 1m/min, 0.2mm

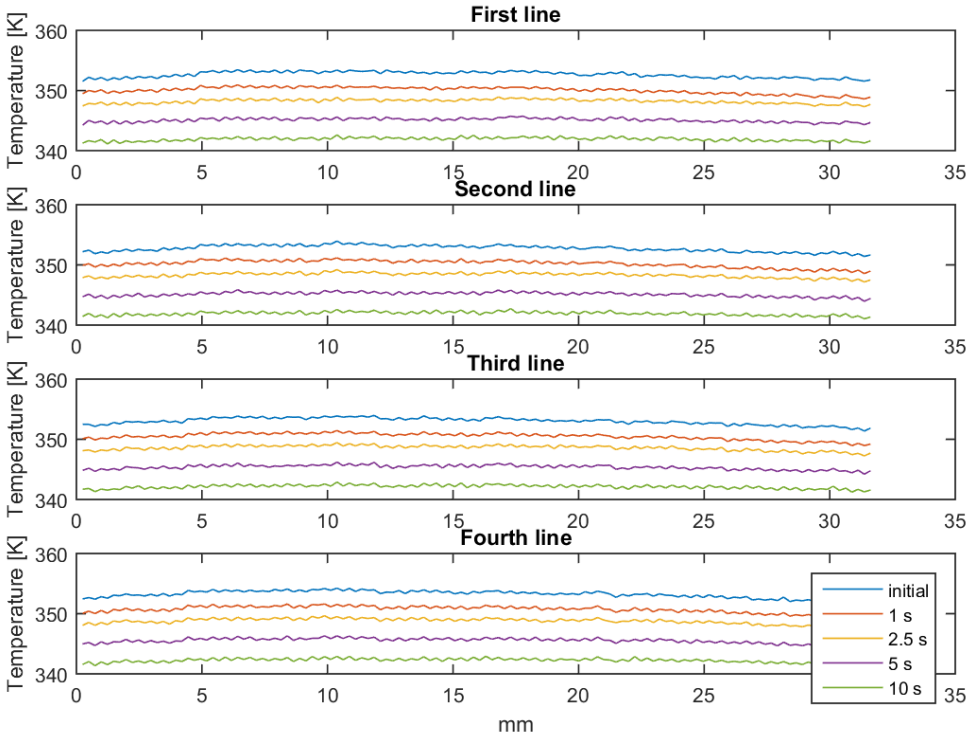

E12: 1m/min, 0.1mm

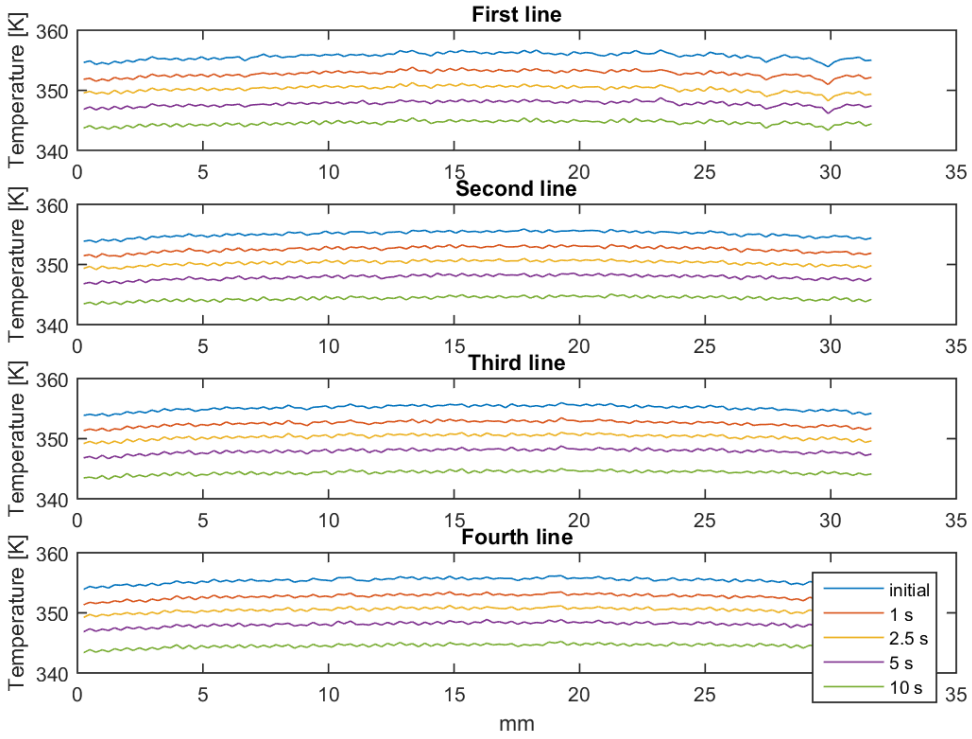

E13: 1m/min, 0.05mm

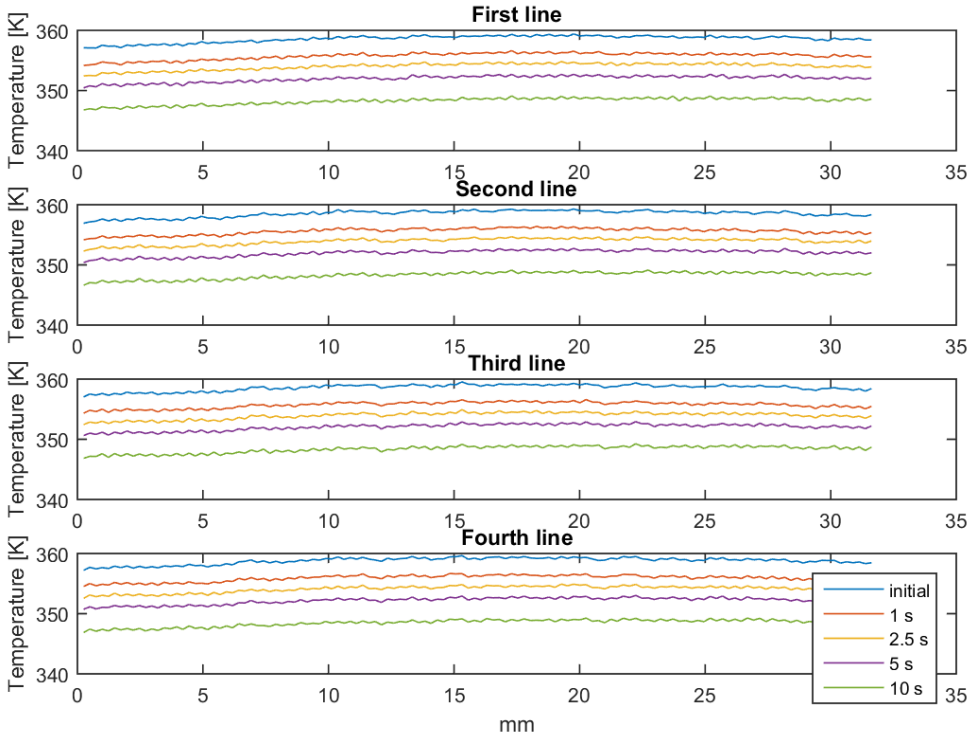

E14: 50m/min, 0.2mm

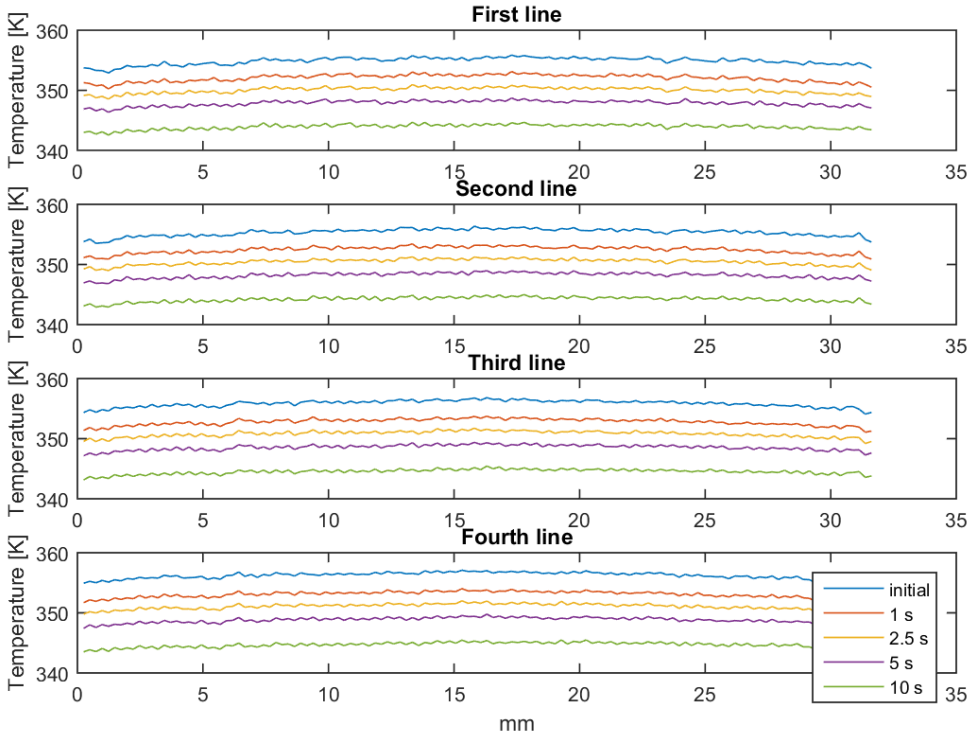

E15: 50m/min, 0.1mm

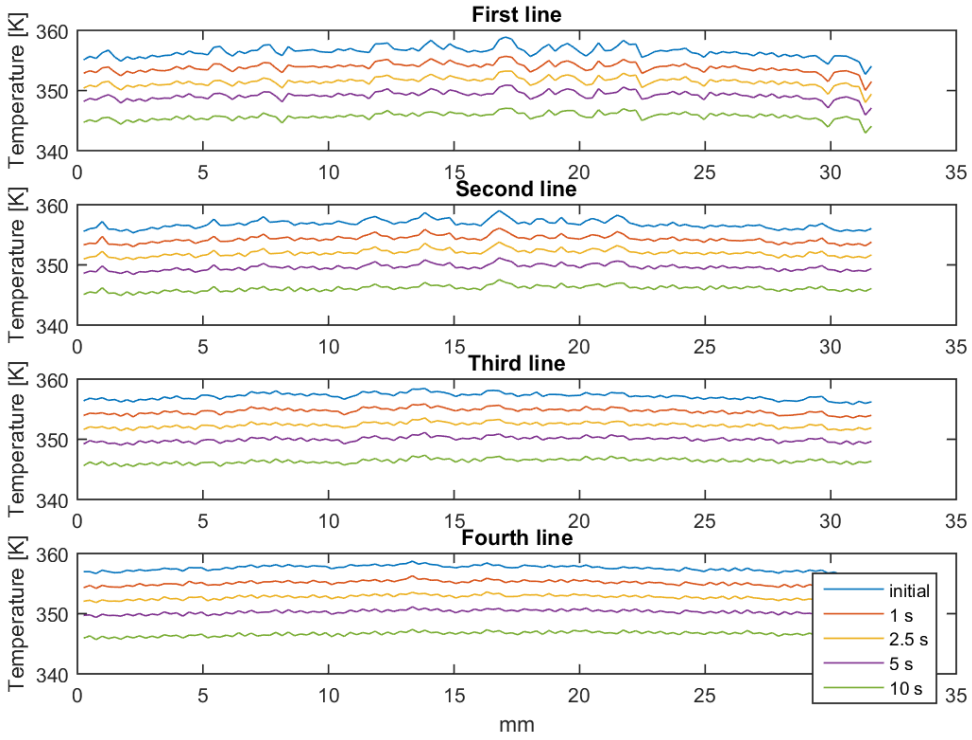

E16: 50m/min, 0.05mm

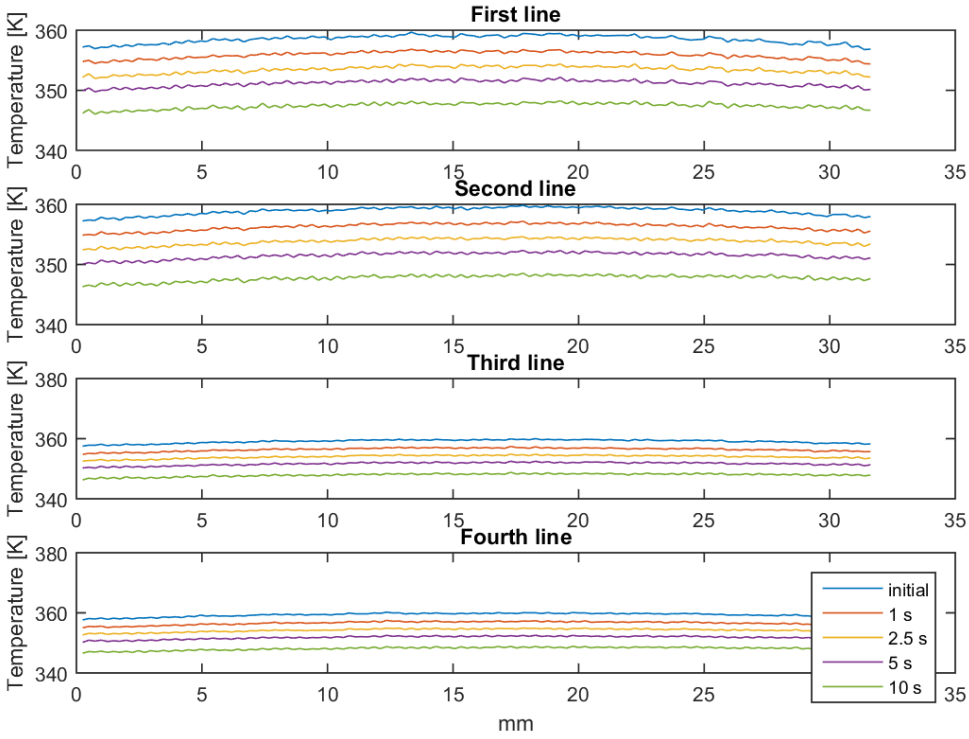

E17: 200m/min, 0.2mm

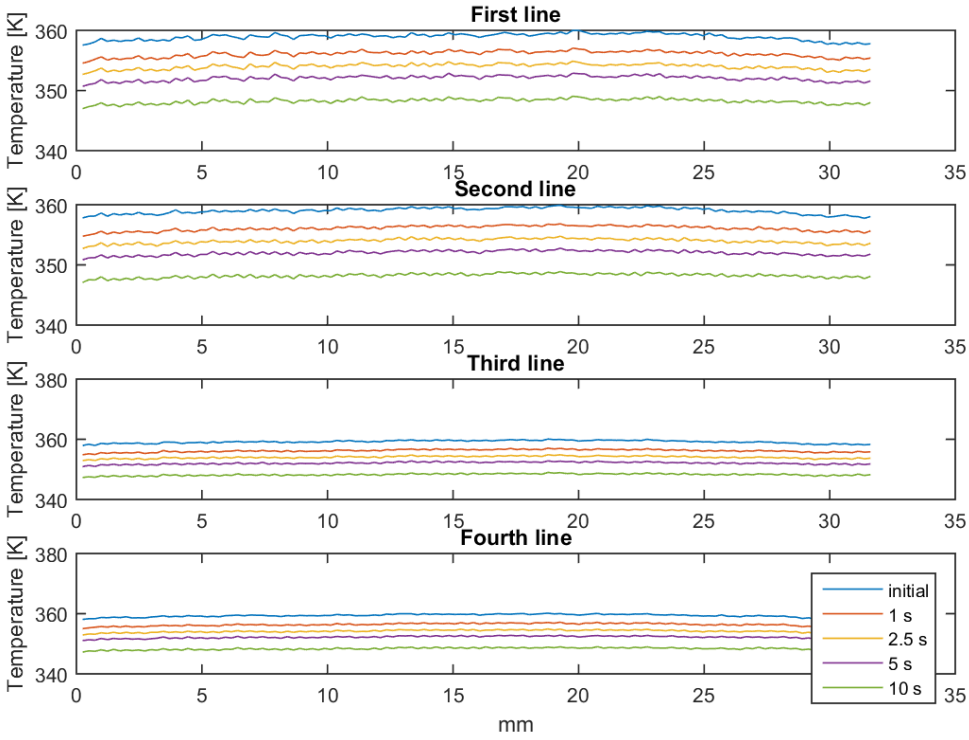

E18: 200m/min, 0.1mm

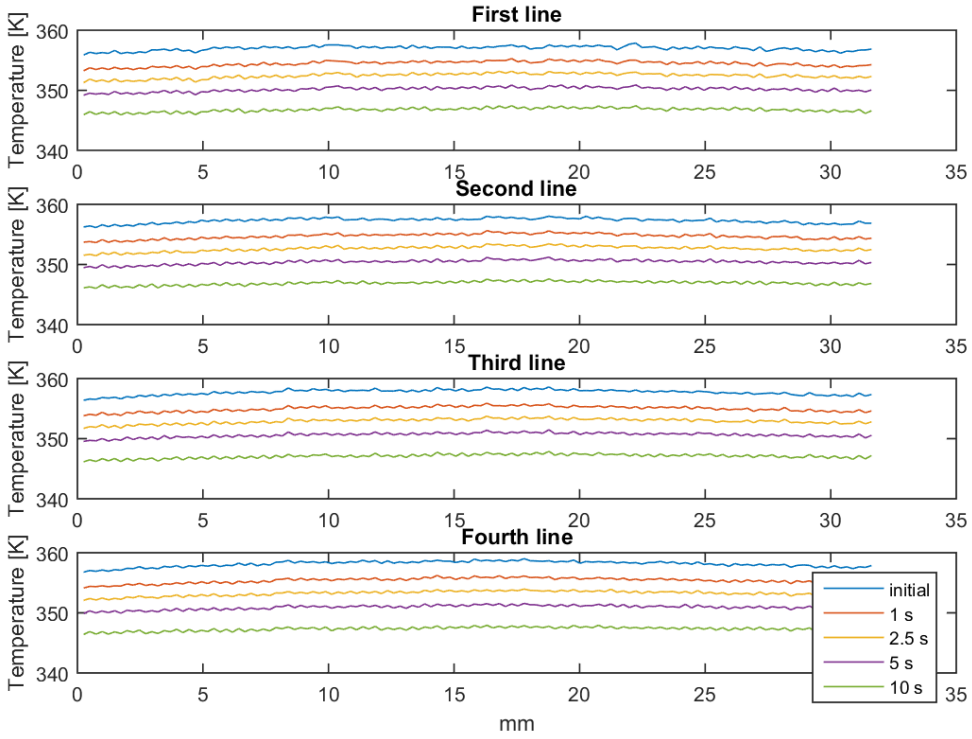

E19: 200m/min, 0.05mm

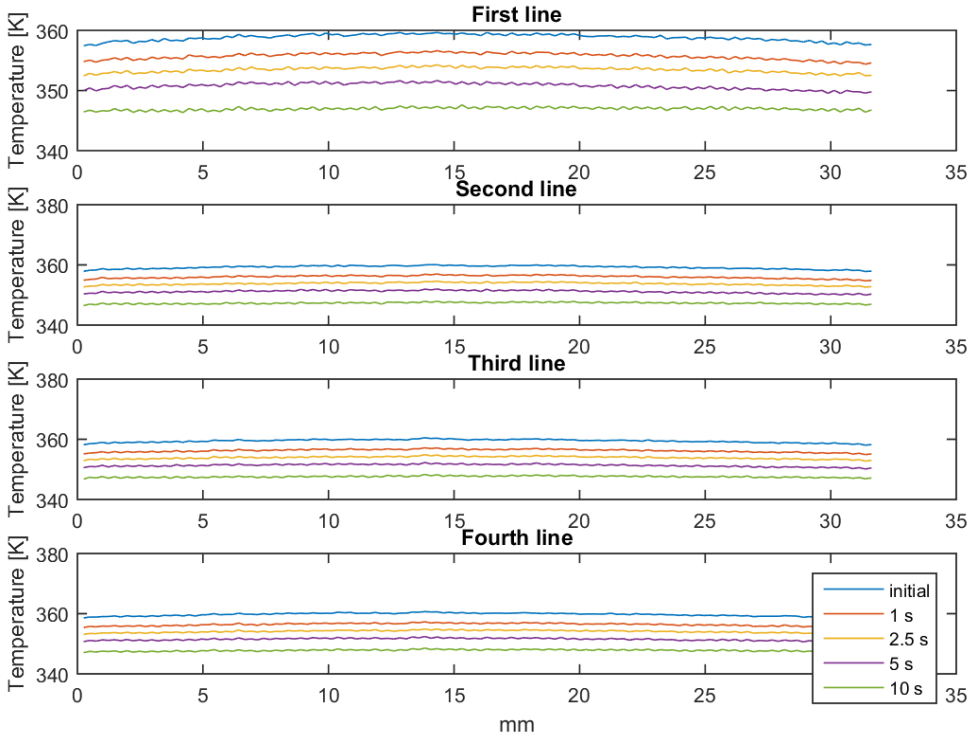

Undamaged specimen